uOttawa

L'Université canadienne
Canada's university

FACULTÉ DES ÉTUDES SUPÉRIEURES ET POSTOCTORALES

uOttawa

L'Université canadienne
Canada's university

FACULTY OF GRADUATE AND POSDOCTORAL STUDIES

Xinlei Zou

AUTEUR DE LA THÈSE / AUTHOR OF THESIS

M.A.Sc. (Electrical Engineering)

GRADE / DEGREE

School of Information Technology and Engineering

FACULTÉ, ÉCOLE, DÉPARTEMENT / FACULTY, SCHOOL, DEPARTMENT

Bandwidth Enhancement Techniques for Probe-Fed Microstrip Patch Antennas

TITRE DE LA THÈSE / TITLE OF THESIS

D. A. McNamara

DIRECTEUR (DIRECTRICE) DE LA THÈSE / THESIS SUPERVISOR

CO-DIRECTEUR (CO-DIRECTRICE) DE LA THÈSE / THESIS CO-SUPERVISOR

EXAMINATEURS (EXAMINATRICES) DE LA THÈSE / THESIS EXAMINERS

M. Yagoub

Q. J. Zhang

Gary W. Slater

LE DOYEN DE LA FACULTÉ DES ÉTUDES SUPÉRIEURES ET POSTDOCTORALES /
DEAN OF THE FACULTY OF GRADUATE AND POSTDOCORAL STUDIES

BANDWIDTH ENHANCEMENT TECHNIQUES FOR PROBE-FED MICROSTRIP PATCH ANTENNAS

By

Xinlei Zou

A thesis submitted to the

Faculty of Graduate and Postdoctoral Studies

in partial fulfillment of the requirements for the degree of

Master of Applied Science

in Electrical Engineering

Ottawa-Carleton Institute for Electrical and Computer Engineering

School of Information Technology and Engineering

Faculty of Engineering

University of Ottawa

January 2005

Your file Votre référence
ISBN: 0-494-11481-9
Our file Notre référence
ISBN: 0-494-11481-9

ABSTRACT

Many bandwidth enhancement techniques for microstrip patch antennas have been developed since the 1970's. Except for an IEEE collection of reprints which appeared in 1995, relatively little work has been done to review and categorize these techniques. As a result, the published research and design of broadband microstrip antennas has become somewhat unsystematic. In this thesis, papers on broadband microstrip antennas have been reviewed. Using full-wave electromagnetic simulation, the important performance parameters such as the bandwidth, realized gain, antenna efficiency, radiation efficiency and radiation patterns of broadband microstrip patch antennas have been considered. Based on these results, bandwidth enhancement techniques have been categorized in two broad classes, namely those applicable when electrically-thick low-permittivity substrates are used, and those applicable to electrically-thin high-permittivity substrates. These broad classes have been sub-divided into several sub-classes in a structured manner that aids the understanding of the bandwidth enhancement methods. A summary of these techniques, linked to a comparison of resulting microstrip patch antenna performance obtained from full-wave analysis of the sub-classes, is provided. It is also shown, through a specific example, how the increased understanding afforded by this categorization can lead to the development of new broad bandwidth geometries that can offer some advantages over existing ones.

Keywords: Probe-fed microstrip patch antennas; bandwidth enhancement; full-wave analysis.

ACKNOWLEDGEMENTS

I would like to thank my supervisor Dr. Derek McNamara for his support, guidance and funding during the research and writing of this thesis. The experience and knowledge I gained from him during our work is, and will be, of great value to me throughout my career.

I owe thanks to my colleagues Ms. Xiangjun Meng, Mr. Wei Fang, Mr. Guangze Zhao, Mr. Prasun Sharma, and my wife, parents, family members and friends for always being there for me, and for unselfishly supporting me from the very beginning of my graduate studies.

TABLE OF CONTENTS

LIST OF FIGURES

CHAPTER 1

INTRODUCTION

1.1 MICROSTRIP PATCH ANTENNAS

The idea of the microstrip patch antenna dates back to the 1950's, its invention being attributed to many sources, including Deschamps [1] and Greig & Engleman [2]. Limited by design and fabrication methods, the microstrip antenna was not given serious attention until the 1970's. The real development of microstrip antennas began in the early 1970's, and by the end of the decade numerous research papers and books had been published [3, 4]. A flurry of further development has taken place since the 1980's. There are several reasons for this, including

- The wide range of improved (i.e. lower loss; repeatability of relative permittivity) substrate products that have been offered by manufacturers.
- The availability of commercial full-wave electromagnetic modeling codes resulting from the work on computational electromagnetics made possible by the widespread availability of computing power.
- The rapid growth in commercial wireless communications.

The reasons for microstrip patch antennas being widely used are many [5, 6, 7, 8, 9, 14, 15], and include its light weight and small volume, its low profile planar configuration, and its low fabrication cost that makes commercial use feasible. As the applications of the basic microstrip patch antenna geometry increased its limitations became clear. Its disadvantages [8, 9, 10] include narrow bandwidth, limited power

capability, poor polarization purity, and unwanted radiation from the feeding mechanism. Much work has been done to overcome or lessen these limitations [8, 10, 11]. Some have been partially alleviated due to improvements in the substrate materials available. Others have been dealt with by using altered feed mechanisms, more complicated patch geometries, electrically thick substrates ("thick" from the point of view of what would be used for non-radiating microstrip circuits), or combinations thereof. Narrow bandwidth has perhaps been the major limitation of traditional microstrip patch antennas. The fractional bandwidth of the original patch antenna was only about 2% [7].

The probe-fed microstrip patch shown in Figure 1.1 was one of the earliest feeding mechanisms used, and it remains the one of choice in a variety of antenna systems. "Feeding a printed antenna via a coaxial probe has long been established as the most robust means of coupling power to and from a microstrip patch. This coupling technique also provides excellent isolation between the components of the feeding network (e.g. phase shifters and amplifiers) and the radiating elements, reducing the likelihood of spurious coupling as well as unwanted back radiation, Such requirements are critical when developing arrays positioned back to back as in typical mobile communications base station environments" [13]. Only probe-fed patch antennas are considered in this thesis. The bandwidth of such a patch antenna, and indeed those used with other feeding mechanisms, is dominated by the impedance variation (and hence mismatch) observed on the feed-line [8]. This variation is due to a combination of the inherent resonator-like properties of the patch and the properties of the feed mechanism. The use of thick substrates provides the most direct way of obtaining increased bandwidth as far as the inherent properties of the patch are concerned. However, when we attempt to use the

probe-feed option with a thick substrate the increased probe length adds an additional input inductance that serves to cause an impedance mismatch that then limits the bandwidth. In recent years there has been considerable work done to overcome these bandwidth limitations of probe-fed microstrip patch antennas. However, less effort has been expended on categorizing the techniques used to do this, with the result that the impression is one of unstructured cut-and-try research. Furthermore, there has been a tendency to declare increased impedance bandwidth without simultaneously monitoring the realized gain, antenna efficiency, radiation efficiency and radiation pattern performance.

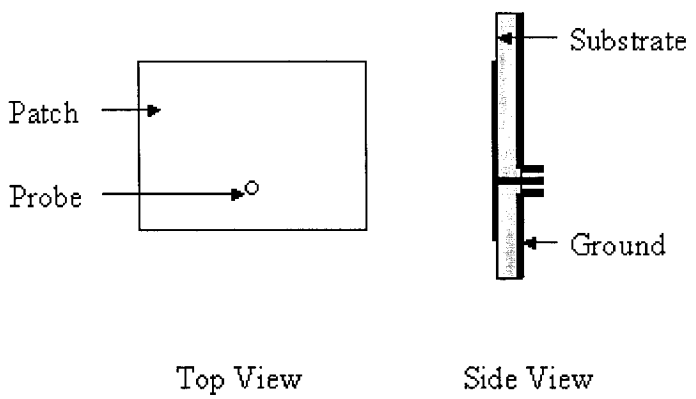

Figure 1.1 : Traditional Probe-Fed Microstrip Patch Antenna

1.2 THESIS OBJECTIVES AND OVERVIEW

The aim of this thesis is to explore and classify the techniques that have been used to increase the bandwidth of probe-fed microstrip patch antennas. One of the greatest difficulties was the extremely large amount of literature on the subject. Two of the early pioneers in pre-microstrip antennas have remarked that the "classification of antennas

into mutually exclusive types is impossible, for we can look at the same antenna from different points of view" [12]. It became evident in the literature survey conducted as part of the work of this thesis that this is almost true for microstrip patch antennas! Nonetheless, we have succeeded in sensibly grouping bandwidth enhancement techniques for probe-fed microstrip patch antennas into two major classes that are further broken down into sub-classes. This has made it significantly easier to relate the work of many authors and to be able to place new work into context. Full-wave analyses have been done of very many patch antenna configurations described by other authors. However, through the understanding afforded by this exercise, we have been able to select one particular example from each sub-class, whose complete computed performance is described in Chapter 3. These examples have been selected such that they are most representative of each of their sub-classes. The same full-wave electromagnetic analysis method is used for all the cases considered in order to allow an "unprejudiced" comparison of their effectiveness. We have found that many authors only provide a limited number of the important performance parameters for the particular antenna configuration they are discussing; here we have provided a complete set of such parameters for all the examples considered. The large amount of data presented in Chapter 3 has been succinctly collected and summarised in tabular form in Chapter 4, to allow a designer to do a proper trade-off selection on the best broadband probe-fed microstrip patch antenna for a particular application. In Chapter 4 we also demonstrate how the increased understanding afforded by the classification of the broadbanding techniques can be used to devise further improvements. In the process we demonstrate the performance of novel antenna that has not previously been described in the literature.

Chapter 2 provides brief technical information on probe-fed microstrip patch antennas that facilitates the discussion in Chapters 3 and 4.

Chapter 5 consists of some general conclusions and suggestions for future work.

1.3 REFERENCES FOR CHAPTER 1

[1] G. A. Deschamps, "Microstrip microwave antennas", 3rd USAF Symp. on Antennas, 1953.

[2] D. D. Greig and H. F. Engleman, "Microstrip – A new transmission technique for the kilomegacycle range", Proc. IRE, pp. 1644-1650, 1952.

[3] I.J. Bahl and P. Bhartia, Microstrip Antennas (Artech House Inc., 1980).

[4] J.R.James, P.S.Hall and C.Wood, Microstrip Antenna Theory and Design (Peter Peregrinus, 1981).

[5] J.R.James and P.S.Hall (Edits.), Handbook of Microstrip Antennas (Peter Peregrinus, 1989).

[6] P.Bhartia, K.V.S.Rao and R.S.Tomar, Millimeter-Wave Microstrip and Printed Circuit Antennas (Artech House, 1991)

[7] D. M. Pozar, "Microstrip antennas", Proc. IEEE, vol. 80, pp. 79–91, Jan. 1992.

[8] D.M.Pozar and D.H.Schaubert (Edits.), Microstrip Antennas: The Analysis and Design of Microstrip Antennas and Arrays (IEEE Press, 1995).

[9] R.Garg, P.Bhartia, I.Bahl and A.Ittipiboon, Microstrip Antenna Design Handbook (Artech House, 2000).

[10] K. L. Wong, Compact and Broadband Microstrip Antennas (Wiley, 2002).

[11] R.Waterhouse, "Microstrip Patch Antennas", Chap.6 in: L.C.Godara (Edit.), Handbook of Antennas in Wireless Communications (CRC Press, 2002).

[12] S.A.Schelkunoff & H.T. Friis, Antennas: Theory and Practice (Wiley, 1952) p.537

[13] D.M.Kokotoff, J.T.Aberle & R.B.Waterhouse, "Rigorous analysis of probe-fed printed annular ring antennas", IEEE Trans. Antennas Propagat., Vol.47, No.2, pp.384-388, Feb.1999.

[14] K.F.Lee & W.Chen, Advances in Microstrip and Printed Antennas (Wiley, 2002).

[15] K.C.Gupta & A.B.Norwood, Microstrip Antenna Design (Artech House, 1988).

CHAPTER 2

MICROSTRIP PATCH ANTENNA PRINCIPLES

2.1 INTRODUCTION

The primary purpose of this chapter is to review certain technical details and descriptions related to the subject of microstrip patch antennas that will facilitate the discussion of Chapter 3. Section 2.2 introduces the microstrip patch antenna concept. Section 2.3 presents an overview of the four types of feed mechanism used to inject a signal into, or extract a received signal from, microstrip patch antennas. Section 2.4 briefly discusses the electromagnetic modeling possibilities for microstrip patch antennas. Section 2.5 concludes the chapter with some definitions of some antenna performance parameters that will be examined in later chapters.

2.2 THE MICROSTRIP PATCH ANTENNA

The "traditional" microstrip patch antenna is shown in Figure 2.1, and consists of a rectangular conducting patch (of conductivity σ) printed on a dielectric substrate (of relative permittivity ε_r, loss tangent $tan\delta$ and thickness h) that is backed by a conducting groundplane [1,2,3].

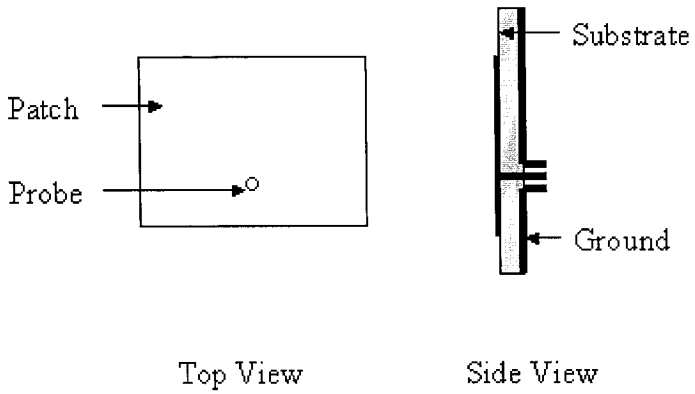

Figure 2.1 : Traditional Rectangular Microstrip Patch Antenna

We consider the radiation as being due to the currents on the conducting patch radiating in the presence of the substrate and the groundplane. The patch can be thought of as a resonator. It is lossy due to the fact that: (a). the conductors have a finite conductivity; (b). the substrate has a non-zero loss tangent and (c). some of the input power propagates away from the patch as a guided surface wave mode(s) of the substrate/ground plane. It is an open cavity, and thus we might expect radiation to take place. It is the fact that this "space wave" is launched that allows it to be used as an antenna. Although patches of rectangular shape are the most common, any shape can be used [2]. Circular, elliptical and triangular patches, as well as annular rings, have been used.

In order to inject a desired signal into the patch (transmissions) or extract it from the patch (reception) there has to be a feed mechanism that forms an interface between the patch and the transmission line feeding the antenna. This "traditional" microstrip configuration is illustrated in Figure 2.2.

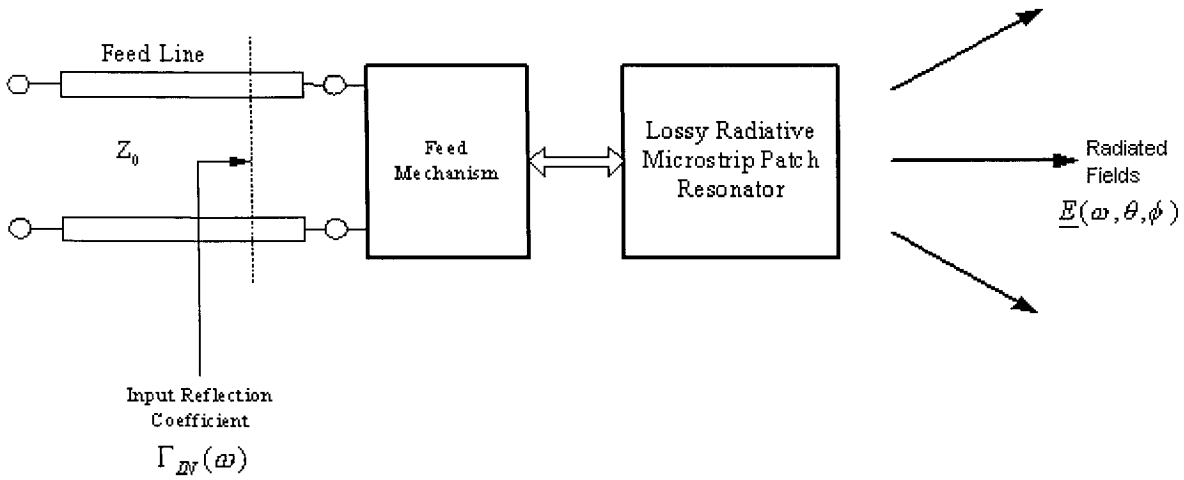

Figure 2.2 : Block Diagram of a "Traditional" Microstrip Patch Antenna

2.3 MICROSTRIP PATCH ANTENA FEED MECHANISMS

The four methods of feeding the traditional microstrip patch antenna are shown in Figure 2.3 through Figure 2.6, along with the appropriate dimensions and parameters [1]. The probe-fed case of Figure 2.3 in effect extends the inner conductor of a coaxial cable through the ground plane and connects it to the patch. The outer conductor of the coaxial line is connected to the ground plane. The microstrip line feed of Figure 2.4 consists of a microstrip transmission line that is connected to one of the edges of the patch (and thus is sometimes called an edge feed). In the aperture-coupled feed mechanism shown in Figure 2.5 the microstrip feed line and the patch are separated by the ground plane; coupling between the feed-line and the patch occurs through the slot in the ground plane. The proximity-coupled feed shown in Figure 2.6 has a microstrip feed-line that is printed on a

substrate layer between the ground plane and the patch. Coupling from the feed-line to the patch takes place simply due to their proximity to each other.

We indicated in Chapter 1 that the probe-fed case has a number of properties that render it very suitable for wireless base station applications. The fact that the feed network is completely separate from the patch means that there is less spurious radiation from the feed network compared to that when the microstrip line or proximity-coupled feed is used. The probe feed is also less sensitive to alignment errors than the aperture-coupled or proximity-coupled feed mechanisms. Furthermore, the fact that the probe is connected directly to the patch means that the antenna structure is quite robust. The probe-feed case has less backward radiation that the aperture-coupled case, something that is important when patches form the elements in back-to-back arrays used in wireless base stations. Finally, the probe-feed also has the advantage (in the intended applications) that it can be driven directly using a coaxial cable, something that, surprisingly, often makes things less expensive than when additional substrate layers are needed for the feed arrangement. Waterhouse [4] notes that, for the above reasons, there has been "a renaissance of the probe-fed-styled patch". In the remainder of this thesis the emphasis will be on probe-fed microstrip patch antennas.

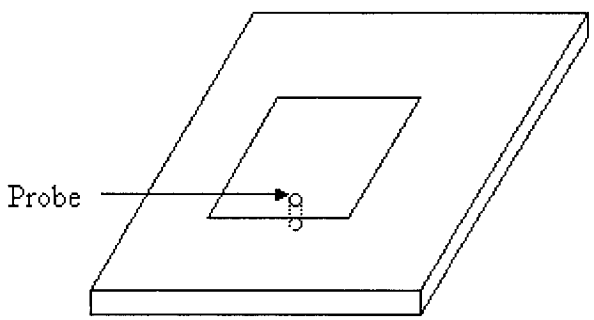

Figure 2.3 : Probe-Fed Microstrip Patch Antenna

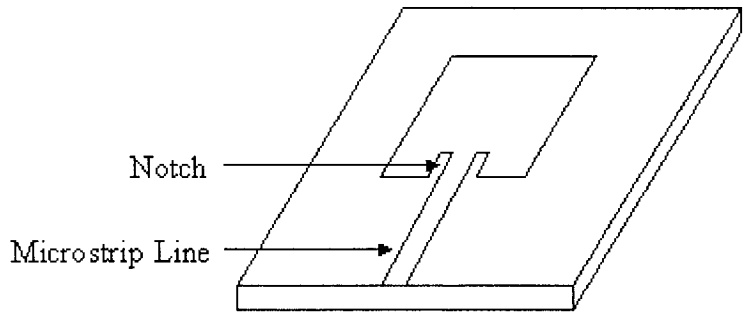

Figure 2.4 : Edge-Fed Microstrip Patch Antenna

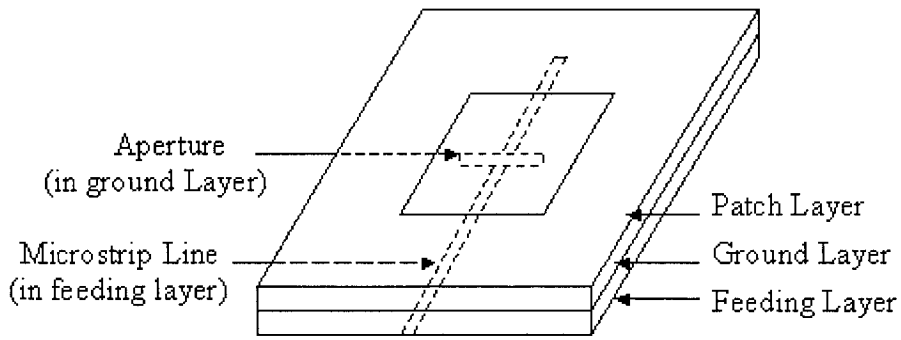

Figure 2.5 : Aperture-Coupled Microstrip Patch Antenna

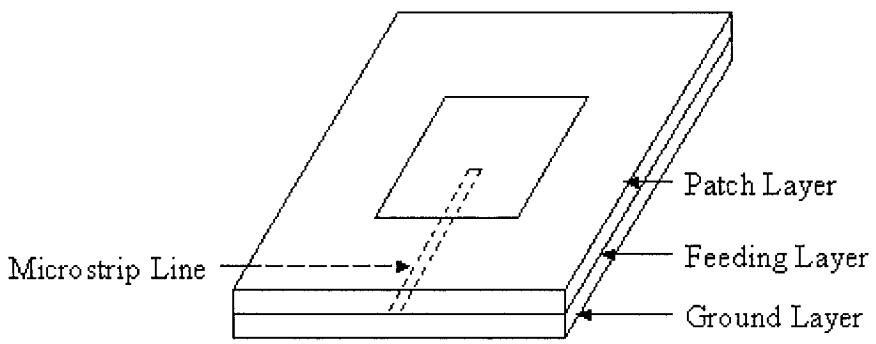

Figure 2.6 : Proximity-Coupled Microstrip Patch Antenna

2.4 THE ELECTROMAGNETIC MODELLING OF MICROSTRIP PATCH ANTENNAS

2.4.1 Detailed Geometry of the Traditional Rectangular Microstrip Patch Antenna

It will be useful for later reference to provide a dimensioned sketch of the traditional rectangular microstrip patch antenna and the radiation pattern coordinate system to be used. This is done in Figure 2.7.

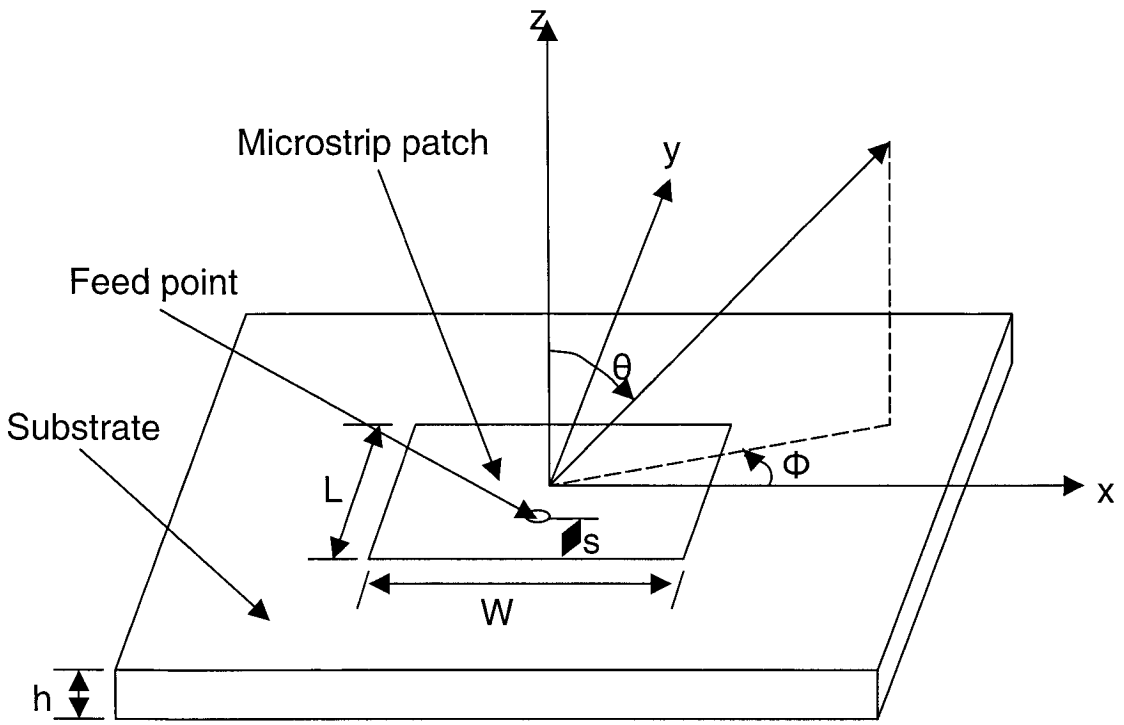

Figure 2.7 : Detailed Geometry of the Traditional Rectangular Probe-Fed Patch Antenna & Radiation Pattern Coordinates

2.4.2 Approximate Electromagnetic Modelling of Microstrip Patch Antennas

The two most useful approximate models for the microstrip patch antenna are the so-called cavity model [2,pp.212-214] and transmission line model [2,pp.205-211]. Although superseded (in terms of accuracy) by models based on numerical techniques, the cavity model is useful in terms of the physical understanding it affords, and the transmission line model in terms of the approximate expressions it provides for the initial design dimensions of the microstrip patch.

In the transmission line model the microstrip patch is considered to radiate from the fringing fields at the two edges of the patch (separated by the length L). This is equivalent to the radiation of two slots, one located at each of these edges. Thus the microstrip antenna is modeled as a transmission line terminated in two slots. In the cavity model the microstrip patch is modeled as a cavity with both electric and magnetic walls. The patch and the groundplane form electric walls on the top and bottom of the cavity. The sides of the cavity are considered to be magnetic walls, which would be exact if there were no fringing at the patch edges. For given centre (resonating) frequency f_0, substrate thickness h, and relative permittivity ε_r, the transmission line model provides expressions for the microstrip patch dimensions. The width is

$$W = \frac{c}{2f_0}\sqrt{\frac{2}{\varepsilon_r + 1}} \tag{2-1}$$

and the physical length

$$L = L_{eff} - 2\Delta L \tag{2-2}$$

The so-called electrical length L_{eff} is given by

$$L_{eff} = \frac{c}{2f_0\sqrt{\varepsilon_{eff}}} \tag{2-3}$$

The effective relative permittivity is determined using

$$\varepsilon_{eff} = \frac{\varepsilon_r + 1}{2} + \frac{\varepsilon_r - 1}{2}\left(1 + 10\frac{h}{W}\right)^{-1/2} \tag{2-4}$$

It accounts for the fact that the associated electromagnetic fields in the vicinity of the patch reside in both the substrate material and free-space (i.e. piecewise homogeneous region) and provides the effective relative permittivity of an equivalent homogenous region.. Because of the fringing field at the patch edges, the patch physical length should be shorter than its electrical length. The length extension is $2\Delta L$, where ΔL is given by

$$\Delta L = \frac{0.412h(\varepsilon_{eff} + 0.3)(\frac{W}{h} + 0.264)}{(\varepsilon_{eff} - 0.258)(\frac{W}{h} + 0.8)} \tag{2-5}$$

The distance between feed point and patch edge **s** will control the input resistance of the probe-fed patch. The approximate models provide the useful expression

$$R_{in}(s) = \frac{1}{2G_s}\cos^2(\frac{\pi}{L}s) \tag{2-6}$$

where

$$G_s = \frac{f_0 W}{120c}[1 - \frac{1}{24}(\frac{2\pi f_0 h}{c})^2] \tag{2-7}$$

Using above equations, the approximate initial values (to be "tweeked" using more complex modeling methods for best performance) of the microstrip antenna length L, width W, and probe location can be determined.

Table 2.1 : Definition of Symbols

Quantity	*Description*
x-Axis	Aligned along the antenna width.
y-Axis	Aligned along the antenna.
z-Axis	Aligned normal to the radiating patch.
(θ,ϕ)	Spherical coordinate angles.
L	Patch length.
W	Patch width.
h	Substrate height (thickness)
s	Distance between the probe attachment point and the edge of the patch
ε_r	Relative permittivity of substrate.
ε_{eff}	Effective relative permittivity of substrate.
f_0	Centre frequency.
c	Speed of light in a vacuum.

2.4.3 Full-Wave Electromagnetic Modelling of Microstrip Patch Antennas

The cavity and transmission line models rely on several assumptions being made about the microstrip patch antenna. These assumptions are not valid, and thus the above-mentioned approximate models fail, in the case of electrically thick substrates or substrates having high relative permittivities. More importantly, the approximate models are not able to model the geometrical modifications needed to render the microstrip patch antenna more broadband. It was thus necessary to use full-wave electromagnetic modeling in the present study. Fortunately, several frequency-domain commercial full-wave codes are available. The most widely used of these have been compared in [5] and

found to have comparable accuracies and run-times. In the case of probe-fed microstrip patches of the type with which this thesis will be principally concerned it appears that the code IE3D [6] provides the most accurate input reflection coefficient values, a quantity that is key to determining the impedance bandwidth of the antennas. There have also been very many independent validations of the code IE3D through comparison with measured data. The conclusion is that it can be used with confidence in design work requiring the comparison between microstrip patch antennas, whose geometries have been altered in efforts to achieve wide bandwidth, and without the need for continual experimental confirmation. We have therefore used the code IE3D in all the computations reported in the thesis. All ground planes are of finite size, and conductors are chosen to be copper (with a finite conductivity = 5.6×10^{8}s) As further confirmation we will, in Chapter 3, provide reference to such experimental validation for each of the classes of microstrip patch antennas to be evaluated in the thesis. In concluding, we mention that finite-difference time-domain (FDTD) commercial codes that can be used for patch antenna modeling are also available. These have not been used in this thesis.

2.5 DEFINITIONS OF MICROSTRIP ANTENNA PERFORMANCE PARAMETERS

There are many parameters that must be used to fully evaluate antenna performance. In the case of the microstrip patch antenna the most important are bandwidth, realized gain, antenna efficiency, radiation efficiency and radiation patterns. The definition of each of these quantities is provided here [7]:

(a). Bandwidth : The range of frequencies within which the performance of the antenna, with the respect to some characteristics, conforms to a specific standard. It includes two main factors, input impedance bandwidth and pattern bandwidth. The bandwidth of the microstrip antenna is mainly limited by the input impedance/reflection coefficient variation [1]. ***In this thesis, by the term bandwidth we mean the input impedance bandwidth, and consider it to be that range of frequencies over which the return loss is less than -10 dB.*** We define the return loss as $10\log|\Gamma_{IN}(\omega)|$ (without a minus sign), where $|\Gamma_{IN}(\omega)|$ is the magnitude of the input reflection coefficient.

(b). Realized Gain : The gain of the antenna reduced by the losses due to the mismatch of the antenna impedance to a specified feedline impedance, namely $10\log\left\{1-|\Gamma_{IN}(\omega)|^2\right\}$.

(c). Antenna Efficiency : The ratio of the total power radiated by the antenna to the net power sent to (i.e. incident on) the input port.

(d). Radiation Efficiency : The ratio of the total power radiated by the antenna to the net power accepted by the antenna from the connected transmitter.

(e). Radiation Pattern : The spatial distribution of a quantity that characterizes the electromagnetic field generated by an antenna. (Normally, two radiation patterns containing the principal E-plane and H-plane are used to describe an antenna's radiation performance.)

(f). Co-Polarization : The polarization that the antenna is intended to radiate.

(g). Cross-Polarization : In a specified plane containing the reference application ellipse, the polarization orthogonal to a specified reference polarization.

2.6 REFERENCES FOR CHAPTER 2

[1] D. M. Pozar, "Microstrip antennas", Proc. IEEE, vol. 80, pp. 79–91, Jan. 1992.

[2] D.M.Pozar & D.H.Schaubert (Edits.), Microstrip Antennas : The Analysis and Design of Microstrip Antennas and Arrays (IEEE Press, 1995).

[3] J. R. James, P. S. Hall, "Handbook of microstrip antennas", IEE, Peter Peregrinus, 1989.

[4] R.Waterhouse, "Microstrip Patch Antennas", Chap.6 in : L.C.Godara (Edit.), Handbook of Antennas in Wireless Communications (CRC Press, 2002).

[5] D.M.Pozar, S.Duffy & N.Hercovici, "A comparison of commercial software packages for microstrip antenna analysis", IEEE International AP-S Symp. Digest, 2000 (Page Numbers Not Available on CD-ROM Digest).

[6] Zeland Software Inc., "IE3D User's Manual", http://www.zeland.com.

[7] IEEE Std 145-1993, "IEEE Standard Definitions of Terms for Antennas"

CHAPTER 3

BROADBAND PROBE-FED MICROSTRIP PATCH ANTENNA CONFIGURATIONS

3.1 INTRODUCTION

The descriptions in this chapter represent the culmination of a relatively exhaustive survey of the literature on bandwidth enhancement techniques for microstrip patch antennas. We have distilled the key concepts from this mass of information and have succeeded in sensibly dividing the approaches into two major classes that are further broken down into sub-classes. This will make it significantly easier to place new work into context. Full-wave analyses have been done of very many patch antenna configurations described by other authors. However, through the understanding afforded by this work, we have been able to select one particular example from each sub-class, whose complete computed performance is described. These have been selected such that they are most representative of each of their sub-classes.

Section 3.2 summarises, in a qualitative fashion, some of the basic principles extracted from the study of the copious literature on the subject. Section 3.3 considers the class of broadbanding methods that utilizes an electrically-thick low-permittivity substrate. Section 3.4 does the same thing for patch antennas that use electrically-thin high-permittivity dielectrics. Section 3.5 concludes the chapter.

3.2 QUALITATIVE CONSIDERATIONS FOR BANDWIDTH ENHANCEMENT

As noted in Section 2.2, the microstrip patch can be considered as being a lossy radiative resonator. We would thus expect to obtain a wider impedance bandwidth if the effective quality factor of the resonator could be decreased. Thus can be achieved by either allowing more power to radiate (which is of course desirable from an antenna point of view) or by purposefully using dissipative lossy materials. The use of especially lossy substrates is not good from an antenna performance point of view since it simply decreases the radiation efficiency. It will therefore not be considered here. Thus only the former suggestion is an option. Figure 3.1 illustrates that this can be achieved if we increase the substrate thickness. In essence the electromagnetic fields become less tightly bound as the substrate thickness increases and/or the relative permittivity decreases. We can conclude that electrically-thick low-permittivity substrates provide a direct way to increase microstrip patch antenna bandwidth. Although this is true, a further issue also needs to be examined. The substrate/ground plane geometry forms a waveguiding structure for surface waves. These can be excited by a microstrip patch in addition to the desired radiated space waves. Even though it is not being dissipated on the antenna structure, the power stolen by the surface waves lowers the radiation efficiency of the patch antenna. If we for the moment consider only the surface wave portion of the non-radiated (but nevertheless lost) power, we would arrive at a curve such as that shown in Figure 3.2. A higher surface wave efficiency requires a thinner substrate. Thus we cannot increase the bandwidth of the microstrip patch antenna by arbitrarily increasing the substrate thickness; at any rate the bandwidth. But an electrically thick substrate (albeit one that not so thick that surface waves destroy the radiation efficiency) used in

conjunction with the additional design strategies to be discussed in the sections that follow, is indeed able to provide the broadest bandwidth patch antennas with the best overall performance.

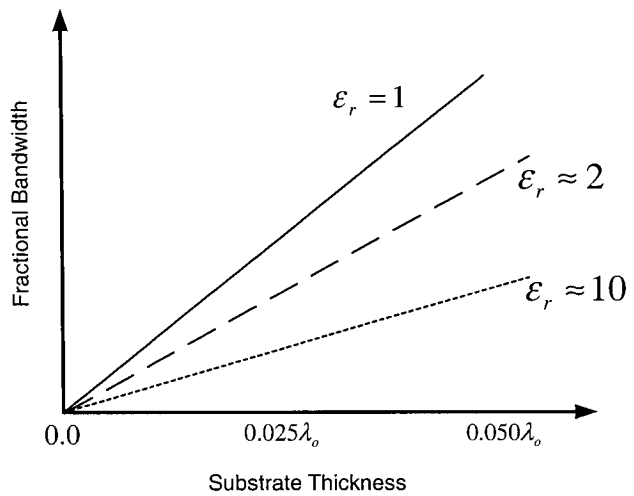

Figure 3.1 : Impedance Bandwidth (Return Loss < -10dB) for a Microstrip Patch Antenna Versus Substrate Electrical Thickness (Adapted from [1,pp.158]).

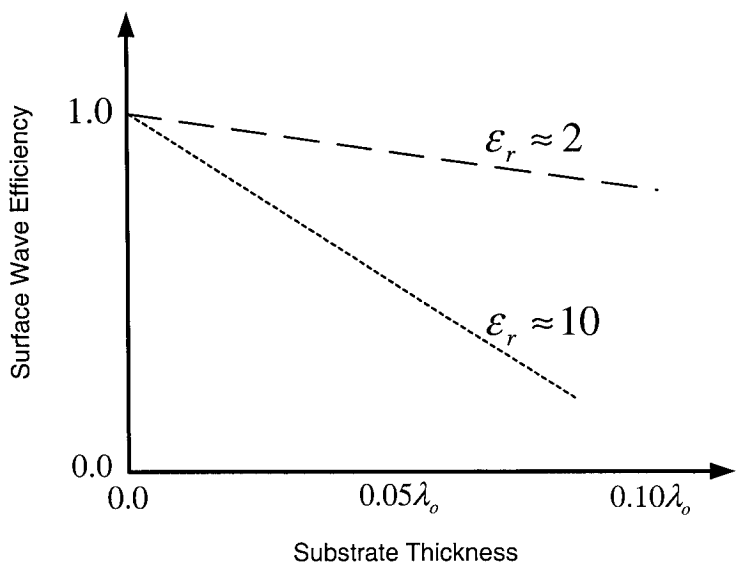

Figure 3.2 : Surface Wave Efficiency for a Microstrip Patch Antenna Versus Substrate Electrical Thickness (Adapted from [1,pp.158]).

In the IEEE Reprint Volume [1] published in 1995 (all of whose articles had appeared prior to 1995) these "additional design strategies" were divided into two approaches; one that uses multiple resonances and one that uses impedance matching. It is not surprising that in the intervening 10 year period there have been dozens of publications purporting to offer new bandwidth enhancement methods, and that as a result a more detailed classification is needed. Based on the literature study performed, we use the categorization shown in Figure 3.3. Although electrically-thick low-permittivity substrates (the first broad class) should be used for the best overall broadband performance, some applications dictate the use of electrically-thin high-permittivity substrates (the second broad class). In the latter situations some of the above-mentioned "additional strategies" provide increased impedance bandwidth but at the cost of lower radiation efficiency. We have divided the above two broad classes into sub-classes, once again based on the literature study. We next proceed to a detailed consideration of each of the sub-classes. Not only the impedance bandwidth, but also the realized gain, antenna efficiency, radiation efficiency *and* radiation pattern results (i.e. overall performance) will be presented. Figure 3.4 shows an embellished version of Figure 2.2; the embellishments will facilitate the description of the "additional strategies" in Sections 3.3 and 3.4.

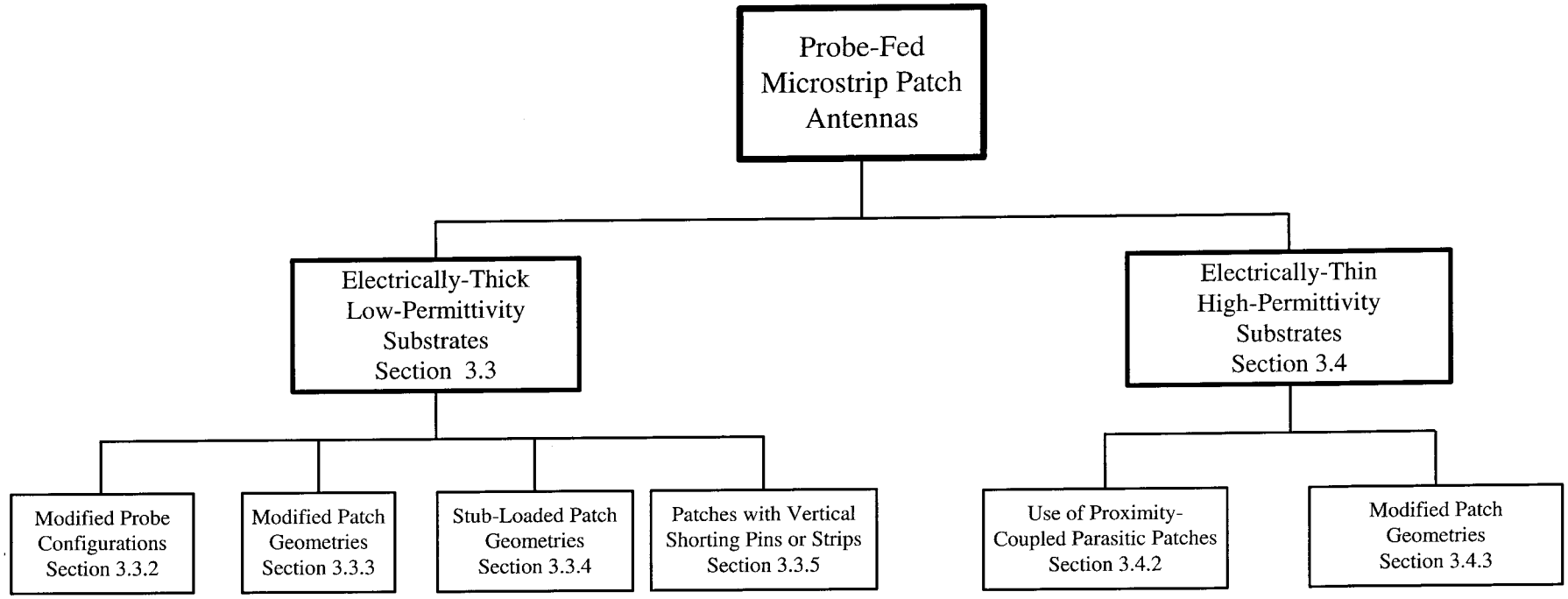

Figure 3.3 : Classification of Probe-Fed Microstrip Patch Antenna Bandwidth Enhancement Techniques

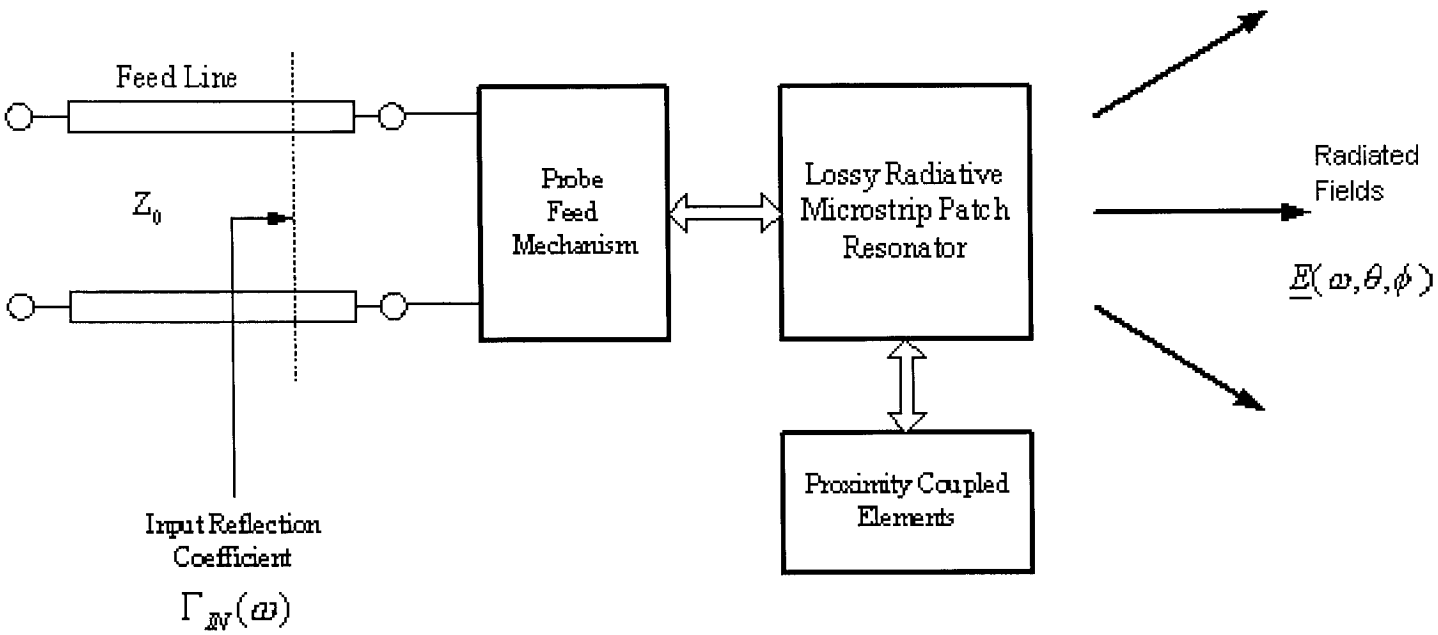

Figure 3.4: Block Diagram of a "Generalised" Probe-Fed Microstrip Patch Antenna

3.3 PROBE-FED MICROSTRIP PATCH ANTENNAS WITH ELECTRICALLY-THICK LOW-PERMITTIVITY SUBSTRATES

3.3.1 Preliminary Remarks

This section deals with strategies applicable to the broadbanding of patch antennas which have electrically-thick low-permittivity substrates. In practice such substrates are usually made of foam that is robust in spite of its low relative permittivity and light weight [2]. We consider each of the four strategies, delineated in Figure 3.3, in turn.

An examination of some of the computed radiation patterns shown reveals a rather sharp discontinuity at the pattern angles 0° and 180°. Clearly this is not physically possible. It is also clear that it is a code error in the IE3D (a fact that has been confirmed with the code developers) since even a cursory glance shows that it is a single pattern point "glitch" in an otherwise smooth radiation pattern.

3.3.2 Antennas with Modified Probe Geometries

A microstrip patch antenna on an electrically-thick low-permittivity substrate has the potential of being broadband. However, when such a thick substrate (on the order of $0.08\lambda_o$ to $0.10\lambda_o$) is used the probe will be electrically long. This adds additional inductance to the probe. The modified probe configuration strategy is to alter the shape of the probe and couple it to the patch capacitively rather than solder it directly to the patch. This added capacitance is then used to compensate for the additional inductance due to the probe length. Designs with T-shaped [4,5,8], L-shaped [6,7], and hook-shaped [10] probes have been proposed. These are illustrated in Figures 3.5, 3.6 and 3.7. The

performance of the geometry of Figure 3.7 is representative of this sub-class, and is the one whose computed performance will be presented.

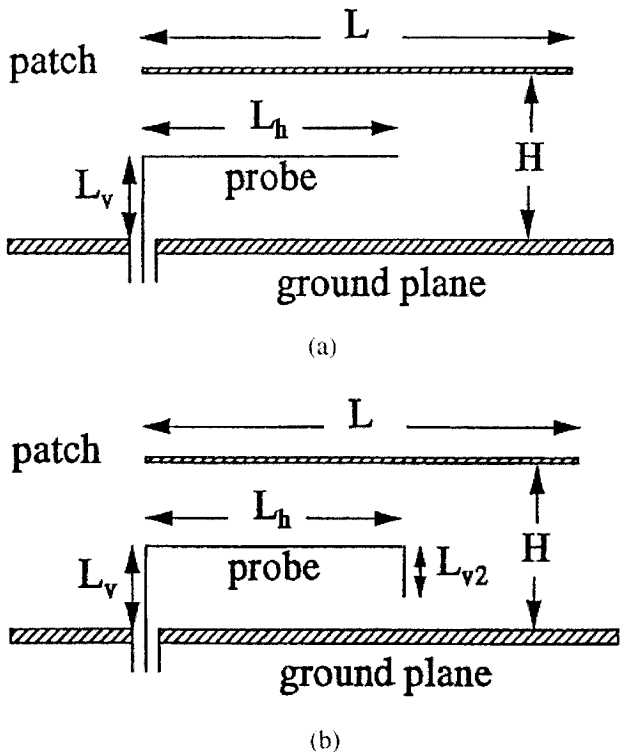

Figure 3.5 : Cross-Section of a Rectangular Microstrip Patch Antenna with an (a). L-Shaped Probe and (b). Hook-Shaped Probe. (After [10]).

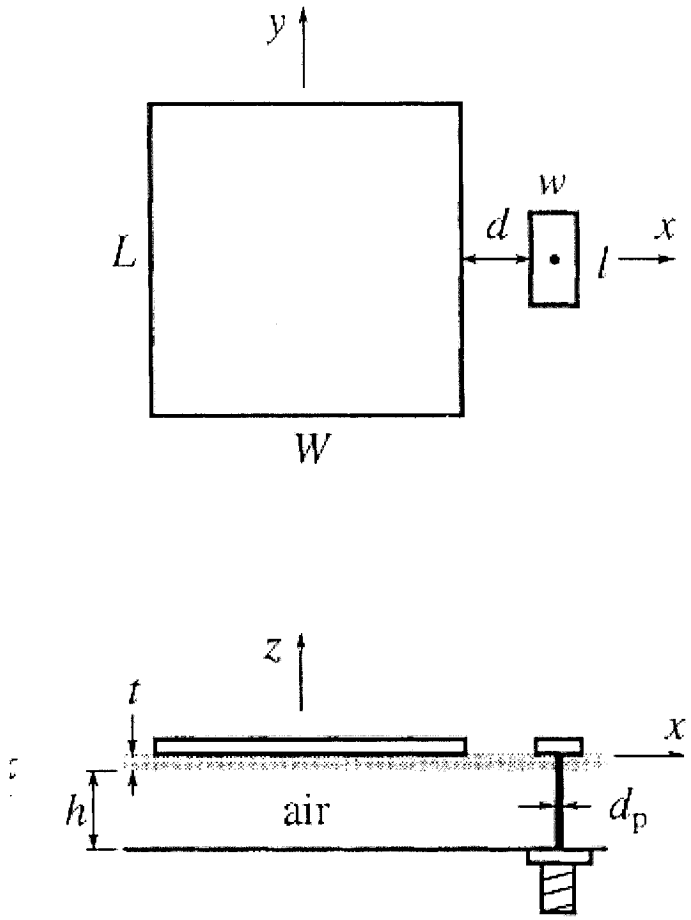

Figure 3.6 : Rectangular Microstrip Patch Antenna with a Single-Layer Capacitively Coupled Probe. (After [8]).

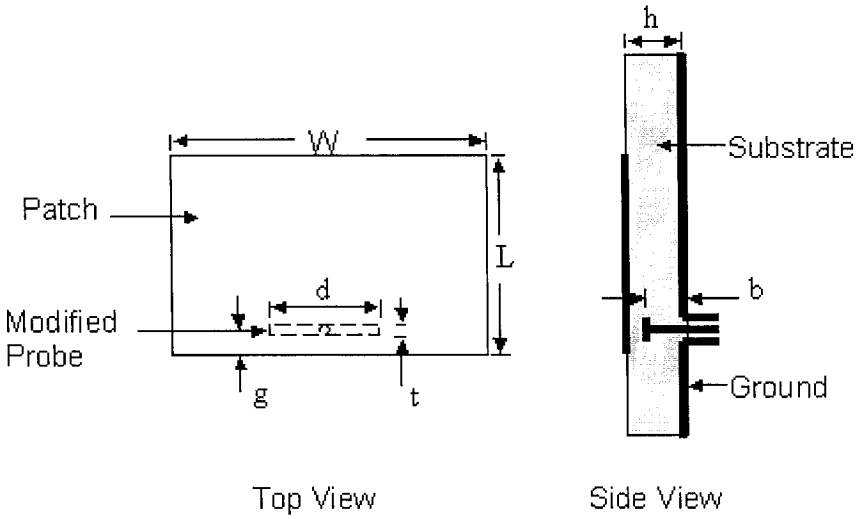

Figure 3.7 : Microstrip Patch Antenna with T-Shaped Probe

The dimensions of the antenna in Figure 3.7 are based on [4]. However, it has been manually optimized using a full-wave analysis to obtain the best performance in the vicinity of 4.5 GHz. The microstrip patch is a rectangle with 25 mm (length L) × 30 mm (width W). The substrate height (h) is 6.6 mm. The probe is a rectangle of size 1 mm (length t) × 11.2 mm (width d), and height (b) equal to 5.8 mm. It is located a distance 1mm (g) from the patch edge. The ground plane is a rectangle of dimensions 60 mm (length) × 60 mm (width). The whole substrate is made of foam (ε_r =1.08, tanδ = 0.001).

We have compared VSWR IE3D simulation result in Figure 3.9 to the measured result [4] in Figure 3.8. The good agreement serves to provide validation of the simulation results. The full-wave simulation results are shown in Figures 3.10 through 3.19. We observe that the return loss is less than -10 dB between 3.7 GHz and 5.5 GHz, implying an impedance bandwidth of 1.8 GHz, which is a fractional bandwidth of about 40% with respect to the center frequency of 4.5 GHz. As shown in Figure 3.11, the antenna realized gain varies between 7.5 dBi and 8.5 dBi over the above frequency band,

and is quite "flat". Figure 3.12 reveals that the antenna efficiency is between 85% and 95% over this same frequency range. Figure 3.13 shows that the radiation efficiency is between 91% and 98% over the operating band. The radiation patterns at 3.7 GHz, 4.5GHz and 5.1 GHz are shown in Figures 3.14 through 3.19. The E-plane co-polarization patterns are stable, with low cross polarization level over the operating band. The H-plane co-polarization patterns are also stable, but with the higher cross-polarization level characteristic of microstrip patch antennas.

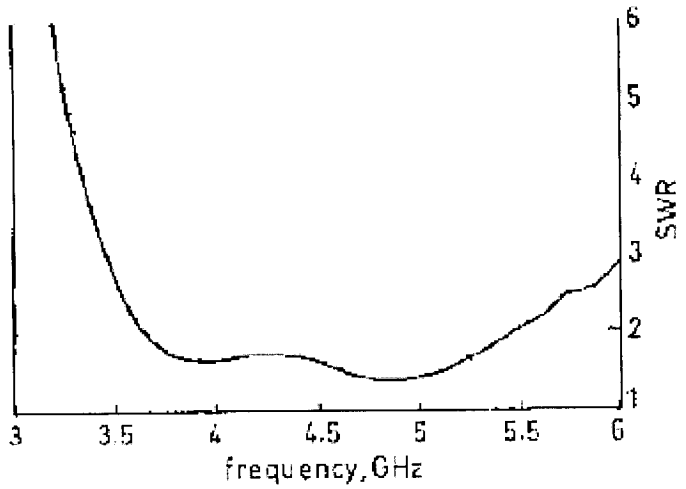

Figure 3.8 : VSWR Measured Result of Antenna with T-Shaped Probe (After [4])

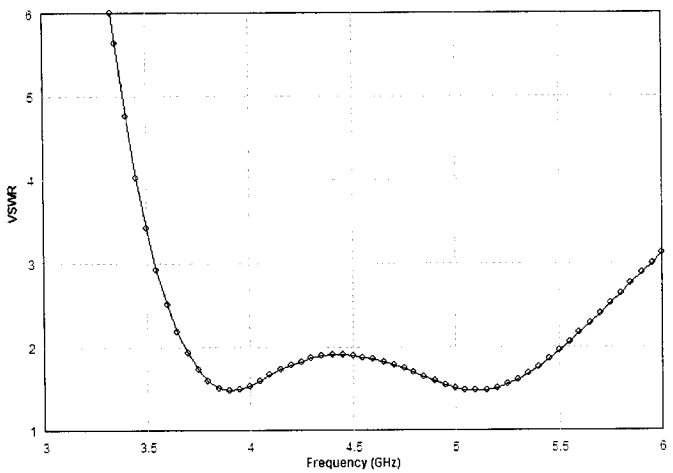

Figure 3.9 : VSWR Simulation Result of Antenna with T-Shaped Probe

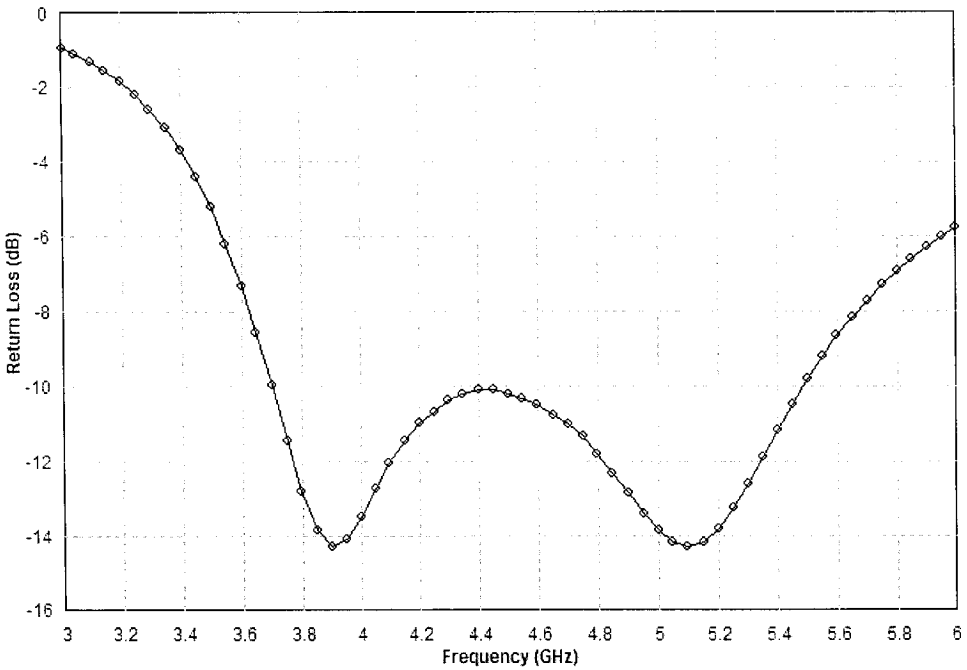

Figure 3.10 : Return Loss of Antenna with T-Shaped Probe

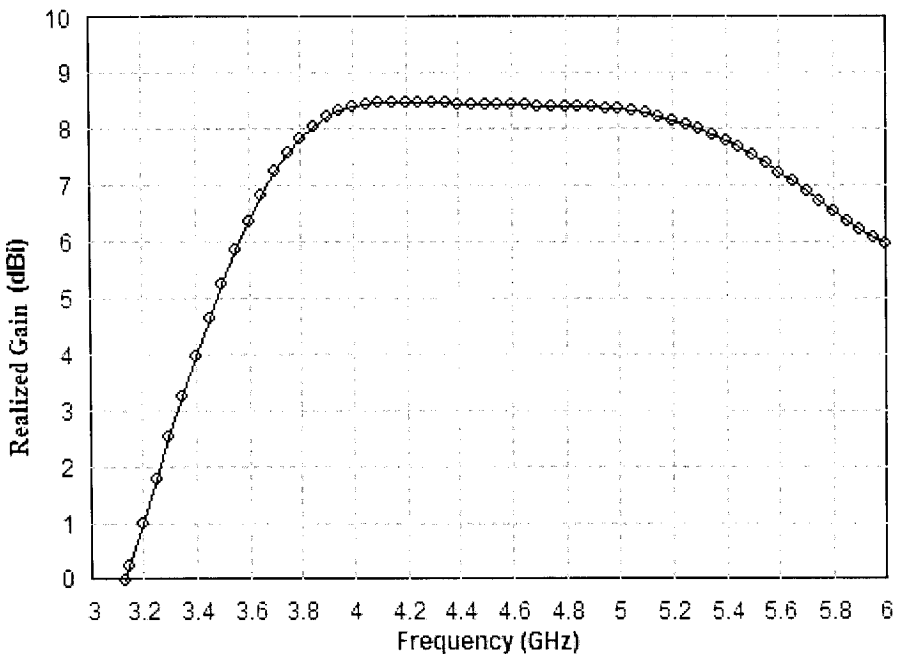

Figure 3.11 : Realized Gain of Antenna with T-Shaped Probe

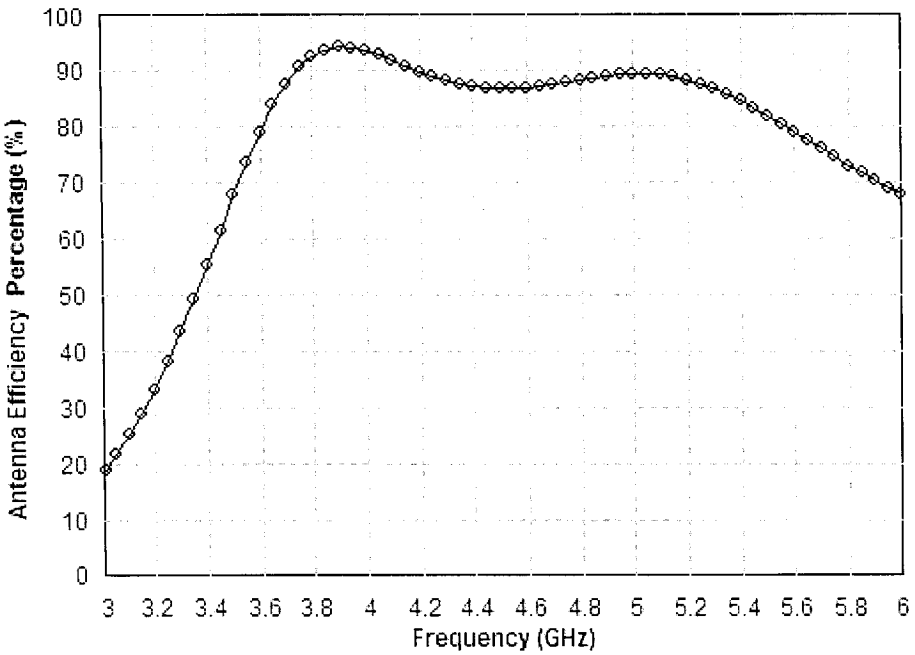

Figure 3.12 : Antenna Efficiency of Antenna with T-Shaped Probe

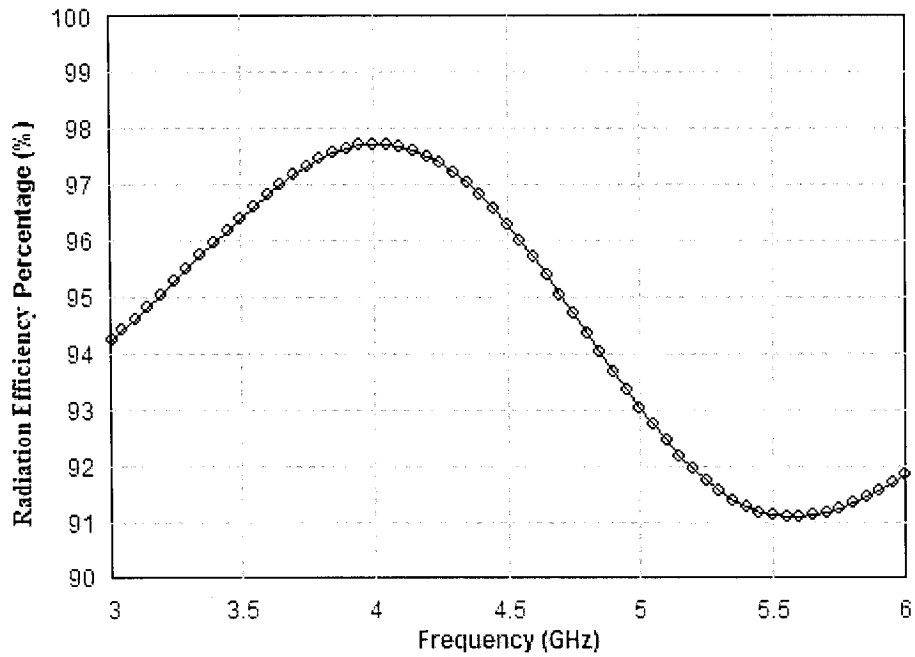

Figure 3.13 : Radiation Efficiency of Antenna with T-Shaped Probe

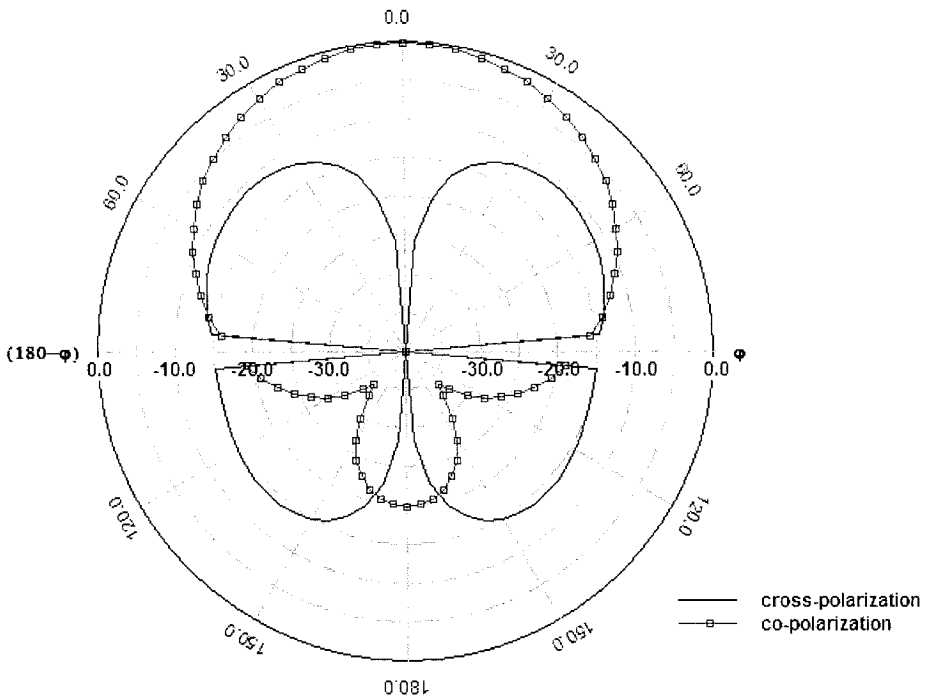

Figure 3.14 : **H-Plane Radiation Patterns of Antenna with T-Shaped Probe at 3.7GHz**

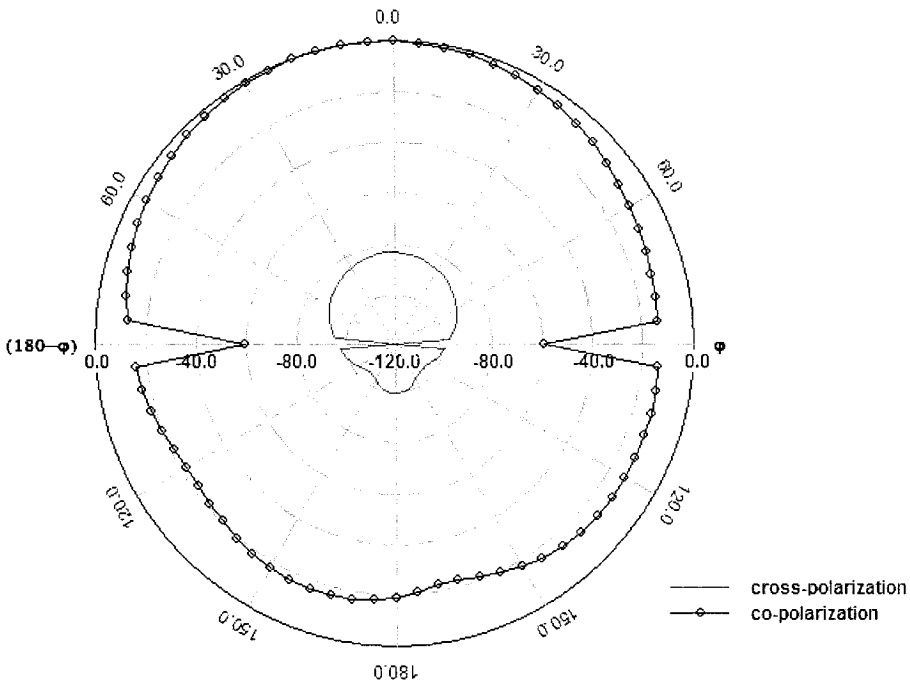

Figure 3.15 : **E-Plane Radiation Patterns of Antenna with T-Shaped Probe at 3.7 GHz**

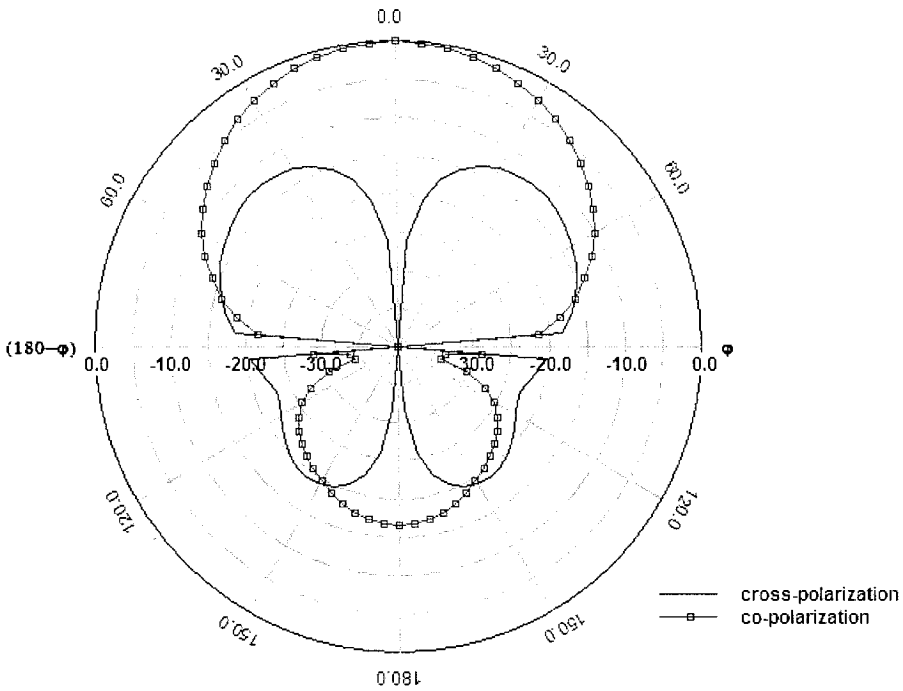

Figure 3.16 : H-Plane Radiation Patterns of Antenna with T-Shaped Probe at 4.5 GHz

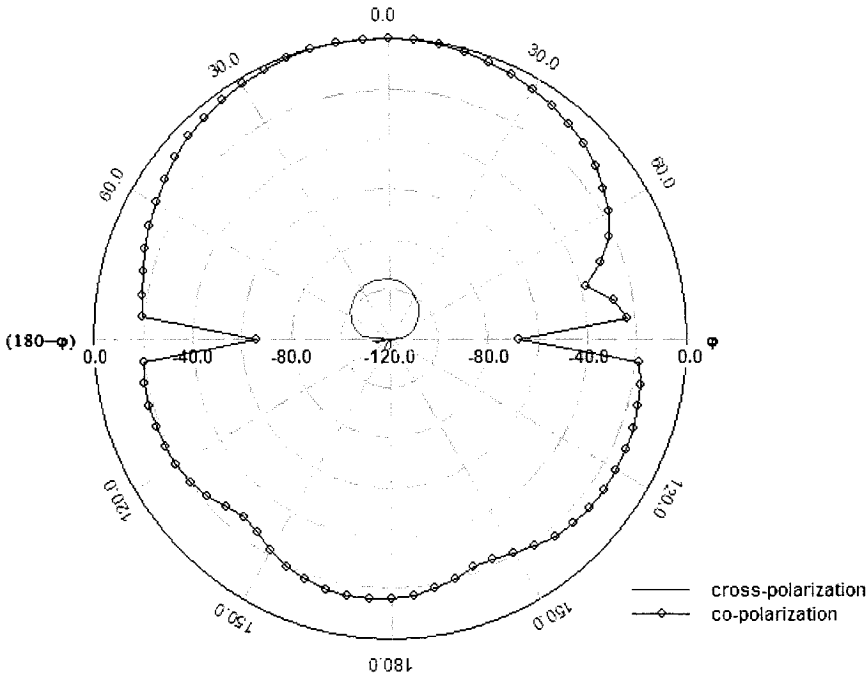

Figure 3.17 : E-Plane Radiation Patterns of Antenna with T-Shaped Probe at 4.5 GHz

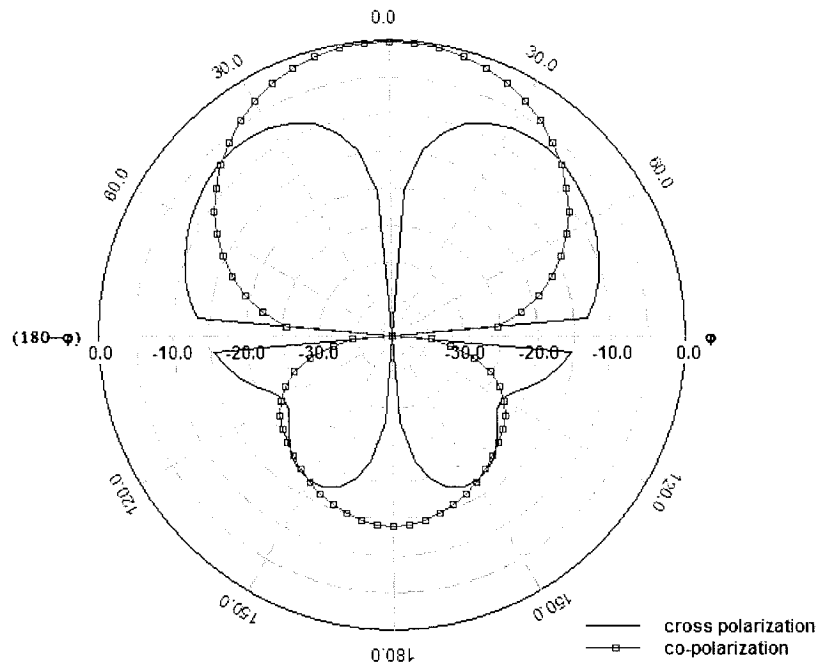

Figure 3.18 : H-Plane Radiation Patterns of Antenna with T-Shaped Probe at 5.1 GHz

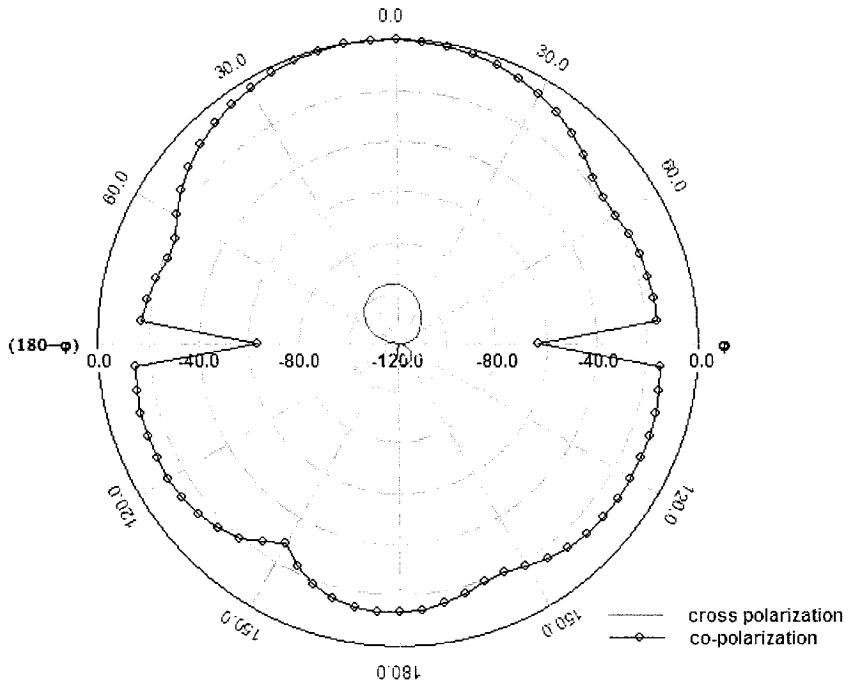

Figure 3.19 : E-Plane Radiation Patterns of Antenna with T-Shaped Probe at 5.1 GHz

Using the representative case of the T-shaped, and available performance information for other probe shapes, we can state that microstrip patch antennas which use electrically-thick low-permittivity substrates with modified probe configurations have the following overall performances :

- Bandwidth : Very Broad (> 35%)
- Realized Gain : High (Around 8 dBi)
- Antenna Efficiency : High (> 80%)
- Radiation Efficiency : High (> 90%)
- E-plane Radiation Pattern : Stable; Very low cross polarization level (cross-polarization < -80 dB relative to the maximum of co-polarization pattern).
- H-plane Radiation Pattern : Stable; High cross polarization level (at the high frequency end of the operating band the cross-polarization may reach -5dB relative to the maximum co-polarization level. To reduce the cross-polarization level, a more complicated feeding technology is needed [4].)

We have interpreted the increased bandwidth of this class of antenna in terms of capacitive compensation for the series inductance of the increased-length probe. But it is important to realize that, due the distributed nature of the capacitive coupling mechanism, the current distribution on the patch will also be altered. Thus while the equivalent circuit viewpoint of adding a capacitor in series with the probe inductance captures the principal effects, the impedance bandwidth is due also to the altered patch current distribution. It is not possible to separate the effects in a rigorous fashion. We will find that this is so for the other "additional strategies" to be discussed in what follows.

3.3.3 Antennas with Modified Patch Geometries

Changing the shape of the patch from rectangular to circular or triangular does not have a major influence on the bandwidth [1]. However, geometry changes which significantly re-route the currents on the patch can be used to achieve a wider bandwidth for probe-fed microstrip antennas through, in essence, changing the equivalent circuit if the patch resonator. An alternative valid view (the "multiple resonances" viewpoint) is that wider bandwidth is achievable because it is possible to alter the patch geometry so that two (or more) of the patch "cavity modes" have closely spaced resonating frequencies. Designs employing U-shaped slots [11,12,13,15], notched patches [14], capacitively coupled strips, and E-shaped patches [18,19,20] have been described. Some of these are illustrated in Figures 3.20 through 3.23, for which fractional bandwidths of up to 20% have been achieved. In the case of the E-shaped patch in Figure 3.24 bandwidths of between 20% and 30% have been reported [19]. We note that sometimes the classification of the patch antennas is not unique. For instance, the antenna in Figure 3.22 is in fact very similar to that in Figure 3.6; the mechanism is one of a T-shaped probe capacitively coupled to the patch. In Figure 3.22 the patch geometry has been altered though; hence its placement in the present sub-class.

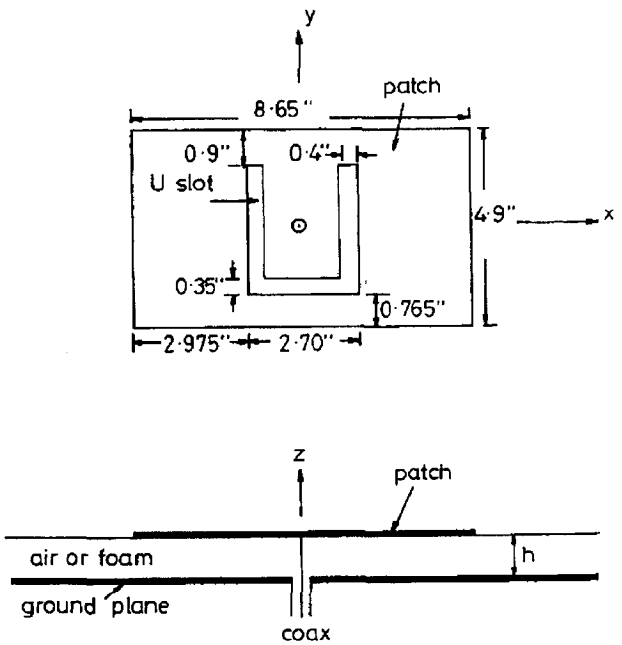

Figure 3.20 : Rectangular Microstrip Patch Antenna with a U-slot (After [11]).

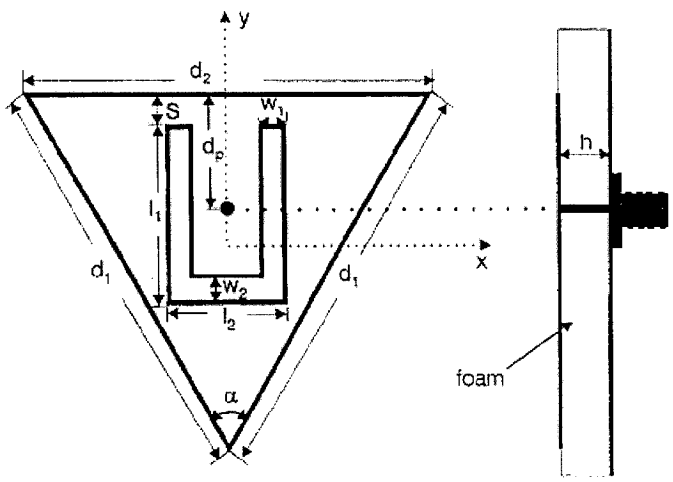

Figure 3.21 : Triangular Microstrip Patch Antenna with a U-slot. (After [13]).

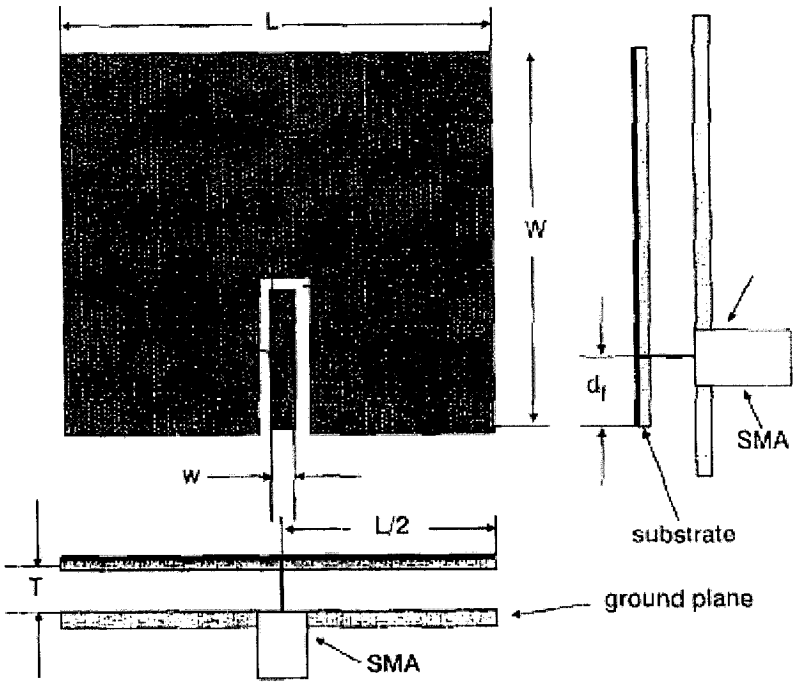

Figure 3.22 : Microstrip Patch Antenna with a Probe-Fed Capacitively Coupled Strip (After [16]).

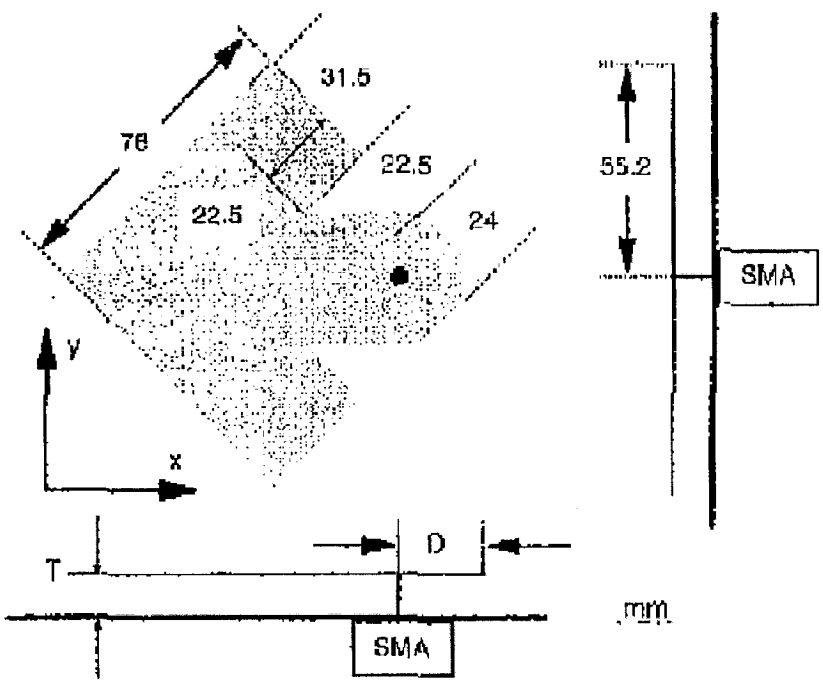

Figure 3.23 : Notched Microstrip Patch Antenna with a U-slot. (After [14]).

Figure 3.24 shows an antenna with E-shaped patch. The dimensions of the antenna are based on [19]. The antenna is designed to operate near 1.75 GHz. The microstrip patch is a rectangle with 65 mm (length L) × 105 mm (width W) at $0.08\lambda_o$=14.3mm (height h) with two slits. The slits are 47 mm (length t) × 6.3 mm (width d) each. The centre part of the patch is 15.3 mm width (c). The probe is 10 mm (g) from the edge. The ground plane is a rectangle with 150 mm × 150 mm. The whole substrate is made of air.

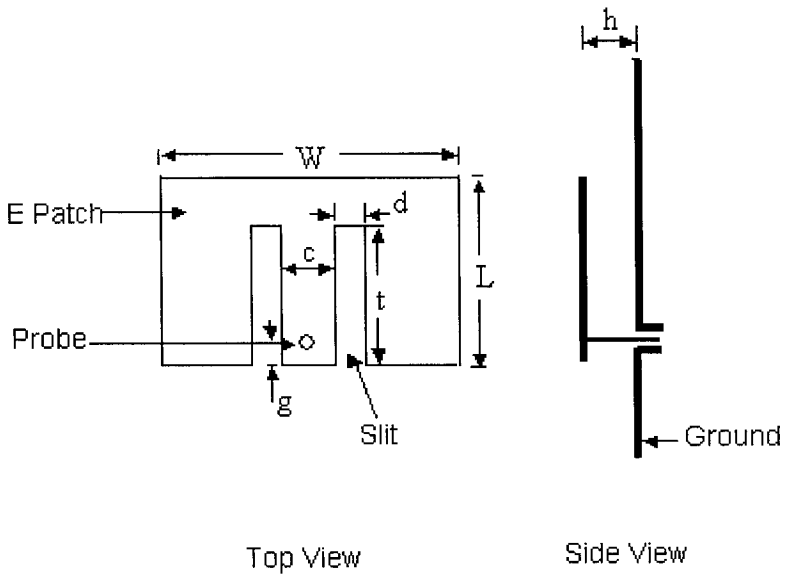

Figure 3.24 : Probe-Fed E-Shaped Patch Antenna

We have compared return loss IE3D simulation result in Figure 3.26 to the measured result [19] in Figure 3.25. There is only small frequency shifting from two results. The good agreement of the bandwidth serves to provide validation of the simulation results. The full-wave simulation results are shown in Figures 3.26 through 3.35. We observe that the return loss is less than -10 dB between 1.61 GHz and 1.93 GHz, implying an impedance bandwidth of 0.32 GHz, which is a fractional bandwidth of about 18% with respect to the center frequency of 1.75 GHz. As shown in Figure 3.27,

the antenna realized gain varies between 9 dBi and 9.5 dBi over the above frequency band, and is quite "flat". Figure 3.28 reveals that the antenna efficiency is above 90% over this same frequency range. Figure 3.29 shows that the radiation efficiency is around 99% over the operating band. The radiation patterns at 1.62 GHz, 1.74GHz and 1.92 GHz are shown in Figures 3.30 through 3.35. The E-plane co-polarization patterns are stable, with low cross polarization level over the operating band. The H-plane co-polarization patterns are also stable, but with the higher cross-polarization level characteristic of microstrip patch antennas.

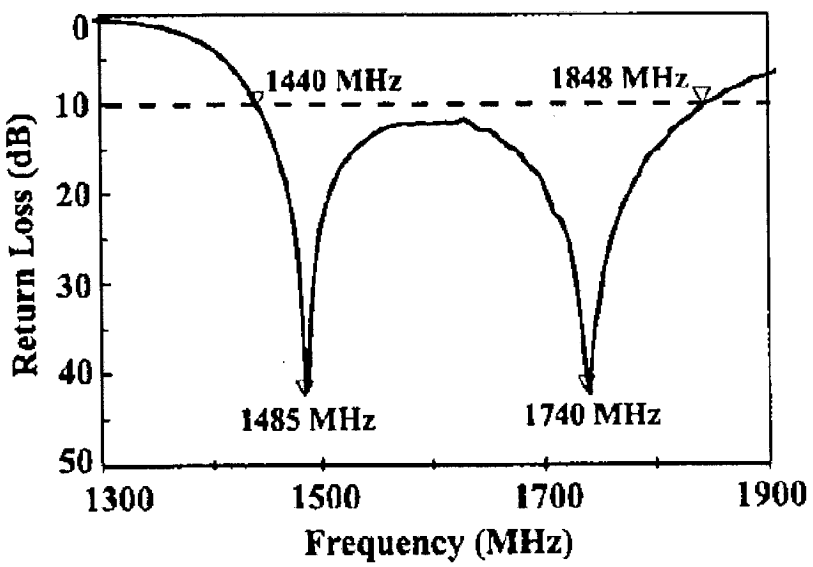

Figure 3.25 : Return Loss Measured Result of Antenna with E-Shaped Patch (After [19])

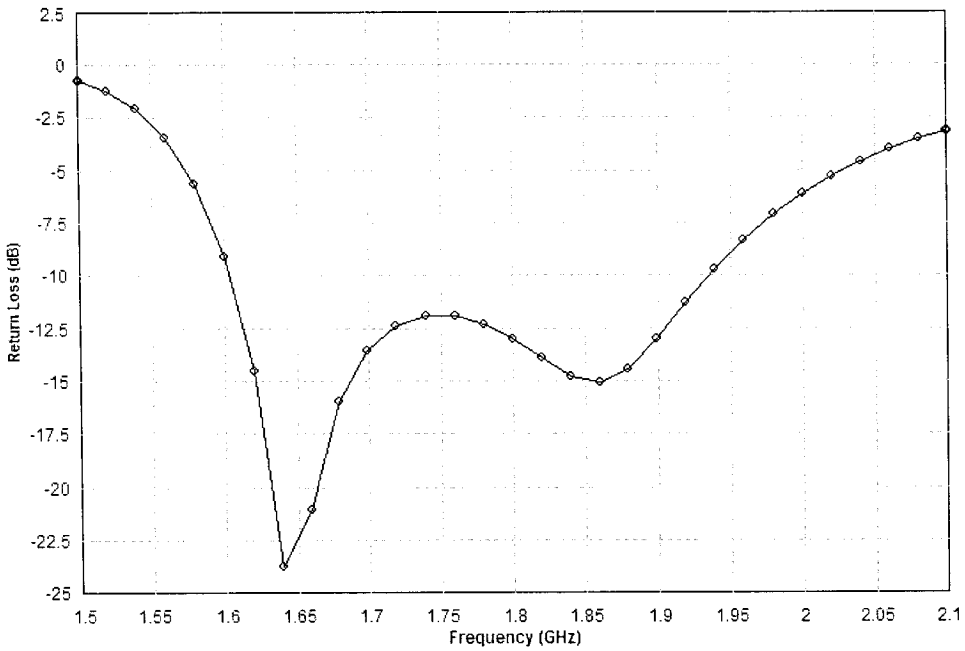

Figure 3.26 : Return Loss Simulation Result of Antenna with E-Shaped Patch

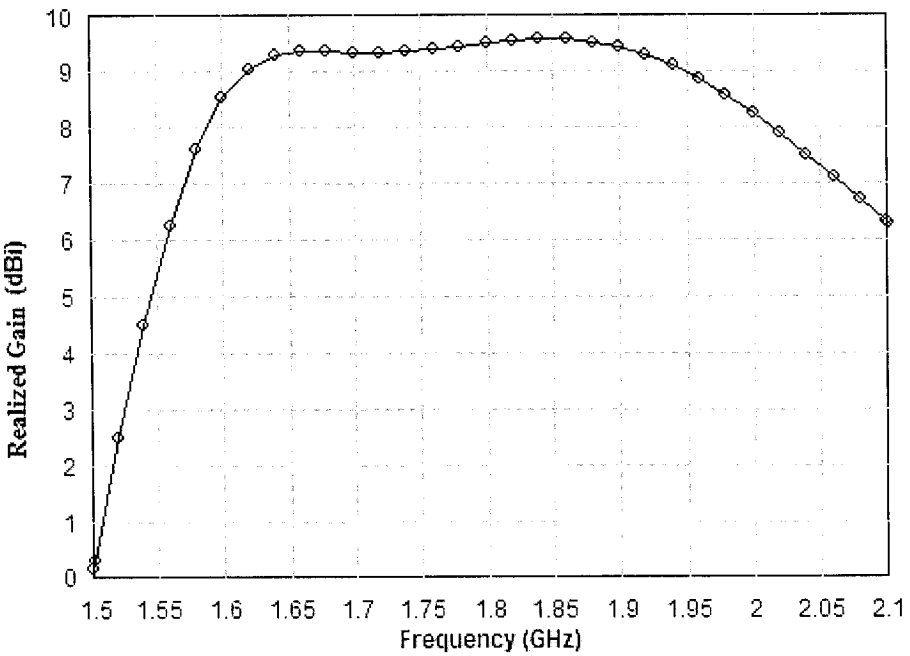

Figure 3.27 : Realized Gain of Antenna with E-Shaped Patch

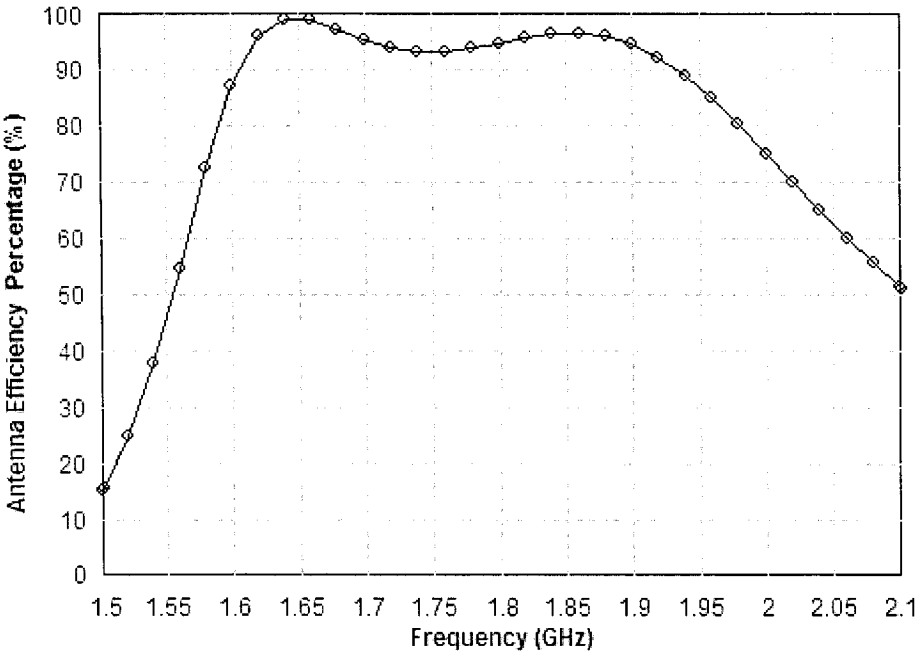

Figure 3.28 : Antenna Efficiency of Antenna with E-Shaped Patch

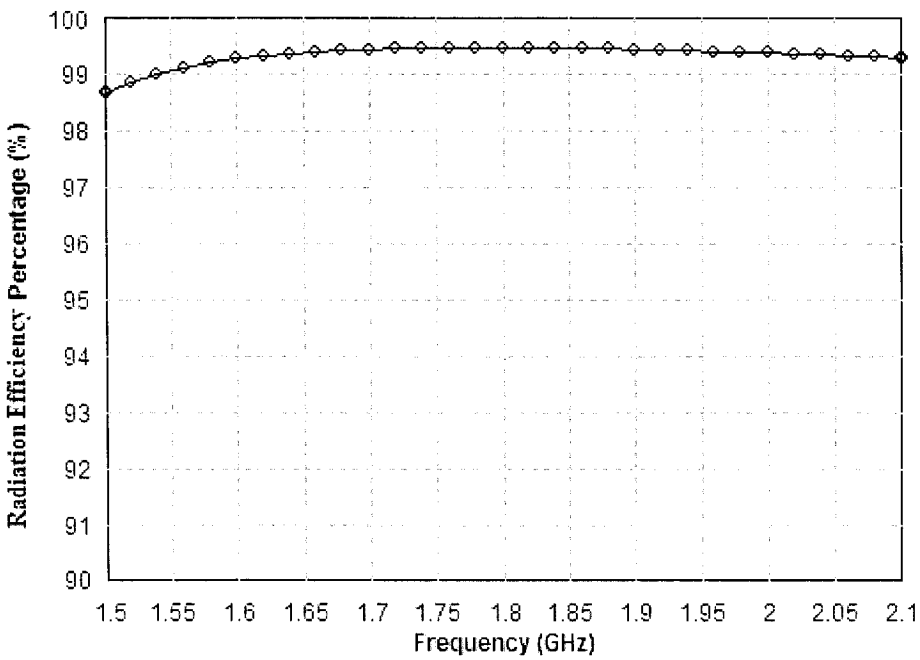

Figure 3.29 : Radiation Efficiency of Antenna with E-Shaped Patch

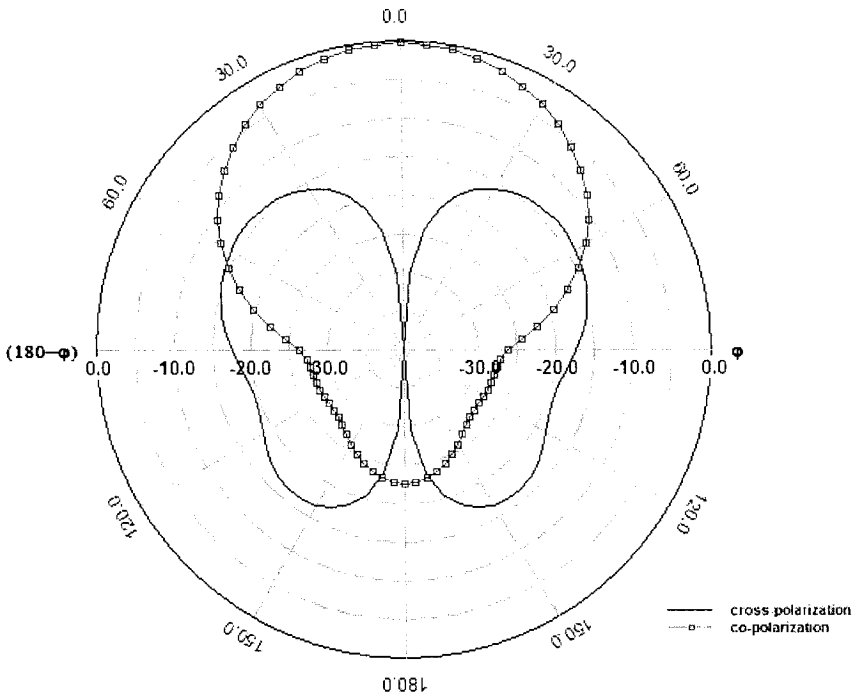

Figure 3.30 : H-Plane Radiation Patterns of Antenna with E-Shaped Patch at 1.62 GHz

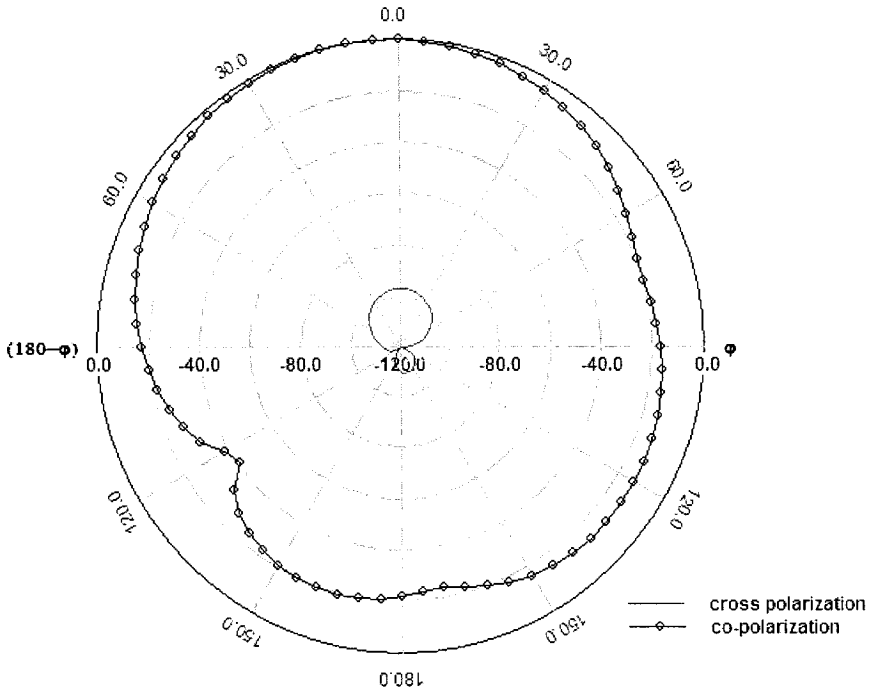

Figure 3.31 : E-Plane Radiation Patterns of Antenna with E-Shaped Patch at 1.62 GHz

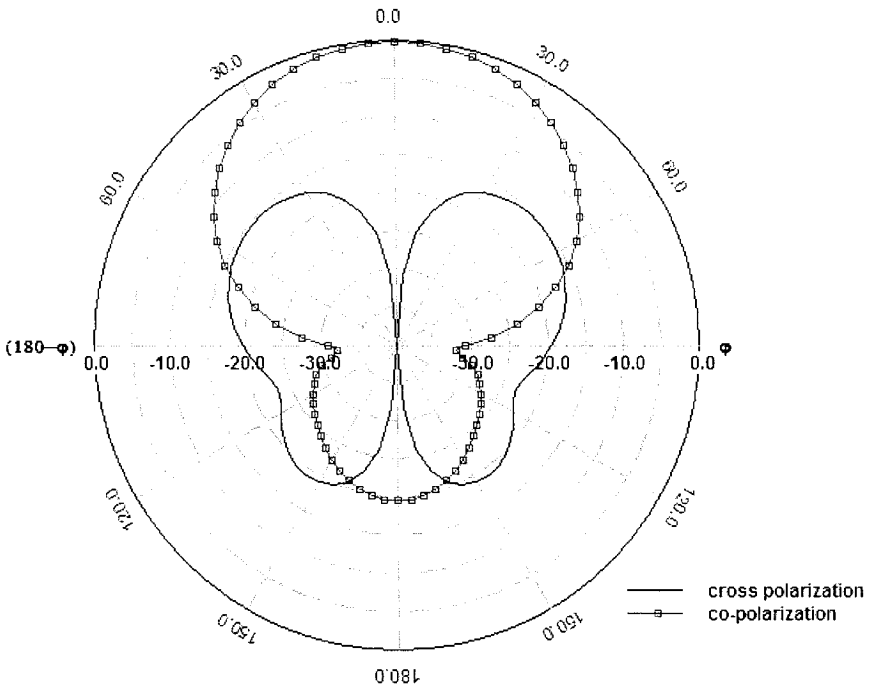

Figure 3.32 : H-Plane Radiation Patterns of Antenna with E-Shaped Patch at 1.74 GHz

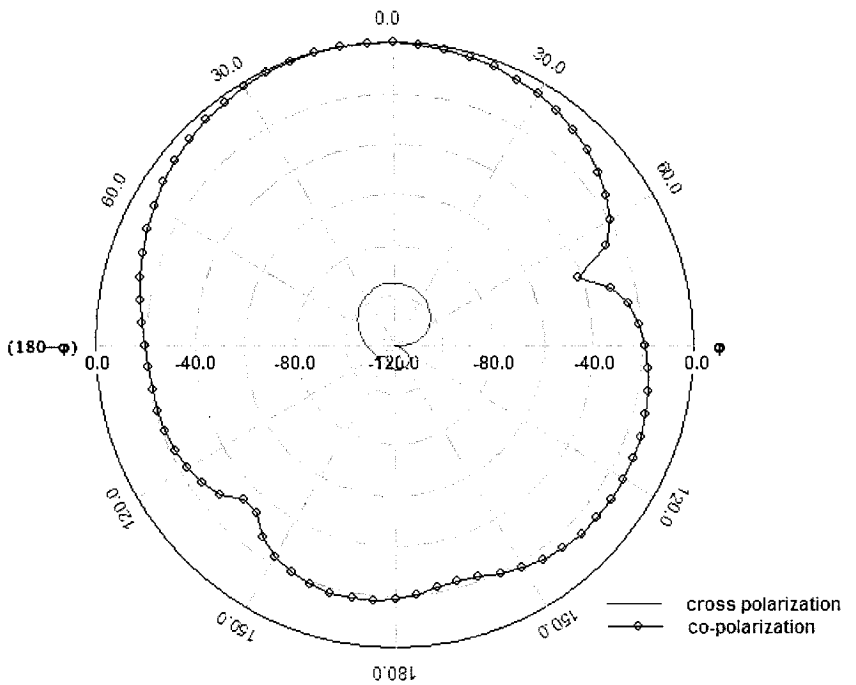

Figure 3.33 : E-Plane Radiation Patterns of Antenna with E-Shaped Patch at 1.74 GHz

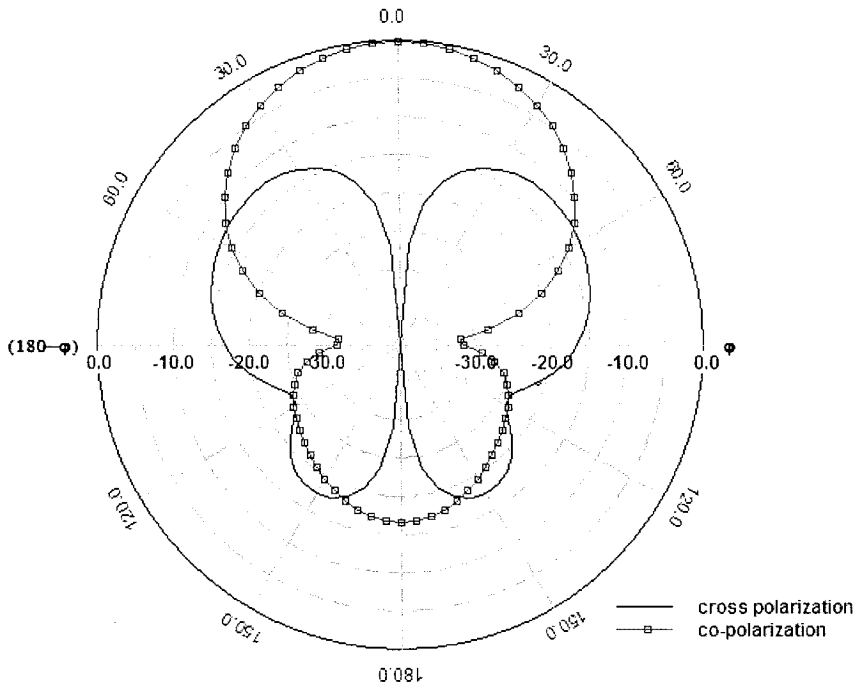

Figure 3.34 : H-Plane Radiation Patterns of Antenna with E-Shaped Patch at 1.92 GHz

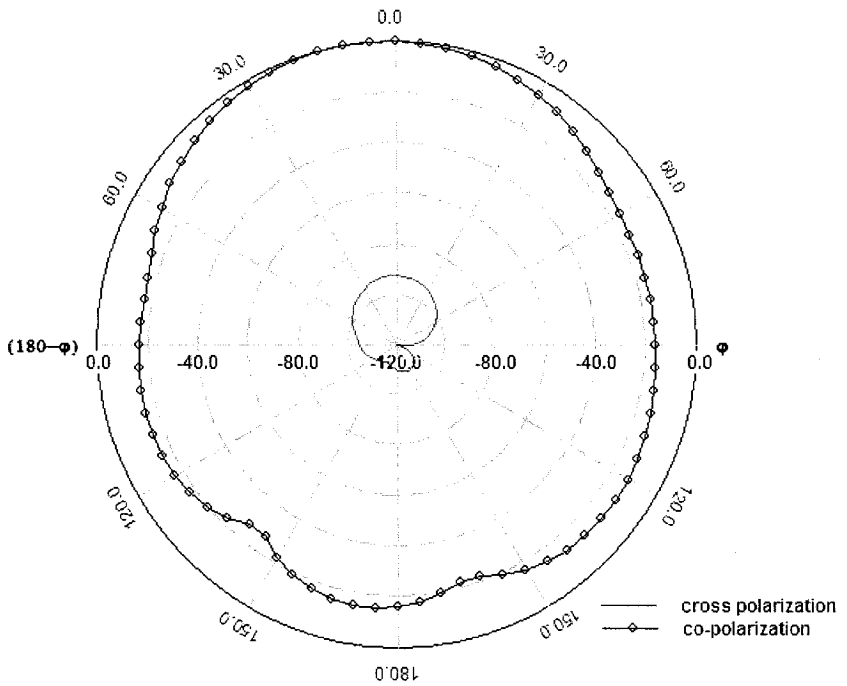

Figure 3.35 : E-Plane Radiation Patterns of Antenna with E-Shaped Patch at 1.92 GHz

Using this representative E-shaped patch case we can state that the "modified patch geometry" sub-class of microstrip patch antennas which use electrically-thick low-permittivity substrates have the following overall performances :

- Bandwidth: broad bandwidth, around 20%
- Realized gain: high, around 9 dBi
- Antenna efficiency: high, > 90%
- Radiation efficiency: high, > 90%
- E-plane radiation pattern: stable, very low cross polarization level (cross-polarization < -90 dB respect to the maximum of co-polarization)
- H-plane radiation pattern: stable, high cross polarization level (cross-polarization may reach -10dB respect to the maximum of co-polarization.)

We observe that the present "modified patch geometry" sub-class has an advantage over the "modified probe configuration" in that it is a single-layer antenna. Comments similar to those given at the end of Section 3.3.2 can be made here. Except for the situation in Figure 3.22, there is no physical alteration of the probe feed itself. It is only the patch geometry that changes. An examination of the current distribution on the patches provides an approximate interpretation (rather than a conventional rigorously determined equivalent circuit) of the behaviour in terms of a double resonance [18,24]. The altered patch geometry is apparently simultaneously providing this double resonance and compensating for the probe inductance. The multiple resonance interpretation is further supported by the fact that the location (in frequency) of these resonances can be altered by changing the length of the "legs" of the E-shaped patch [22].

3.3.4 Antennas with Stub-Loaded Patch Geometries

This technique has been used to broadband a microstrip patch antenna with an electrically-thick low-permittivity substrate [25], and illustrated in Figure 3.36. This could have been included in the sub-class "modified patch geometry" discussed in the previous section. However, the modification, namely an addition of a stub, represents such a well-known concept, that it makes sense to categorise it separately.

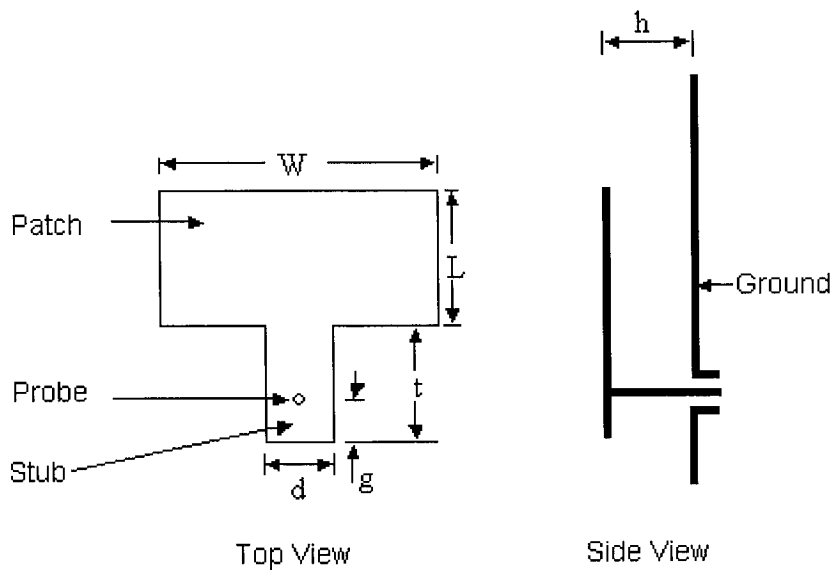

Figure 3.36 : Probe-Fed Rectangular Microstrip Partch Antenna with Stub

The antenna was designed to operate near 2.0 GHz. The dimensions of the antenna are based on [25], with some manual optimizations performed using the full-wave simulator. The radiating patch is 65 mm (length L) and 96 mm (width W). The stub is 37.5 mm (length t) × 16.7 mm (width d). The feed point is 17 mm (g) from the lower edge. The ground plane is 150 mm × 150 mm. The substrate is air of thickness 10 mm (h).

We have compared return loss IE3D simulation result in Figure 3.38 to the measured result [25] in Figure 3.37. The good agreement of the bandwidth serves to provide validation of the simulation results. The full-wave simulation results are shown in Figures 3.39 through 3.48. We observe that the return loss is less than -10 dB between 1.85 GHz and 2.25 GHz, implying an impedance bandwidth of 0.4 GHz, which is a fractional bandwidth of about 20% with respect to the center frequency of 2 GHz. As shown in Figure 3.40, the antenna realized gain varies between 8.5 dBi and 10 dBi over the above frequency band, and is quite "flat". Figure 3.41 reveals that the antenna efficiency is high than 85% over this same frequency range. Figure 3.42 shows that the radiation efficiency is around 99% over the operating band. The radiation patterns at 1.85 GHz, 2GHz and 2.2 GHz are shown in Figures 3.43 through 3.48. The E-plane co-polarization patterns are stable, with low cross polarization level over the operating band. The H-plane co-polarization patterns are also stable, but with the higher cross-polarization level characteristic of microstrip patch antennas.

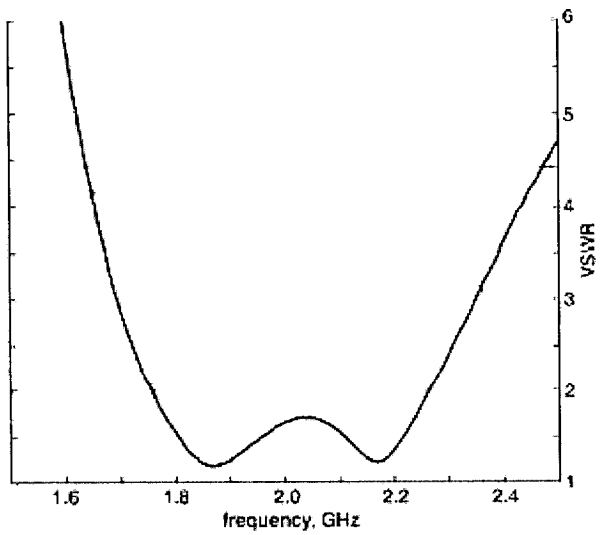

Figure 3.37 : VSWR Measured Result of Antenna with Stub (After [25])

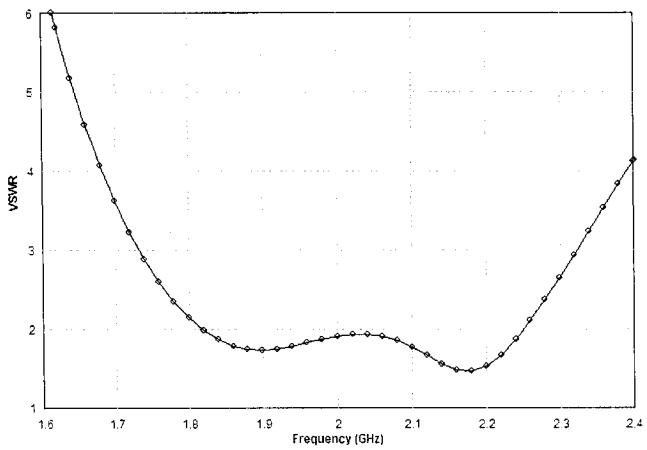

Figure 3.38 : VSWR Simulation Result of Antenna with Stub

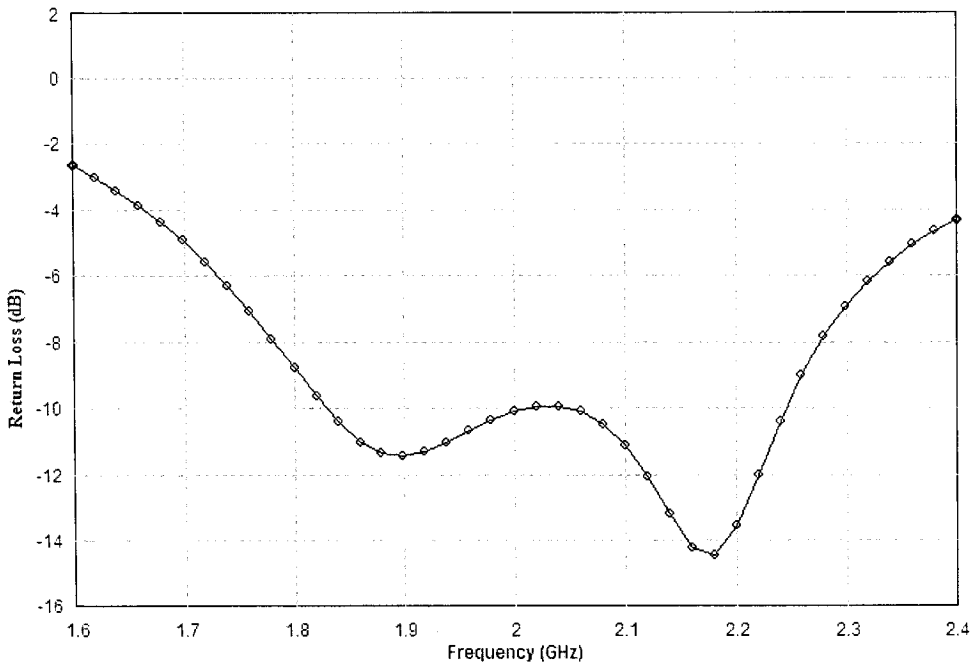

Figure 3.39 : Return Loss of Antenna with Stub

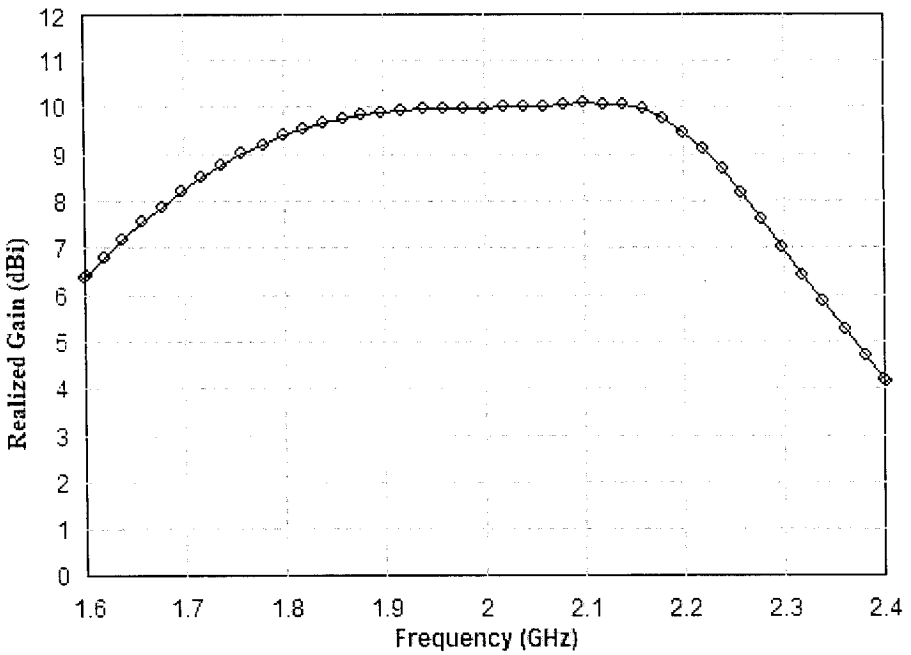

Figure 3.40 : Realized Gain of Antenna with Stub

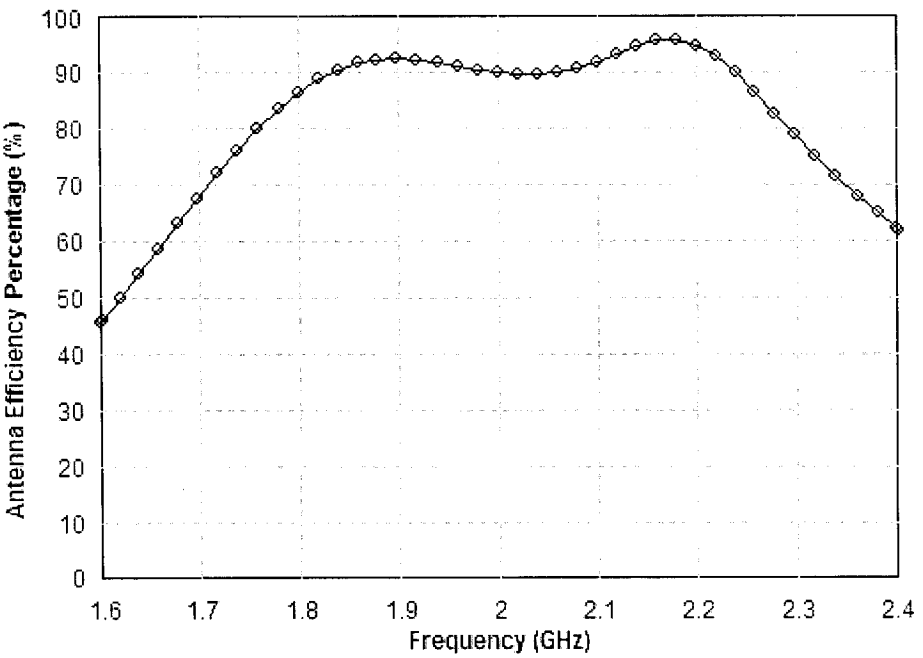

Figure 3.41 : Antenna Efficiency of Antenna with Stub

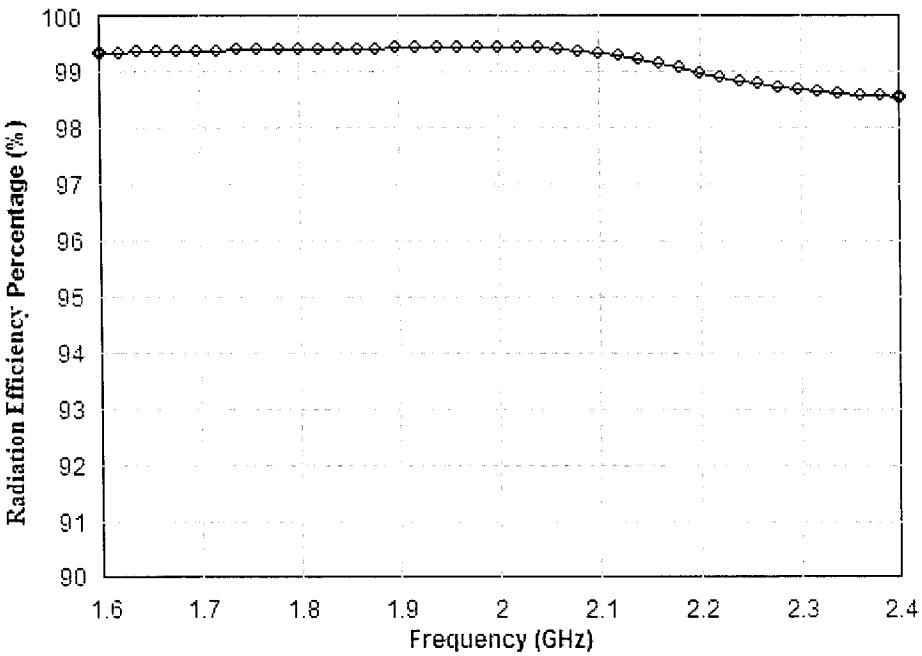

Figure 3.42 : Radiation Efficiency of Antenna with Stub

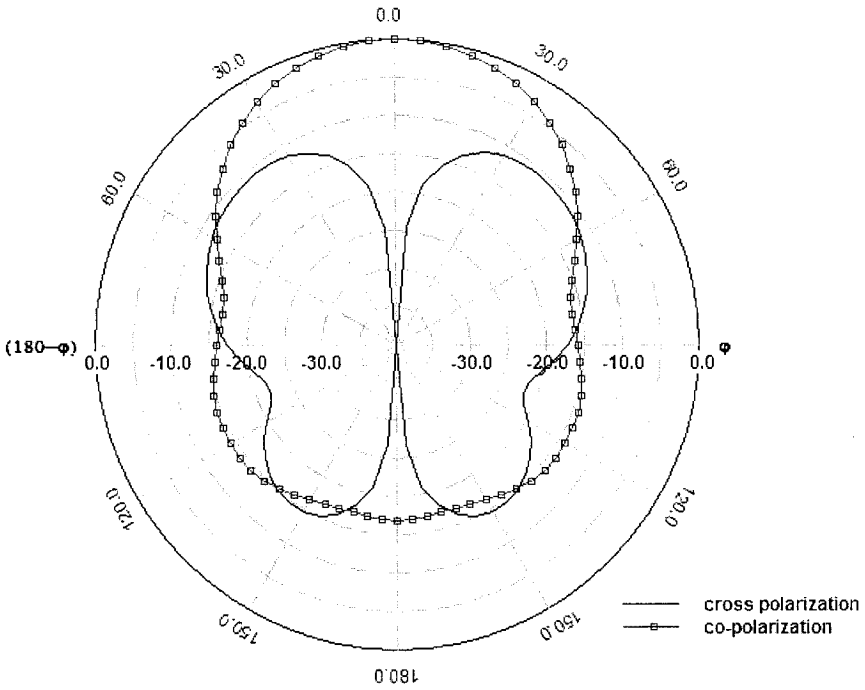

Figure 3.43 : H-Plane Radiation Patterns of Antenna with Stub at 1.85 GHz

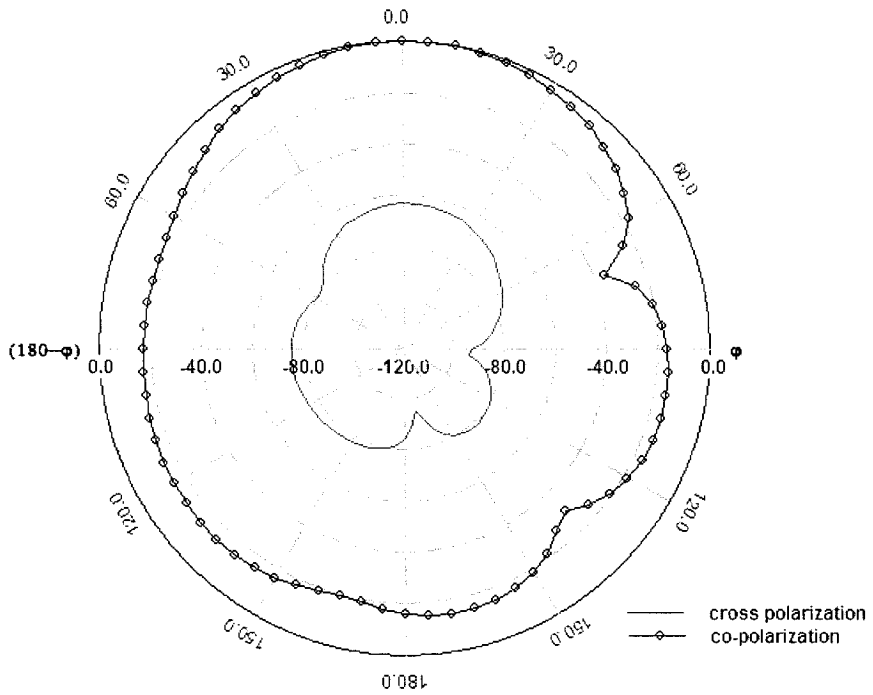

Figure 3.44 : E-Plane Radiation Patterns of Antenna with Stub at 1.85 GHz

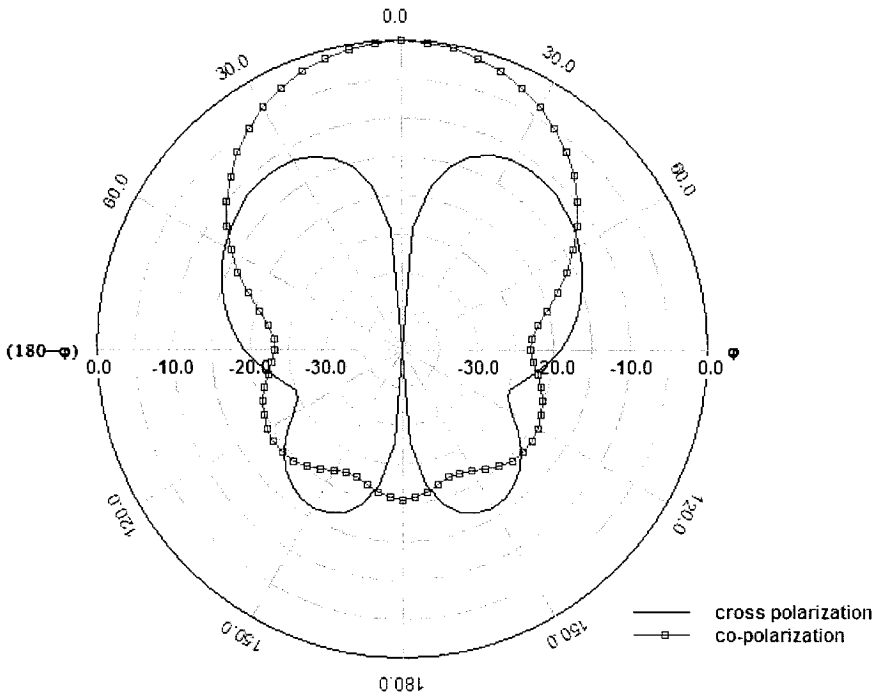

Figure 3.45 : H-Plane Radiation Patterns of Antenna with Stub at 2 GHz

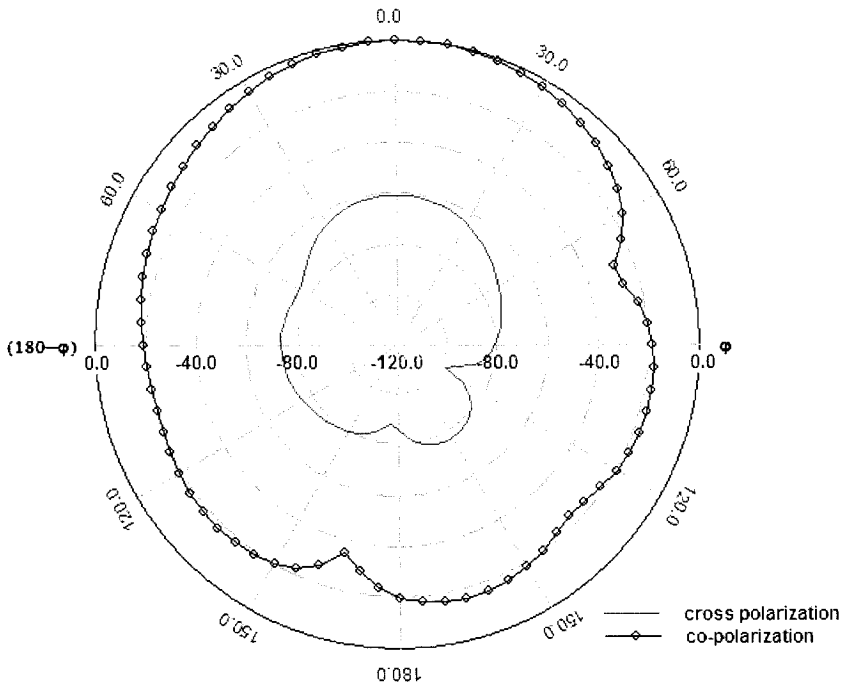

Figure 3.46 : E-Plane Radiation Patterns of Antenna with Stub at 2 GHz

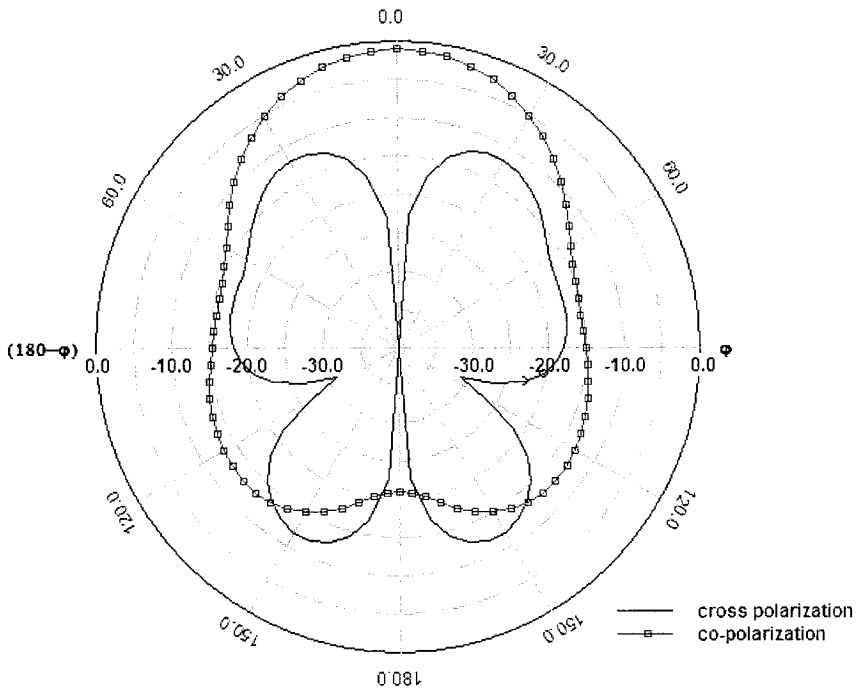

Figure 3.47 : H-Plane Radiation Patterns of Antenna with Stub at 2.2 GHz

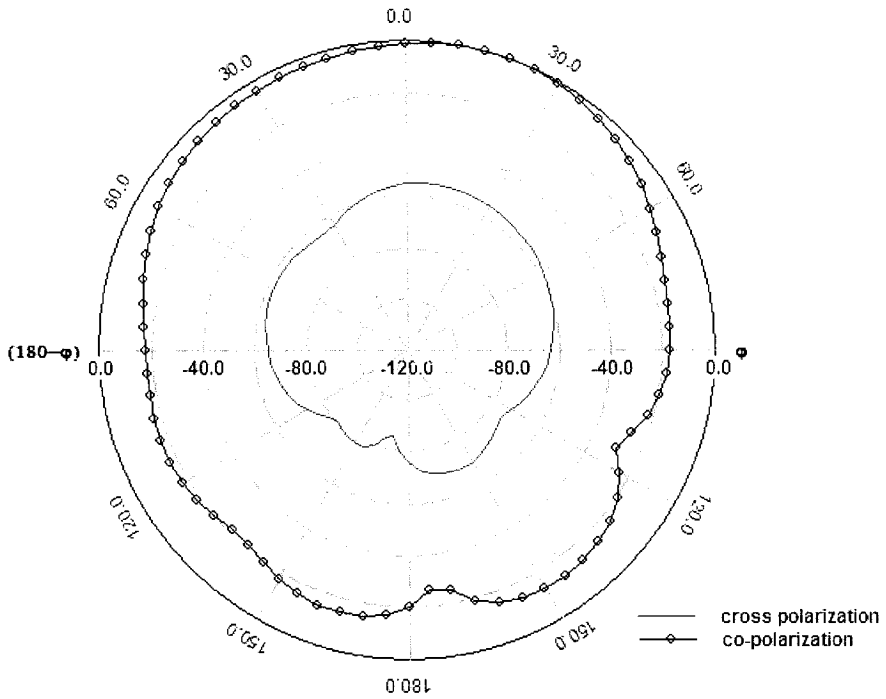

Figure 3.48 : E-Plane Radiation Patterns of Antenna with Stub at 2.2 GHz

We are able to state that, for microstrip patch antennas using electrically-thick low-permittivity substrate, appropriate stub-loading can be used as an "additional strategy" to realise antennas with the following performance:

- Bandwidth: broad bandwidth, around 20%
- Realized gain: high, around 9 dBi
- Antenna efficiency: high, > 80%
- Radiation efficiency: high, > 90%
- E-plane radiation pattern: stable, low cross polarization level (cross-polarization < -60 dB respect to the maximum of co-polarization)
- H-plane radiation pattern: stable, high cross polarization level (cross-polarization may reach -10dB respect to the maximum of co-polarization.)

3.3.5 Antennas Using Patches with Vertical Shorting Walls or Pins

Shorting walls or pins technique is commonly used to reduce the size of microstrip antennas. It is found that there are several shorting walls or pins microstrip antennas which obtain compact size and broadband simultaneously. In the equivalent circuit point of view, this can be explained as: the shorting walls or pins introduce small inductances parallel to the probe inductance, which will decrease the total inductance in the circuit, so broadband can be achieved. Designs employing edge-shoring wall [26], shorting fence [27], shorting pin and wall [28] have been illustrated in Figure 3.49 through 3.51, for which fractional bandwidths of above 20% have been reported. The performance of geometry Figure 3.51 is presented as the representative of this sub-class.

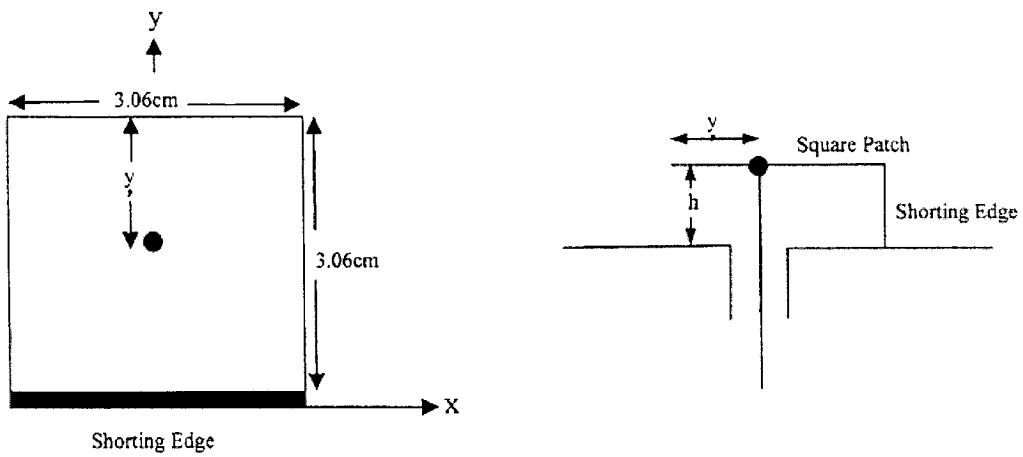

Figure 3.49 : Probe-Fed Microstrip Patch Antenna with Edge-Shorting Wall (After [26])

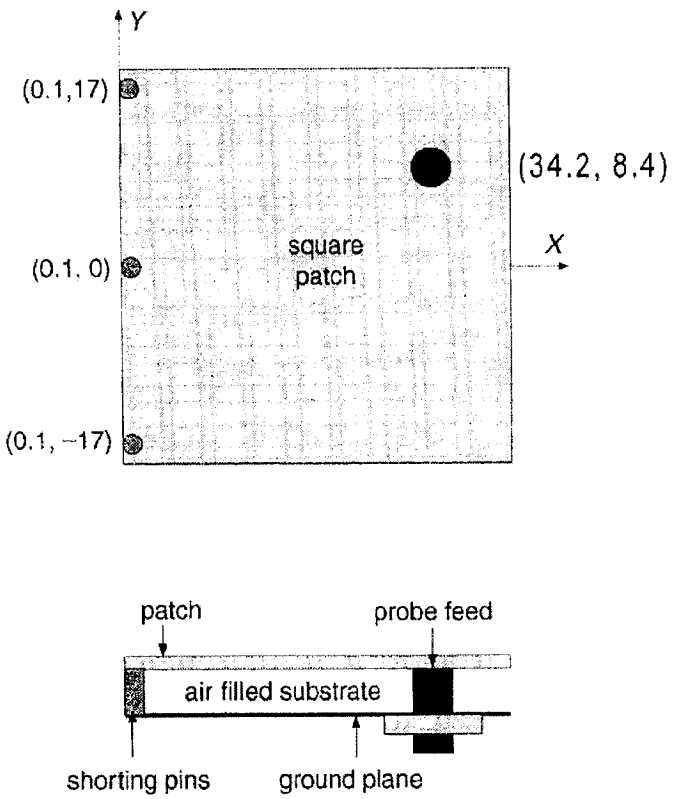

Figure 3.50 : Microstrip Patch Antenna with Shorting Fence (After [27])

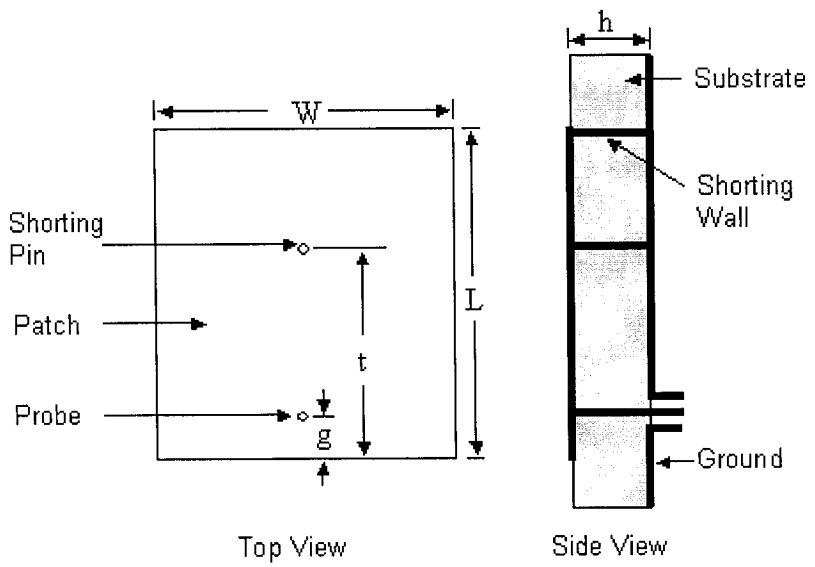

Figure 3.51 : Antenna with Shorting Pin and Wall

The antenna in Figure 3.51 was designed to operate near 3.3 GHz. The dimensions of the antenna are based on [28] with some manual optimization performed using the full-wave simulator. The radiation patch is 30 mm (length L) × 25 mm (width W). The feed point is 5 mm (g) from the lower edge of the patch. The shorting pin is 20 mm (t) from the lower edge of the patch. The ground plane is 60 mm × 60 mm. The substrate is foam of thickness 7 mm (h).

Figure 3.52 provides the comparison of VSWR IE3D simulation result and measured result [28]. The good agreement of the bandwidth serves to provide validation of the simulation results. The full-wave simulation results are shown in Figures 3.53 through 3.62. We observe that the return loss is less than -10 dB between 3 GHz and 3.7 GHz, implying an impedance bandwidth of 0.7 GHz, which is a fractional bandwidth of about 21% with respect to the center frequency of 3.3 GHz. As shown in Figure 3.54, the antenna realized gain varies between 3 dBi and 4 dBi over the above frequency band, and is quite "flat". Figure 3.55 reveals that the antenna efficiency is between 55% and 65% over this same frequency range. Figure 3.56 shows that the radiation efficiency is between 70% and 85% over the operating band. The radiation patterns at 3.05 GHz, 3.3 GHz and 3.65 GHz are shown in Figures 3.57 through 3.62. We observe that the E-plane radiation patterns are stable with low cross polarization level over the operating band, and the maximum co-polarizations are 30° excursive from the centre. The H-plane radiation patterns are stable with very high cross-polarization level. The maximum cross-polarization level is even higher than the maximum co-polarization level.

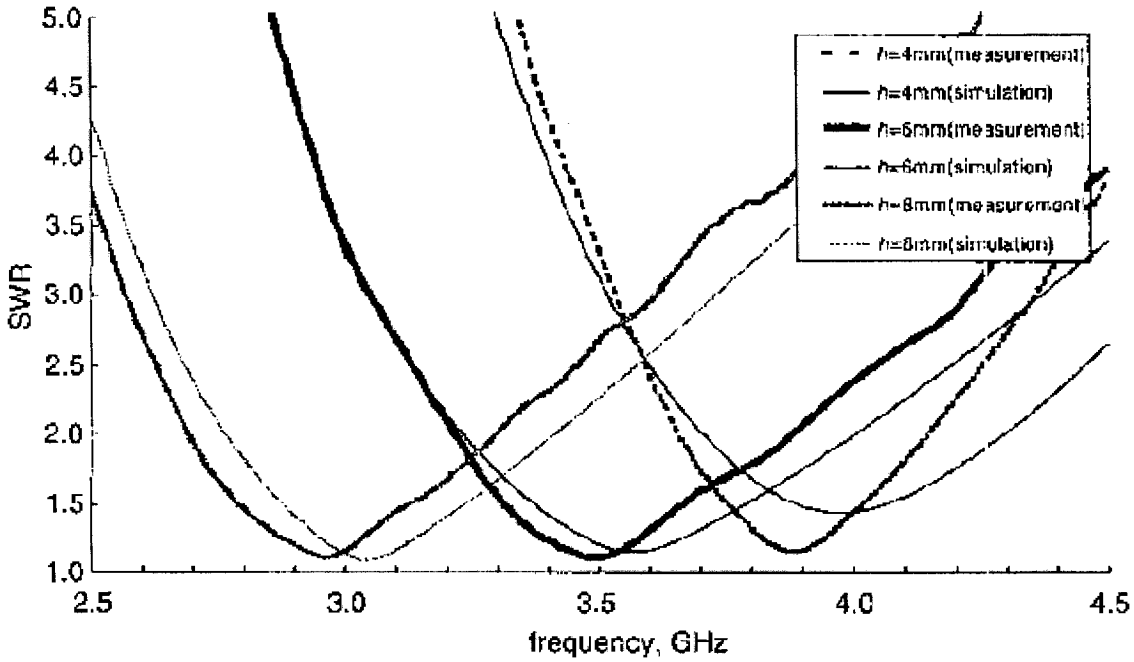

Figure 3.52 : Comparison of VSWR Measured and IE3D Simulation Result of Antenna with Shorting Pin and Wall (After [28])

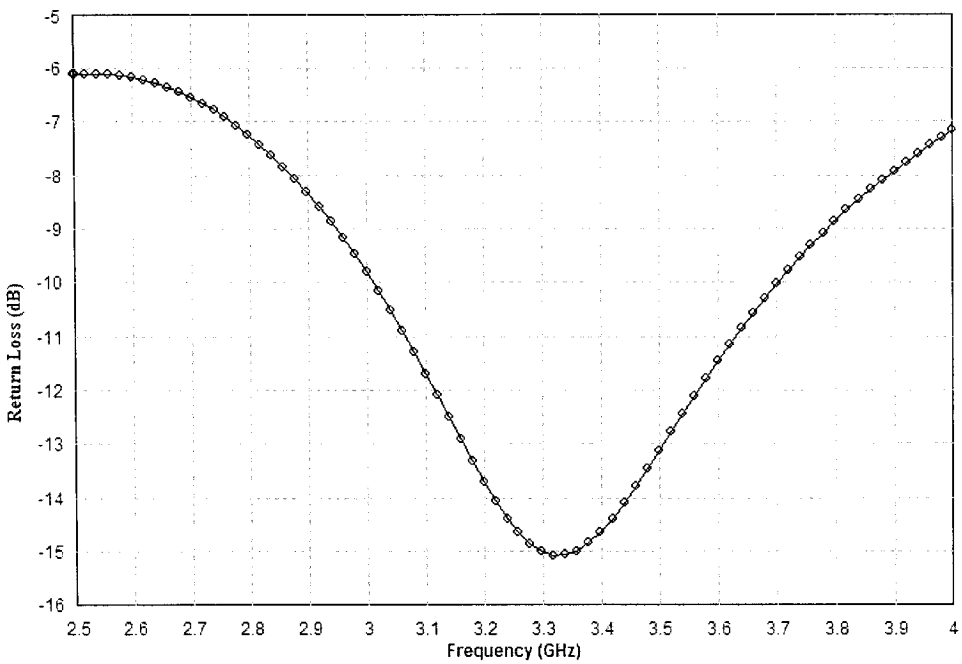

Figure 3.53 : Return Loss of Antenna with Shorting Pin and Wall

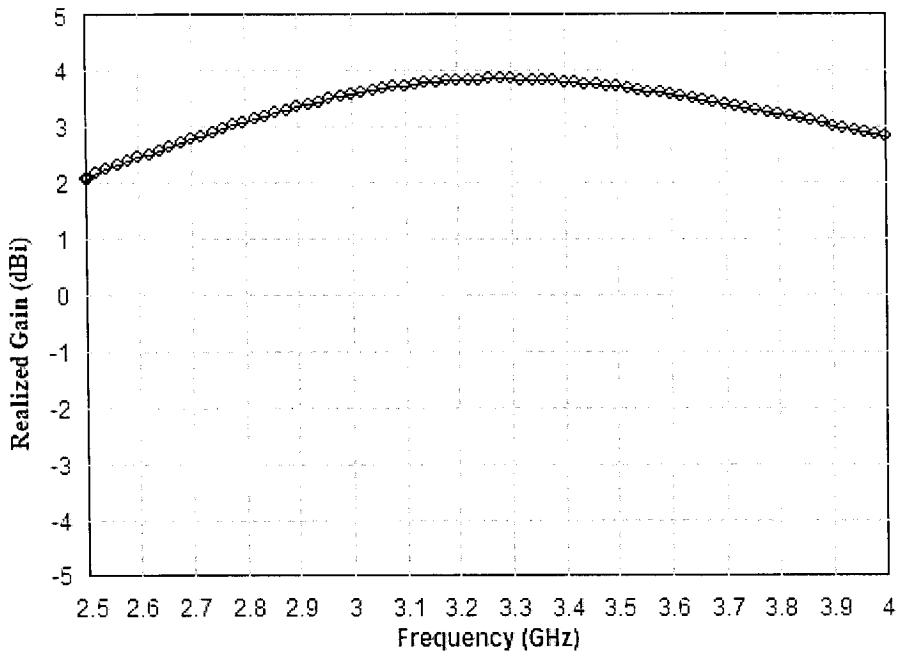

Figure 3.54 : Realized Gain of Antenna with Shorting Pin and Wall

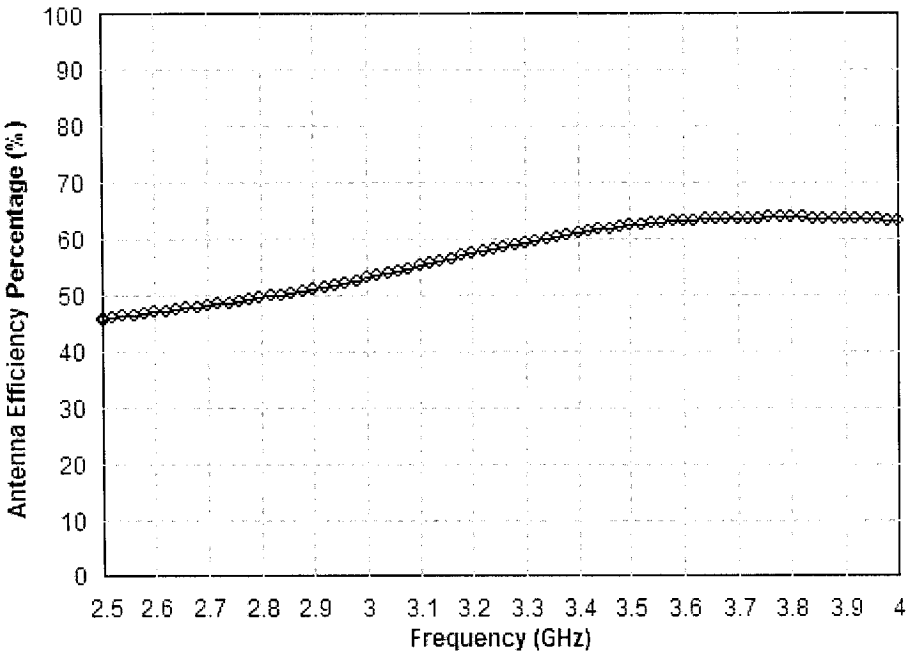

Figure 3.55 : Antenna Efficiency of Antenna with Shorting Pin and Wall

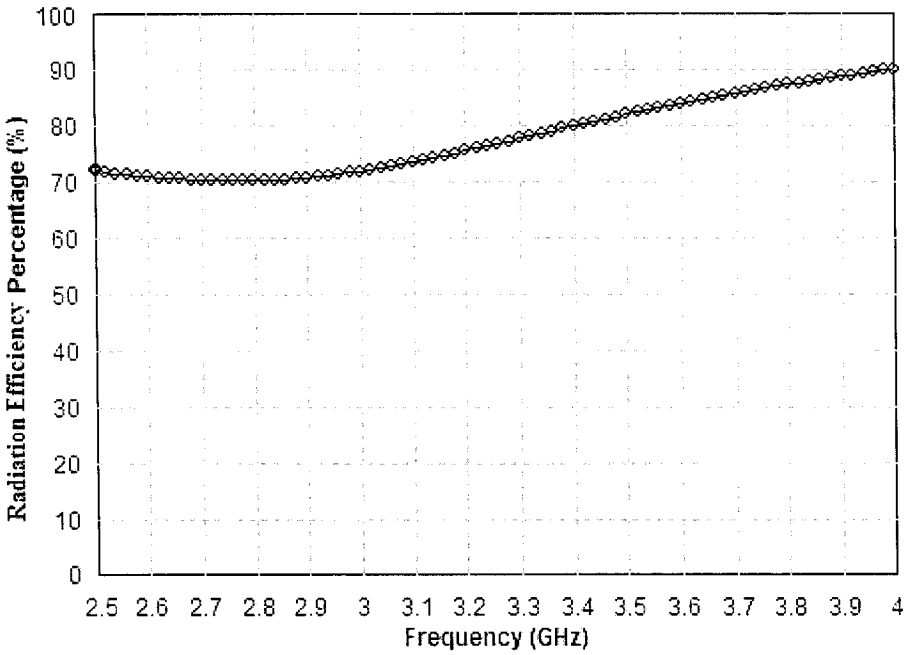

Figure 3.56 : Radiation Efficiency of Antenna with Shorting Pin and Wall

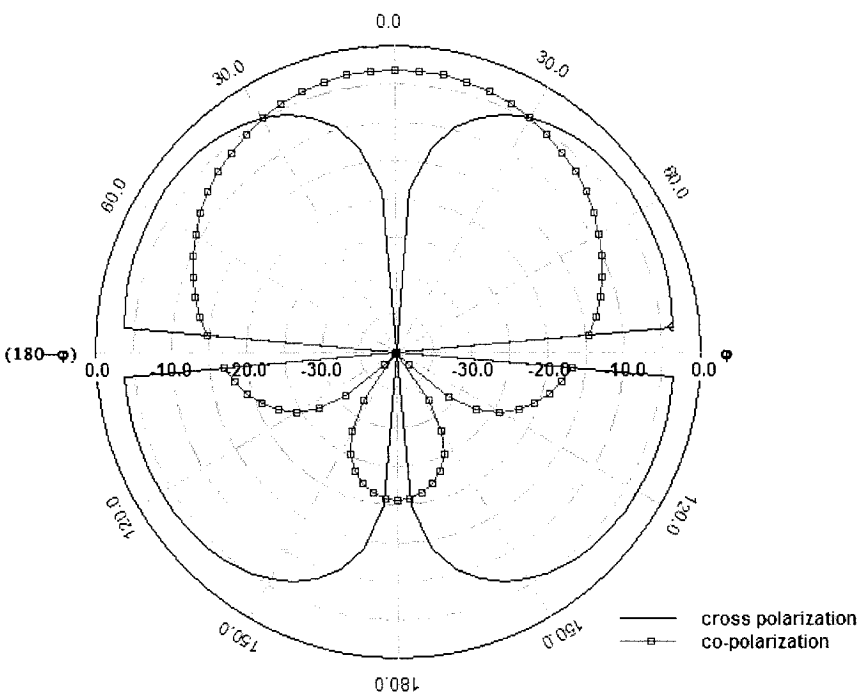

Figure 3.57 : H-Plane Radiation Patterns of Antenna with Shorting Pin and Wall at 3.05 GHz

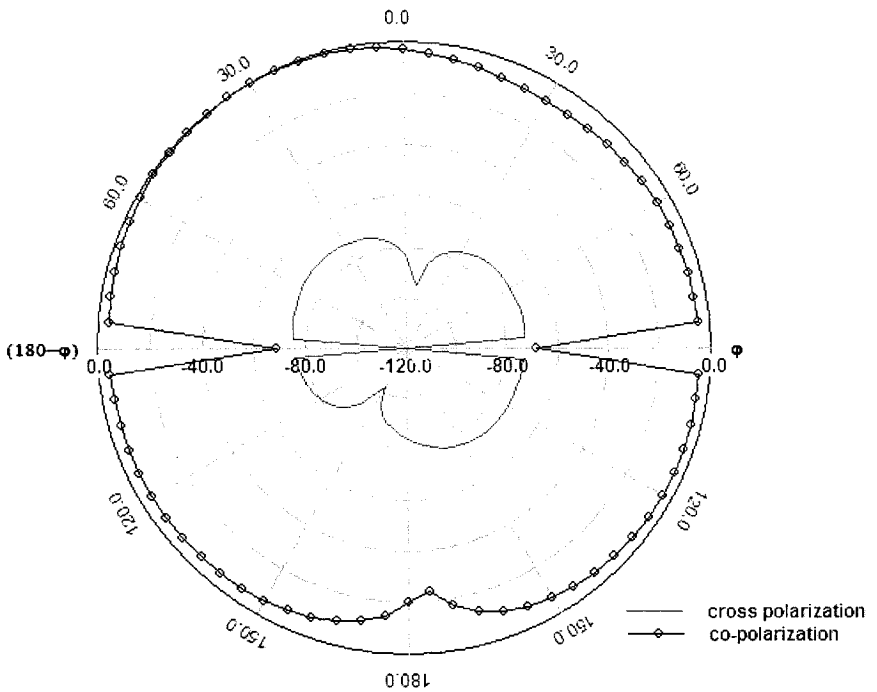

Figure 3.58 : E-Plane Radiation Patterns of Antenna with Shorting Pin and Wall at 3.05 GHz

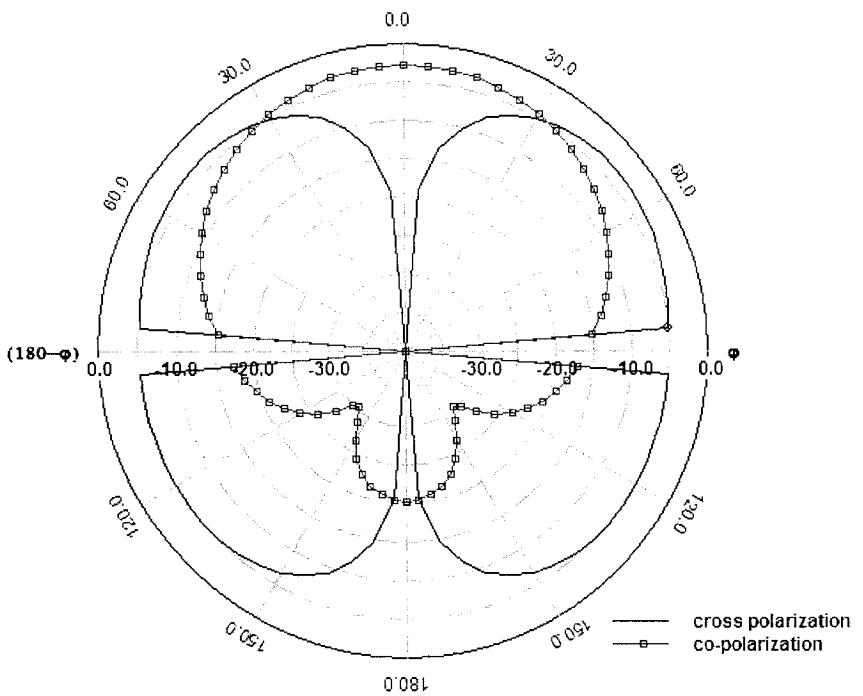

Figure 3.59 : H-Plane Radiation Patterns of Antenna with Shorting Pin and Wall at 3.3 GHz

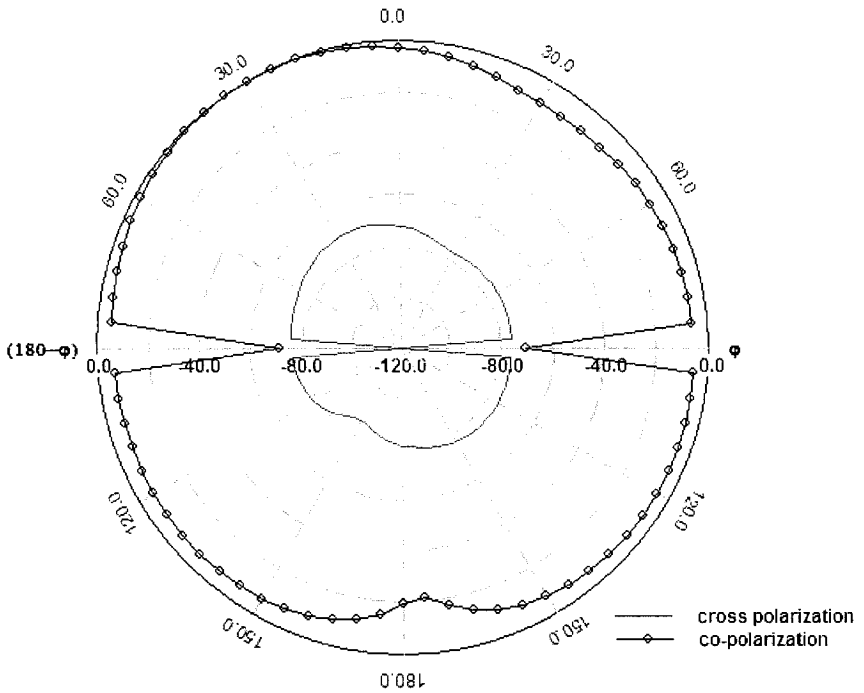

Figure 3.60 : E-Plane Radiation Patterns of Antenna with Shorting Pin and Wall at 3.3 GHz

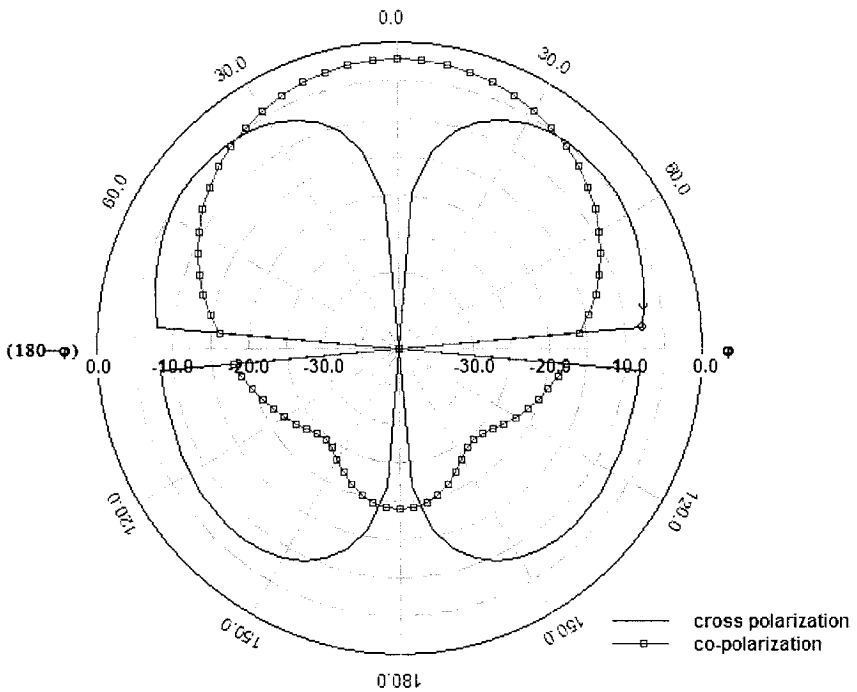

Figure 3.61 : H-Plane Radiation Patterns of Antenna with Shorting Pin and Wall at 3.65 GHz

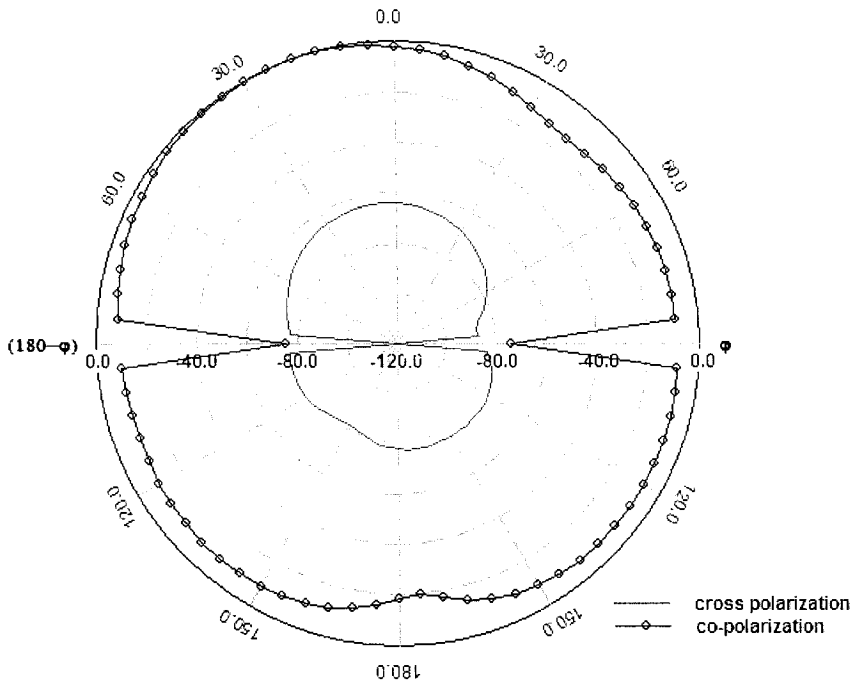

Figure 3.62 : H-Plane Radiation Patterns of Antenna with Shorting Pin and Wall at 3.65 GHz

Microstrip antennas using electrically-thick low-permittivity substrates, with shorting pins or walls judiciously used as the "additional strategy", are able to attain the following performance:

- Bandwidth: broad bandwidth, around 20%
- Realized gain: moderate, around 3.5 dBi
- Antenna efficiency: moderate, around 60%
- Radiation efficiency: moderate, around 80%
- E-plane radiation pattern: stable, maximum co-polarization may offset from centre, low cross polarization level (cross-polarization < -60 dB respect to the maximum of co-polarization)
- H-plane radiation pattern: stable, very high cross polarization level (The maximum cross-polarization level may be higher than the maximum co-polarization level.)

It is worth commenting at this point that some of the members of the sub-class of microstrip antennas in question actually take on a geometry viewed by many not as patch antennas, but as so-called planar-inveretd-F (PIFA) antennas, as shown in Figure 3.63 [30].

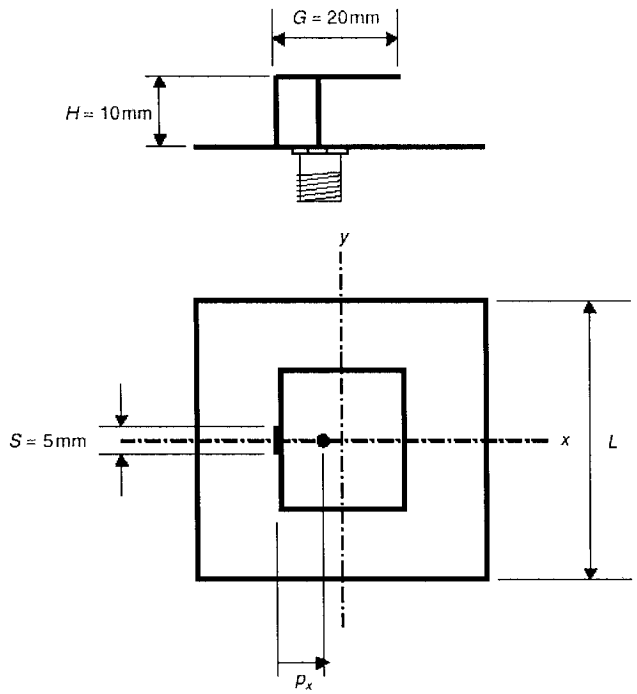

Figure 3.63 : Planar Inverted-F Antenna (PIFA) (After [30]). Height H = 0.065λo.

3.4 PROBE-FED MICROSTRIP PATCH ANTENNAS WITH ELECTRICALLY-THIN HIGH-PERMITTIVITY SUBSTRATES

3.4.1 Introductory Comments

Microwave circuits are usually built on electrically-thin substrate of relative permittivity larger than unity, such as FR4 (ε_r = 4.4, tanδ = 0.02), in order to limit unwanted radiation from the circuit. If some application demands that we realize a patch antenna on the same substrate as the circuitry, then we know from Section 3.2 that such an antenna will have a very narrow bandwidth. Strategies have, however, been developed to increase the bandwidth of such antennas, albeit not for fractional bandwidths as large as those for the electrically-thick substrate cases discussed in Section 3.3. One begins with a patch antenna whose bandwidth is on the order of 2% (and which has a single resonating frequency), and then adds some additional features in order to arrive at a geometry that possesses more than one resonating frequency. Since the feed probe is short its inductance is small and arguments related to its compensation are not required. With electrically-thin high-permittivity patch antennas the multi-resonance viewpoint provides the best physical "picture" of the reason for the broader bandwidth.

We have sorted the techniques available in the literature for obtaining these multiple resonances into two sub-classes: the use of additional resonating patches and the modification of the patch geometry. These are discussed in Sections 3.4.2 and 3.4.3, respectively. It is noted that the second of these methods are based on the same principle as those described for the electrically-thick situation in Section 3.3.3. However, the bandwidths obtained are never as large as the latter and, more importantly, other

performance parameters (e.g. realized gain) are different from their electrically-thick counterparts even at the antenna centre frequencies.

3.4.2 Antennas with Parasitic Elements

It is known from circuit theory that if one couples two circuits, each of which separately has it's own resonating frequency, the combined circuit exhibits a "double-hump" response that is broader than the responses of the individual resonating circuits when they are uncoupled. This is the multiple-resonance phenomenon. It can be achieved for microstrip patch antennas using parasitic elements, and several possibilities exist. The so-called stacked patch configuration is illustrated in Figure 3.64; the disadvantage here is that it is multilayered. Figure 3.65 shows the so-called edge-coupled case, where the driven patch (to which the probe is connected) and the parasitic patched lie in the same plane. Note that two or four parasitic resonators (patches) have been attempted, the latter providing slightly wide bandwidth.

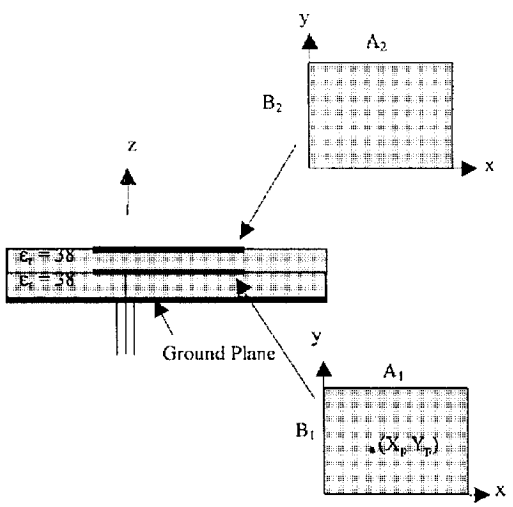

Figure 3.64 : Proximity Coupled Parasitic Patch Configuration : Stacked Patch Geometry (After [39]).

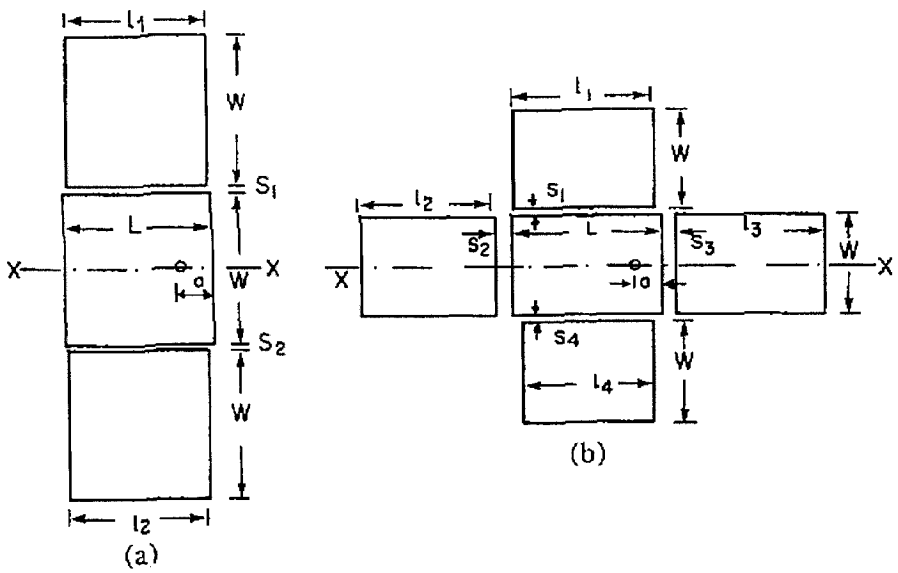

Figure 3.65 : Proximity Coupled Parasitic Patch Configuration : Coplanar Patch Geometry (After [34]).

A combination of both stacked and coplanar parasitic patches is used in Figure 3.66. Here the driven patch has two edge-coupled coplanar parasitic patches, plus a third (stacked) parasitic patch. Figure 3.67 shows yet another of what is a large number of possibilities, namely a situation in which the additional patches are directly coupled. Clearly, these configurations are more demanding on substrate real estate than those not employing such large additional patches.

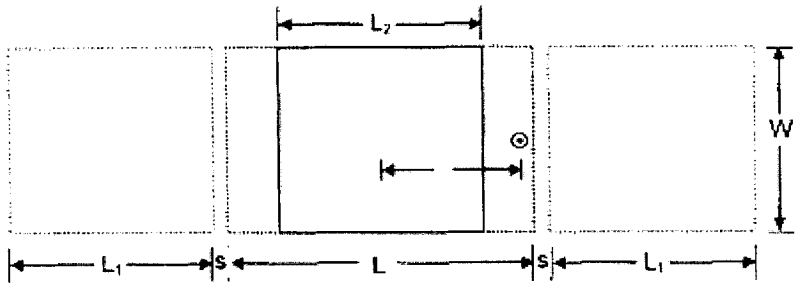

Figure 3.66 : Proximity Coupled Parasitic Patch Configuration : Mixed Coplanar-Stacked Patch Geometry (After [40]).

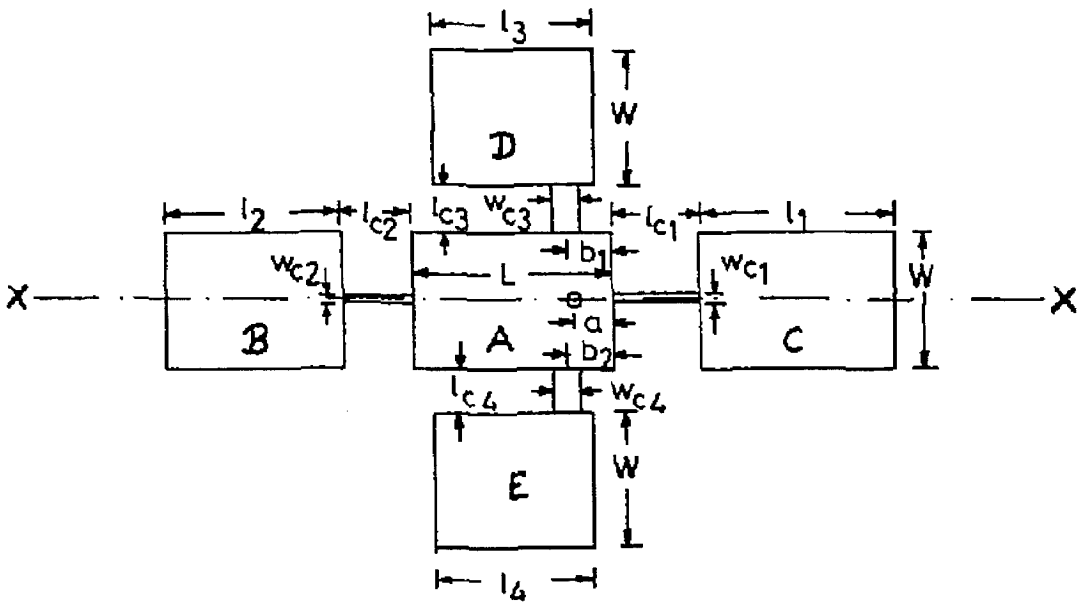

Figure 3.67 : Direct Coupled Parasitic Patch Configuration (After [35]).

A further possibility is shown in Figure 3.68. The antenna consists of the probe-fed patch, a directly coupled parasitic patch, plus two edge-coupled parasitic patches. It is examine din detail here as representative of what can be achieved with this sub-class of broadbanding technique. The dimensions of the antenna are based on [38], with some manual optimization performed using the full-wave simulator.

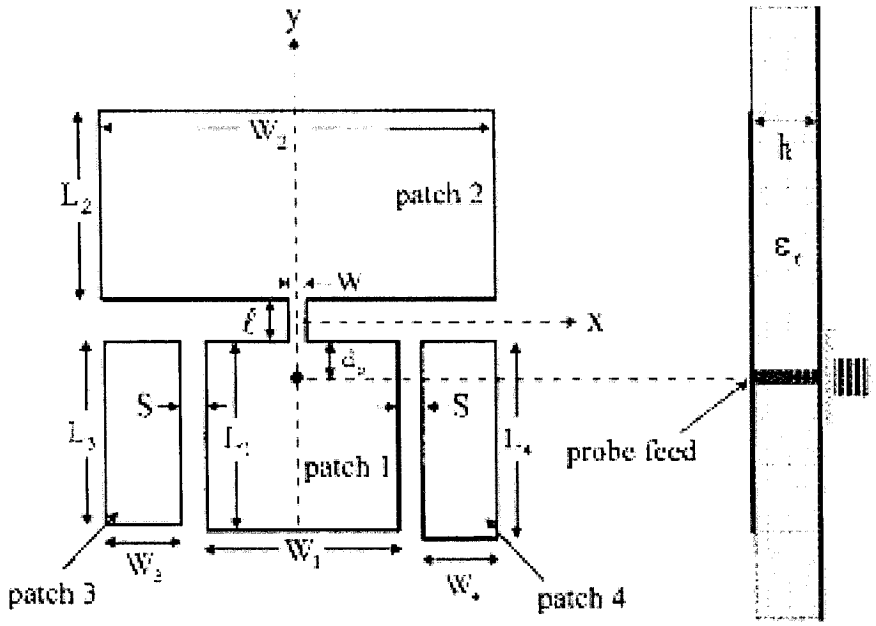

Figure 3.68 : Geometry of Antenna with Parasitic Elements (After [38])

The patch#1 is 26.6 mm (length L1) × 16 mm (width W1). The patch#2 is 24.4 mm (length L2) × 40 mm (width W2). The patch#3 is 26.47 mm (length L3) × 10 mm (width W3). The patch 4 is 27 mm (length L4) × 10 mm (width W4). The transmission line between patch#1 and patch#2 is 2 mm (length l) × 0.5 mm (width w). Distance S between patch#1 and patch#3, patch#1 and patch#4 is 2 mm. The feed point is dp = 1.2 mm from upper edge of patch#1. The substrate is made of FR4 (ε_r = 4.4) with thickness h = 1.6 mm. The ground plane is 75 mm (length) × 60 mm (width). The antenna is designed to operate about a centre frequency of 2.75 GHz.

We have compared return loss IE3D simulation result in Figure 3.70 to the measured result [38] in Figure 3.69. The results quite agree with each other except that we can not get the 3 GHz dip. The good agreement serves to provide validation of the simulation results. The full-wave simulation results are shown in Figures 3.70 through

3.79. We observe that the return loss is less than -10 dB between 2.65 GHz and 2.97 GHz, implying an impedance bandwidth of 0.32 GHz, which is a fractional bandwidth of about 11.6% with respect to the center frequency of 2.75 GHz. As shown in Figure 3.71, the antenna realized gain varies between 0.5 dBi and 3 dBi over the above frequency band, and is quite "flat". Figure 3.72 reveals that the antenna efficiency is between 20% and 30% over this same frequency range. Figure 3.73 shows that the radiation efficiency is between 20% and 30% over the operating band. The radiation patterns at 2.65 GHz, 2.8 GHz and 2.9 GHz are shown in Figures 3.74 through 3.79. The H-plane co-polarization patterns are stable, with very low cross polarization level over the operating band. The E-plane co-polarization level is much higher than cross polarization level, and the maximum co-polarization levels are excursive from the center.

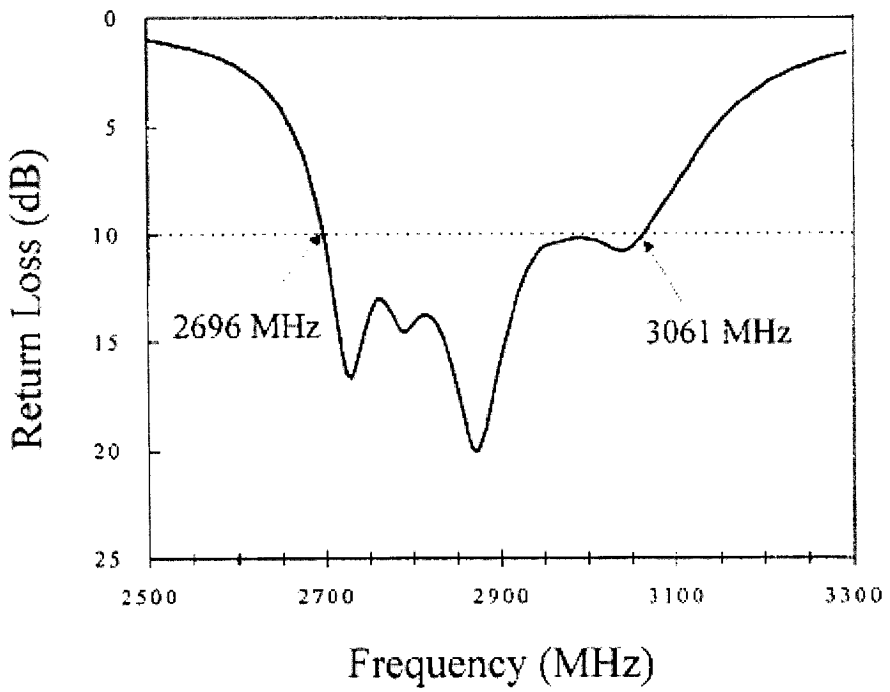

Figure 3.69 : Return Loss Measured Result of Antenna with Parasitic Elements (After [38])

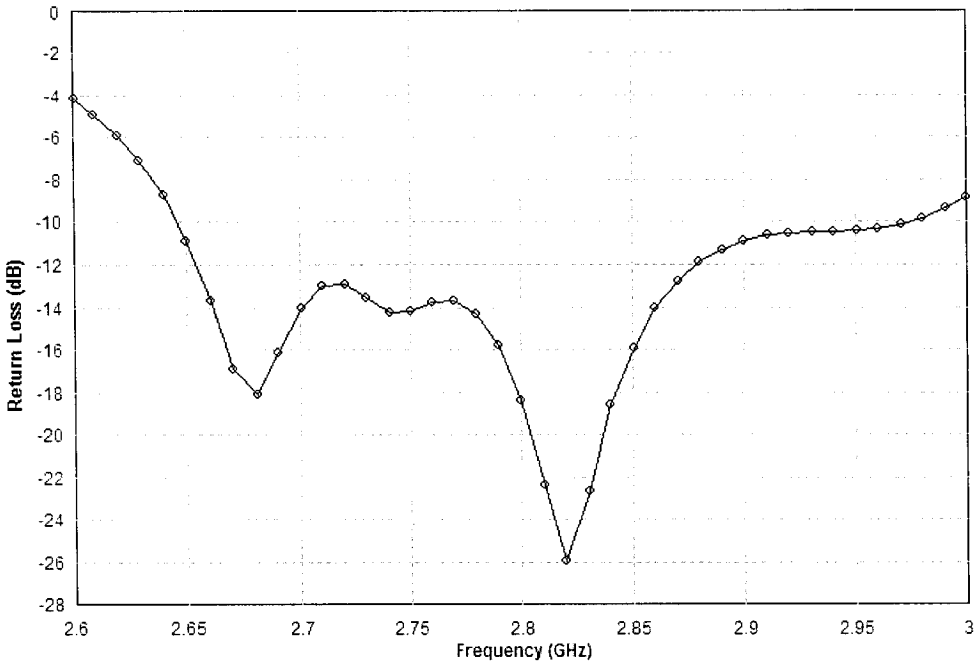

Figure 3.70 : Return Loss Simulation Result of Antenna with Parasitic Elements

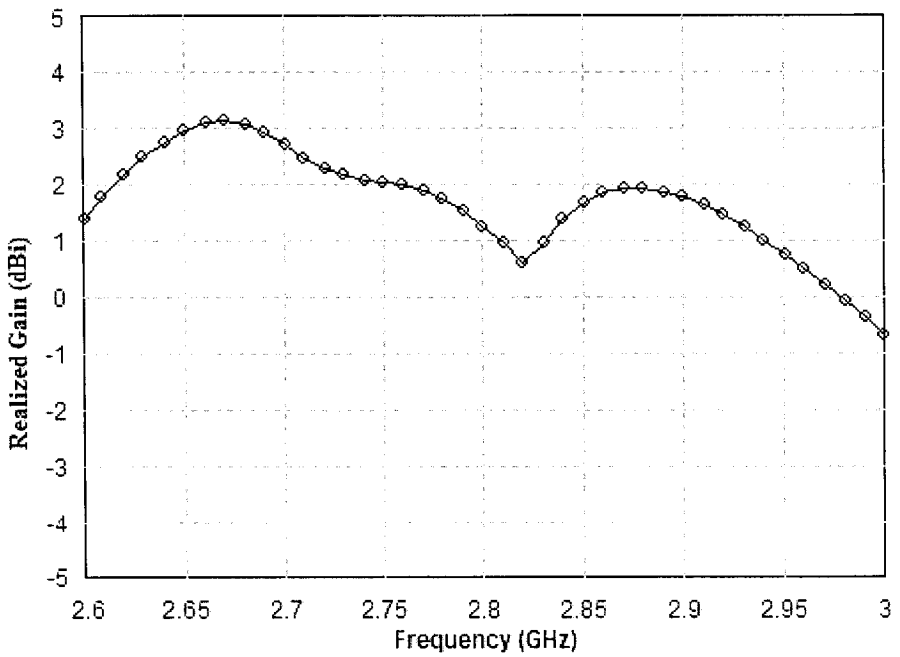

Figure 3.71 : Realized Gain of Antenna with Parasitic Elements

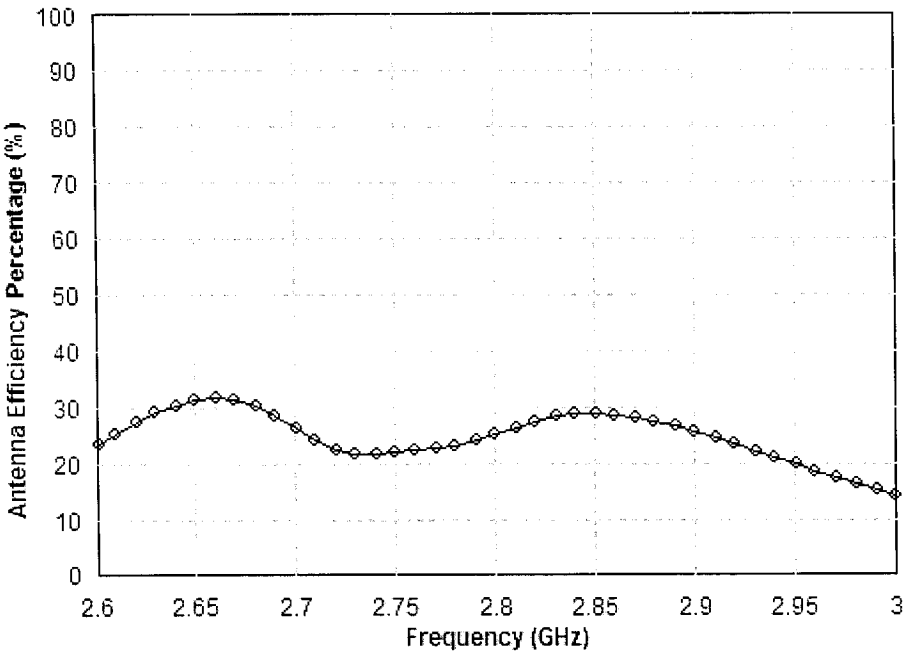

Figure 3.72 : Antenna Efficiency of Antenna with Parasitic Elements

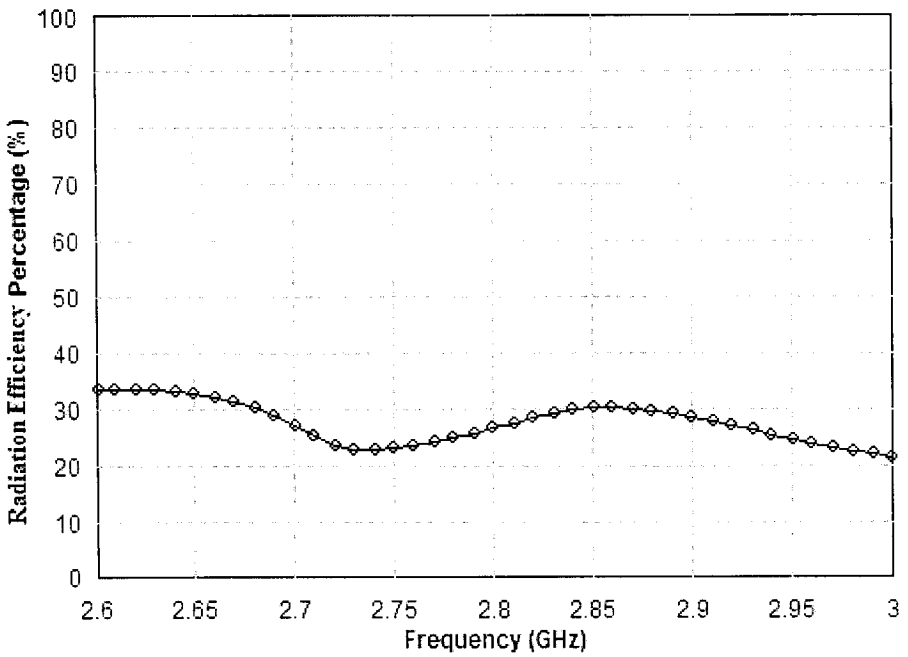

Figure 3.73 : Radiation Efficiency of Antenna with Parasitic Elements

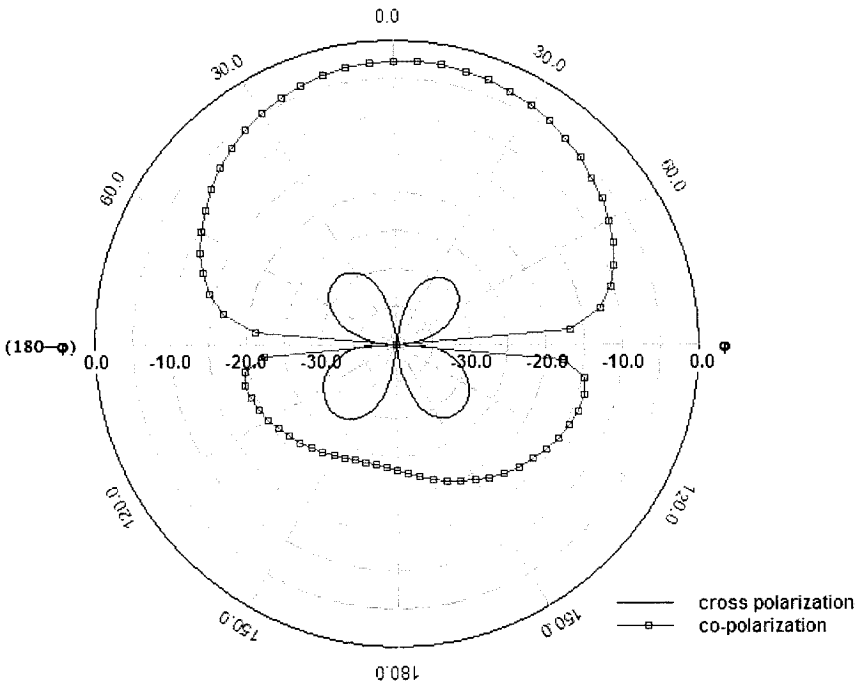

Figure 3.74 : H-Plane Radiation Patterns of Antenna with Parasitic Elements at 2.65 GHz

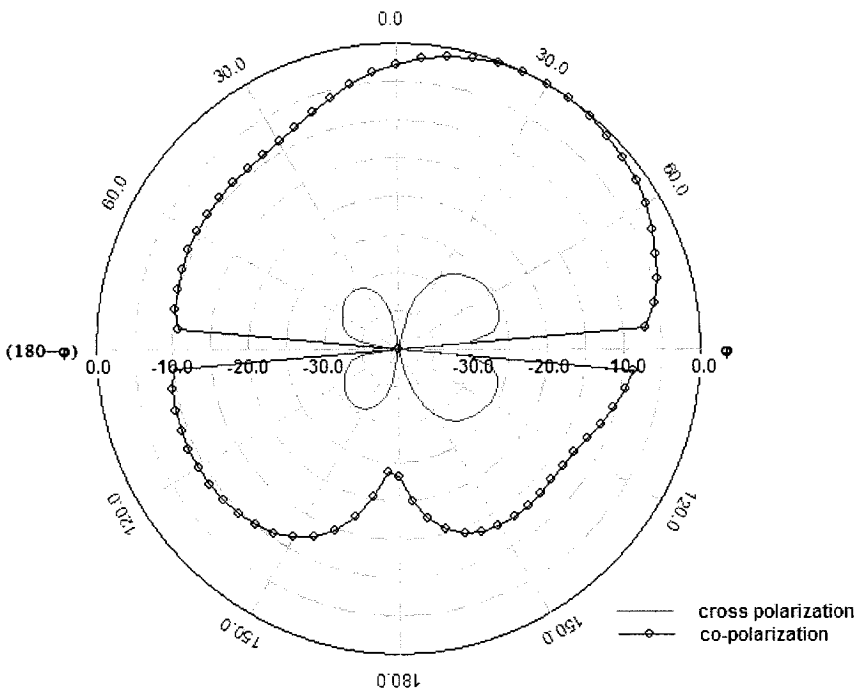

Figure 3.75 : E-Plane Radiation Patterns of Antenna with Parasitic Elements at 2.65 GHz

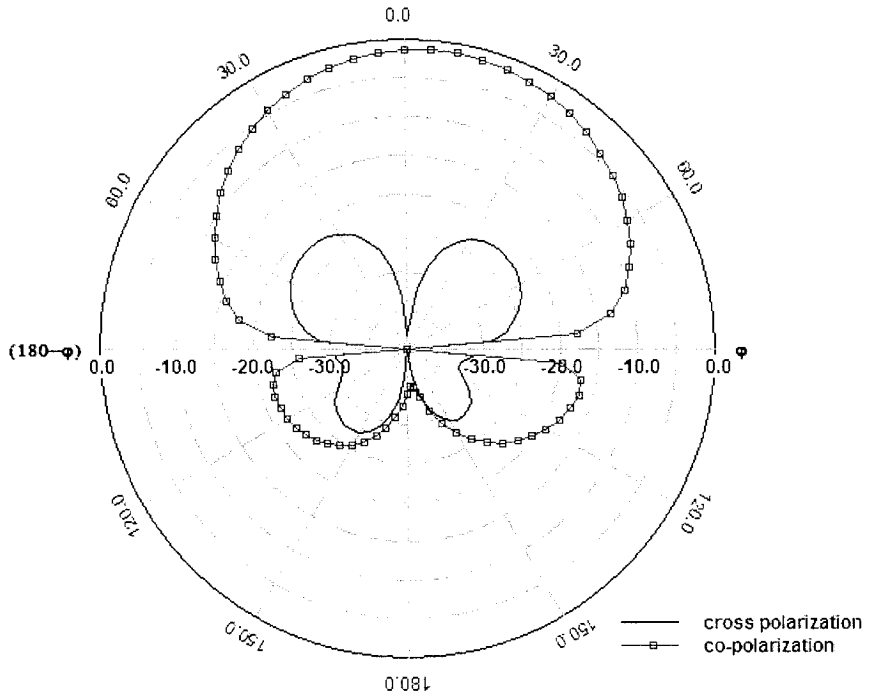

Figure 3.76 : H-Plane Radiation Patterns of Antenna with Parasitic Elements at 2.8 GHz

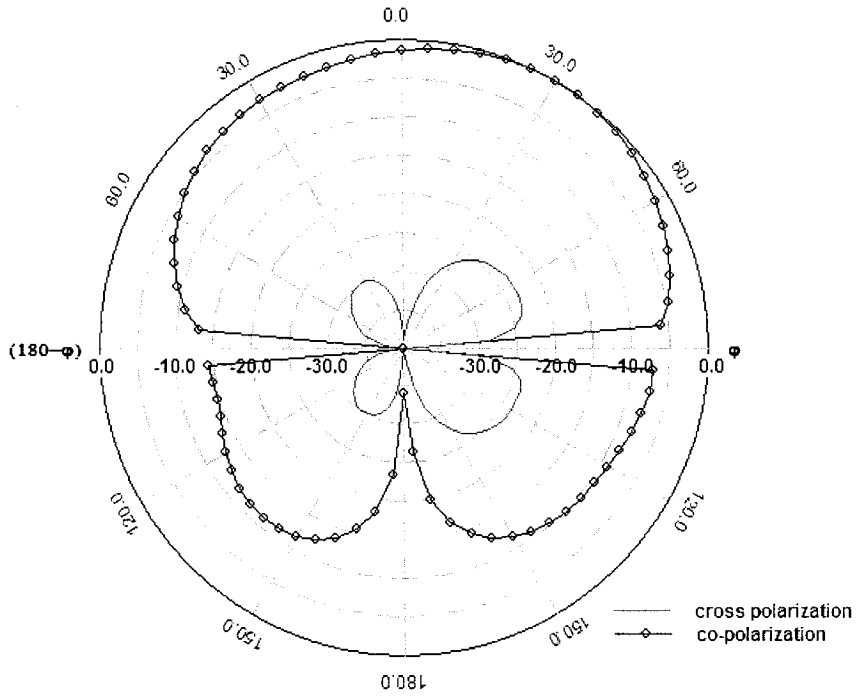

Figure 3.77 : E-Plane Radiation Patterns of Antenna with Parasitic Elements at 2.8 GHz

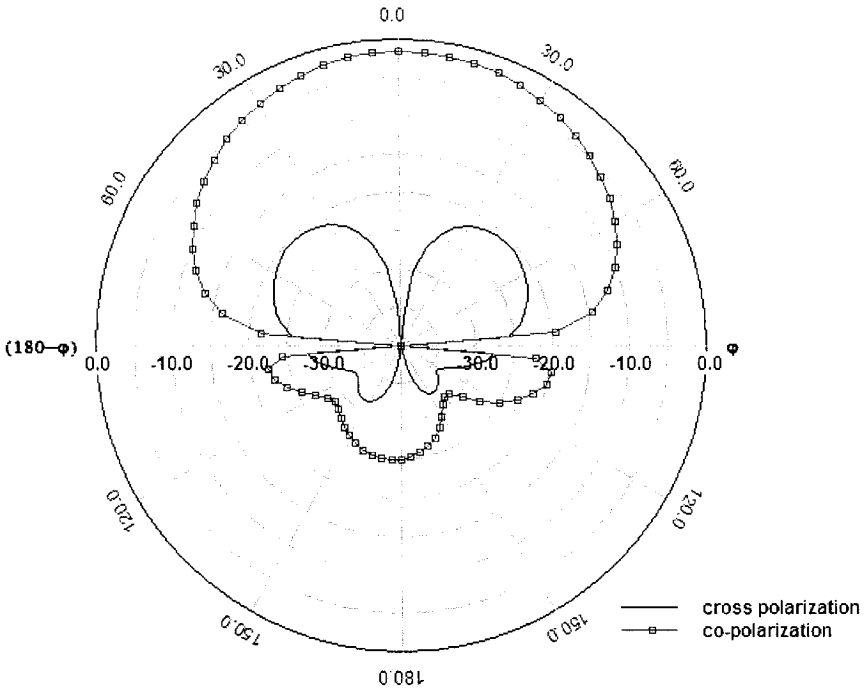

Figure 3.78 : H-Plane Radiation Patterns of Antenna with Parasitic Elements at 2.9 GHz

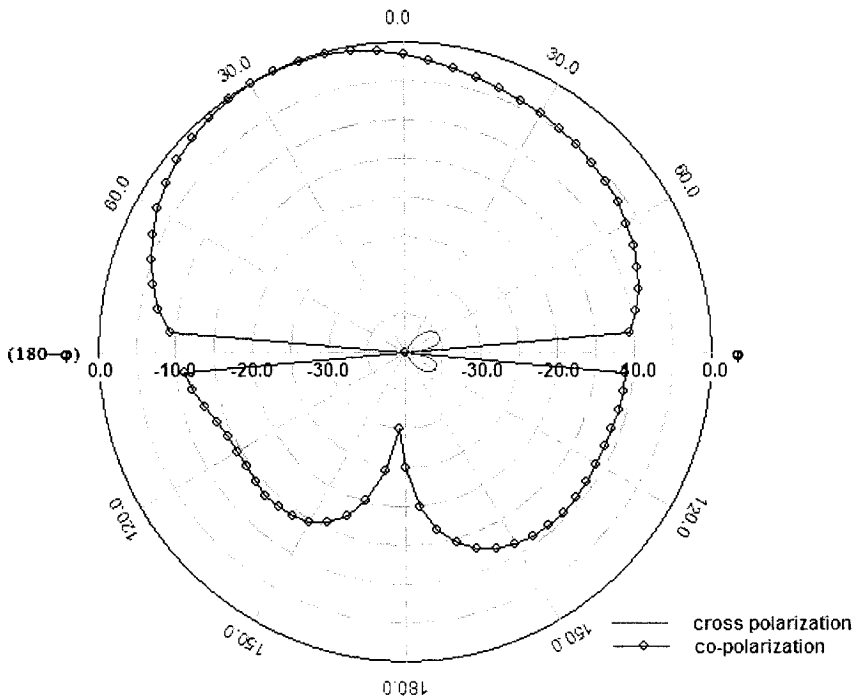

Figure 3.79 : E-Plane Radiation Patterns of Antenna with Parasitic Elements at 2.9 GHz

Microstrip antennas using electrically thin and high permittivity substrate with parasitic elements have performances as follows:

- Bandwidth: broad bandwidth, around 10%
- Realized gain: low, around 2 dBi
- Antenna efficiency: low, around 25%
- Radiation efficiency: low, around 25%
- E-plane radiation pattern: stable, low cross polarization level (cross-polarization is 20 dB less than co-polarization), the maximum co-polarization level may be excursive from the center.
- H-plane radiation pattern: stable, low cross polarization level (cross-polarization is 20 dB less than co-polarization).

3.4.3 Antennas with Modified Patch Geometries

Multiple resonances may also be realized by using a single patch but altering its geometry. This is the same approach as was done in Section 3.3.3 for the electrically-thick low-permittivity substrate antenna. As was the case there, altering the patch geometry moves the resonating frequencies of the "cavity modes" (or equivalently, altered patch current distributions) closer together. An equally valid viewpoint is one that maintains that altering the patch geometry is equivalent to reactively loading the patch resonating circuit in such a way that there are closely spaced resonating frequencies. It is for this reason that different authors name the technique differently. Some refer to it as the use of "embedded slots" while others simply call it "reactively loaded patches". We have classified these in the sub-class "modified patch geometries" [41-46]. We will consider the two of these geometries in some detail, namely that in Figure 3.80 and Figure 3.92.

Figure 3.80 shows the geometry of a microstrip antenna with patch geometry modifications that might be called "embedded slot". The antenna is a rectangular patch with a pair of toothbrush-shape slots. The dimensions of the antenna are based on [41], with some manual optimization performed using the full-wave simulator. The patch is 37.3 mm (length L) × 24.87 mm (width W). The slots consist of a pair of bent slots with 15° bent angle and a pair of three protruding slots which are 2 mm spacing to the next one and different widths as 9 mm (w_1), 8.5mm (w_2) and 8 mm (w_3). The feed point is g = 15.15mm from lower edge of the patch. The substrate is made of FR4 with thickness h = 1.6 mm. The ground plane is 60 mm × 60 mm. The antenna is designed to operate near 1.73 GHz.

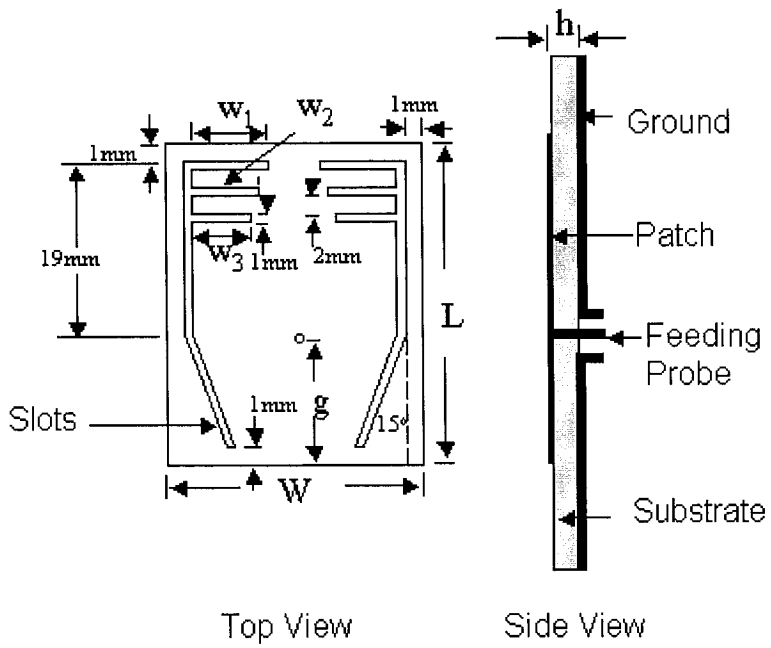

Figure 3.80 : Geometry of Antenna with Embedded Slots

We have compared return loss IE3D simulation result in Figure 3.82 to the measured result [41] in Figure 3.81.There is only a small frequency shifting between the results. The good agreement serves to provide validation of the simulation results. The full-wave simulation results are shown in Figures 3.81 through 3.90. We observe that the return loss is less than -10 dB between 1.69 GHz and 1.77 GHz, implying an impedance bandwidth of 0.08 GHz, which is a fractional bandwidth of about 4.6% with respect to the center frequency of 1.73 GHz. As shown in Figure 3.83, the antenna realized gain varies between -9 dBi and -2 dBi over the above frequency band. Figure 3.84 reveals that the antenna efficiency is less than 20% over this same frequency range. Figure 3.85 shows that the radiation efficiency is less than 20% over the operating band. The radiation patterns at 1.7 GHz, 1.73 GHz and 1.76 GHz are shown in Figures 3.86 through 3.91. The H-plane co-polarization patterns are stable, with low cross polarization level over the operating band. The E-plane co-polarization patterns are also stable, with very low cross polarization level over the operating band.

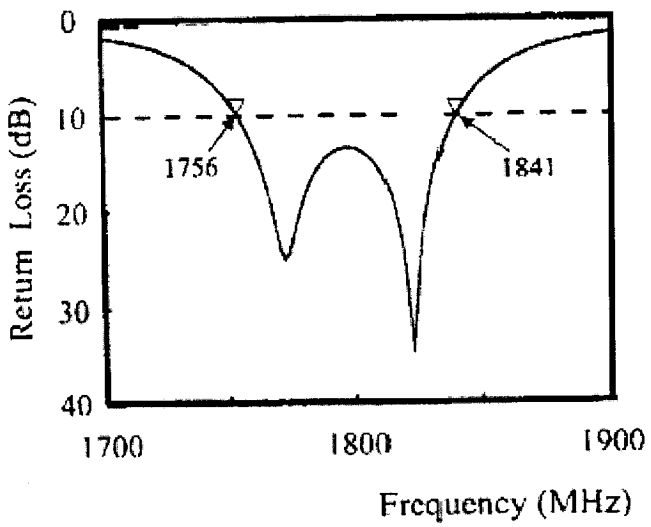

Figure 3.81 : Return Loss Measured Result of Antenna with Embedded Slots (After [41])

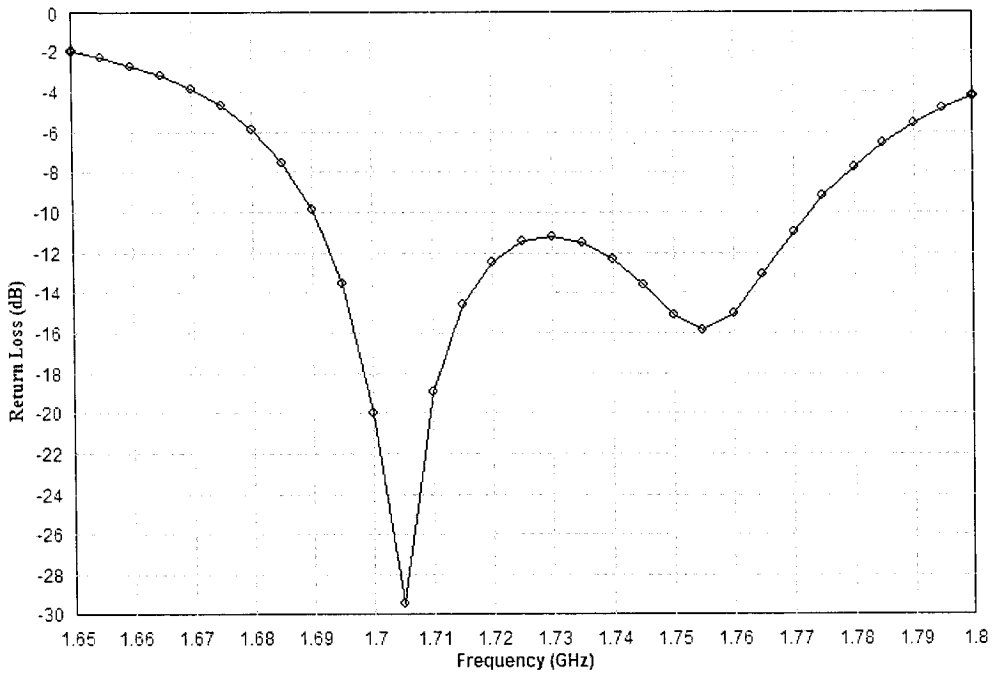

Figure 3.82 : Return Loss Simulation Result of Antenna with Embedded Slots

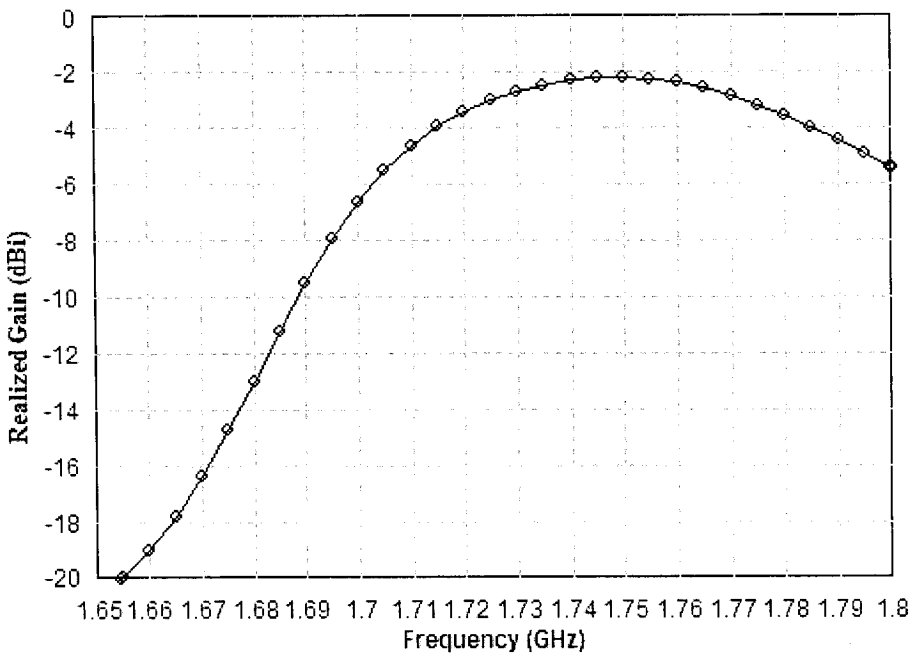

Figure 3.83 : Realized Gain of Antenna with Embedded Slots

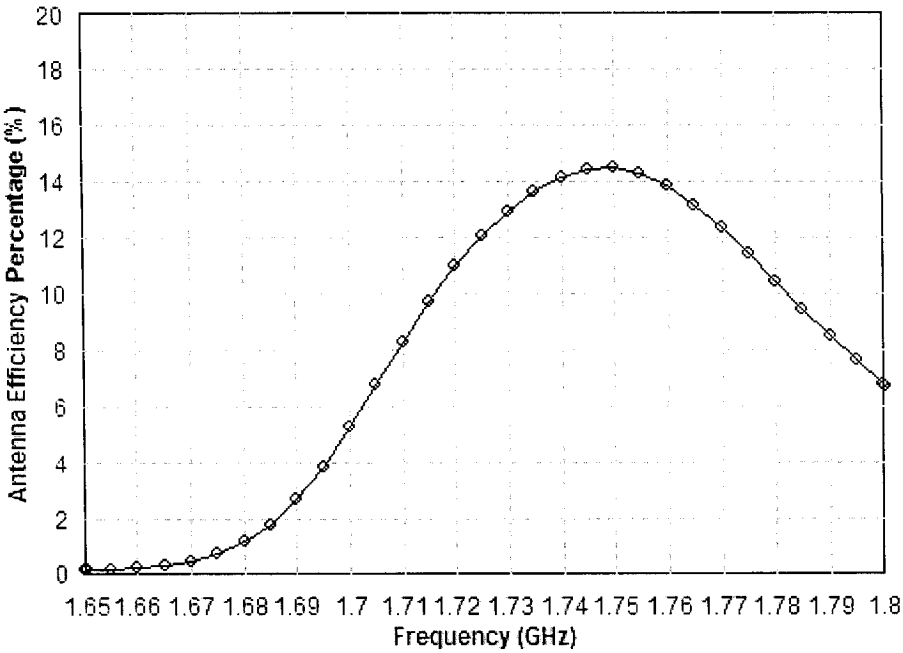

Figure 3.84 : Antenna Efficiency of Antenna with Embedded Slots

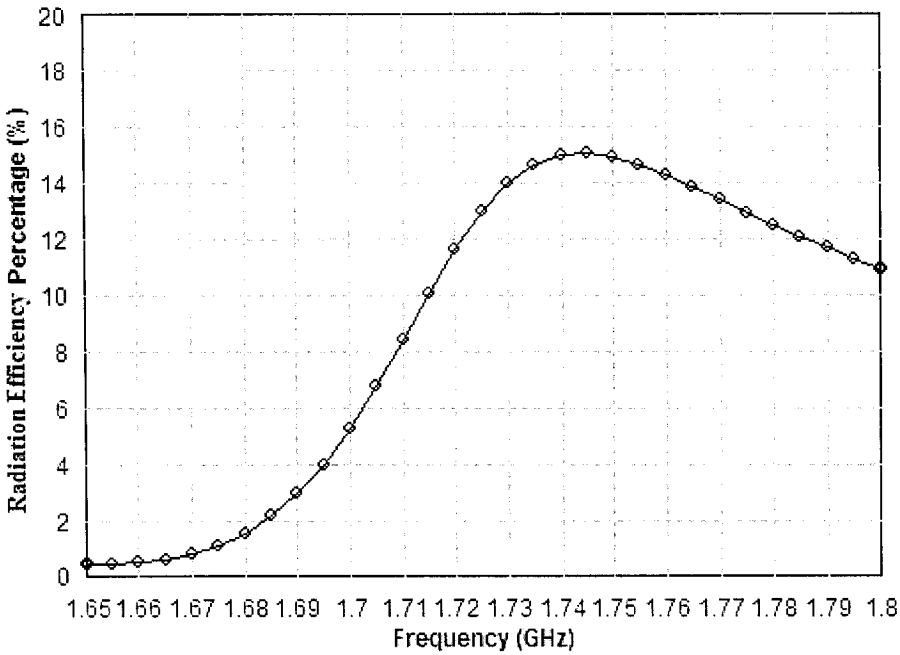

Figure 3.85 : Radiation Efficiency of Antenna with Embedded Slots

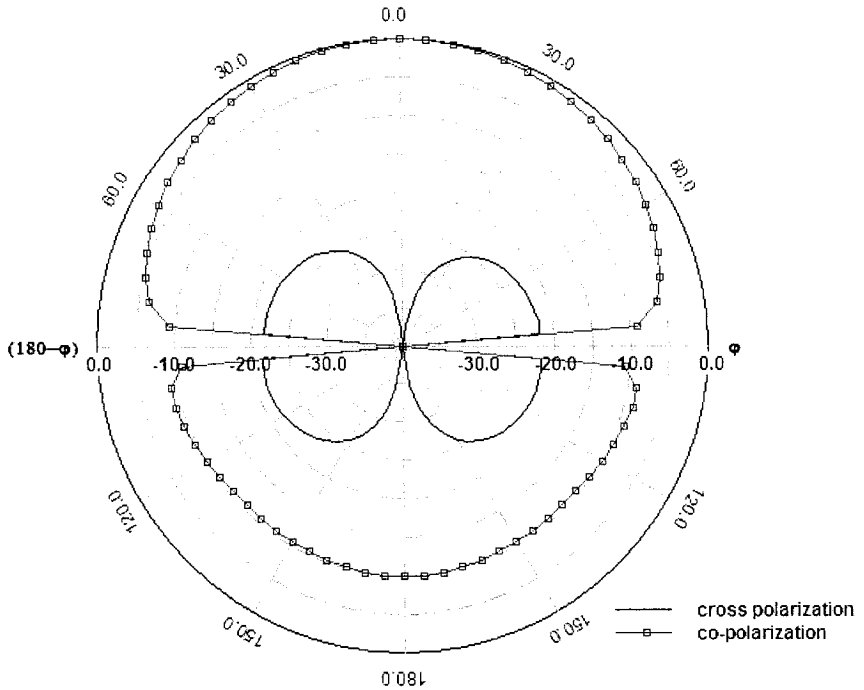

Figure 3.86 : H-Plane Radiation Patterns of Antenna with Embedded Slots at 1.7 GHz

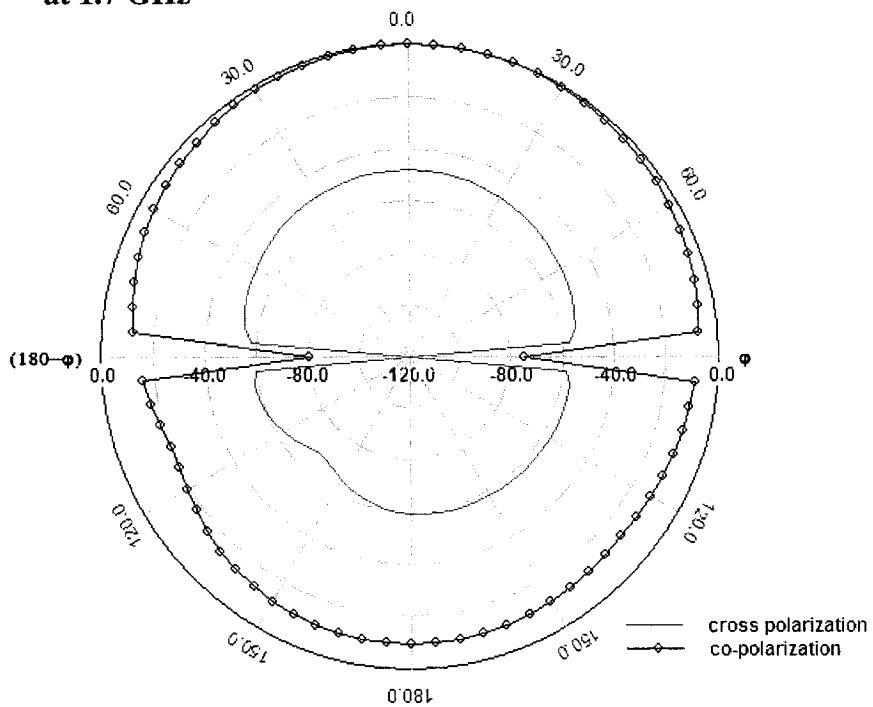

Figure 3.87 : E-Plane Radiation Patterns of Antenna with Embedded Slots at 1.7 GHz

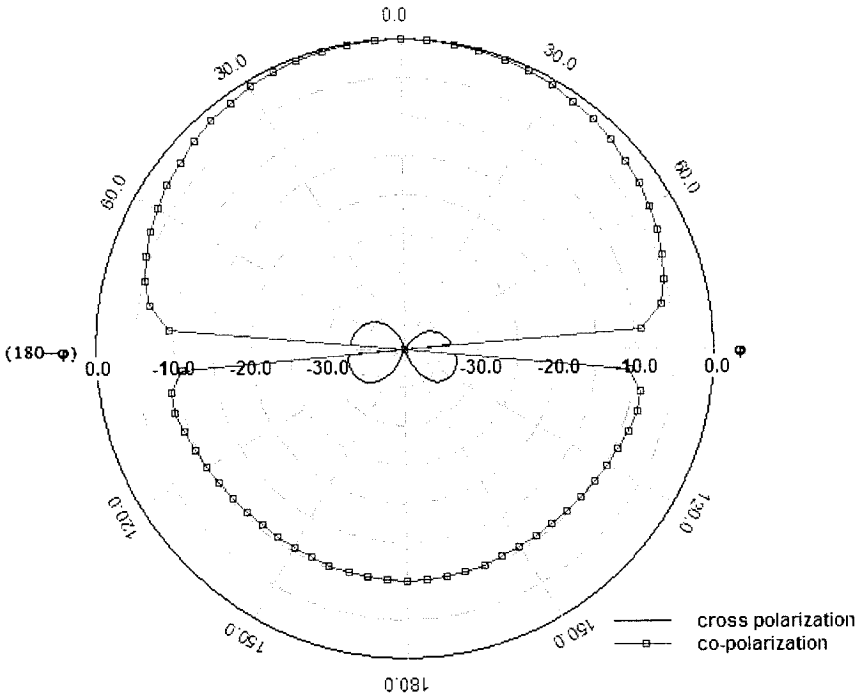

Figure 3.88 : H-Plane Radiation Patterns of Antenna with Embedded Slots at 1.73 GHz

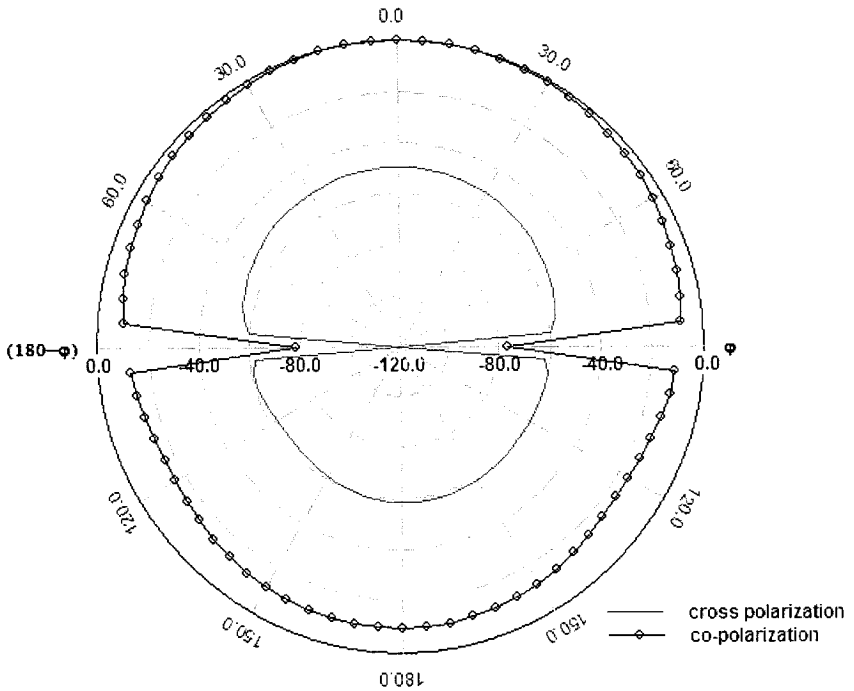

Figure 3.89 : E-Plane Radiation Patterns of Antenna with Embedded Slots at 1.73 GHz

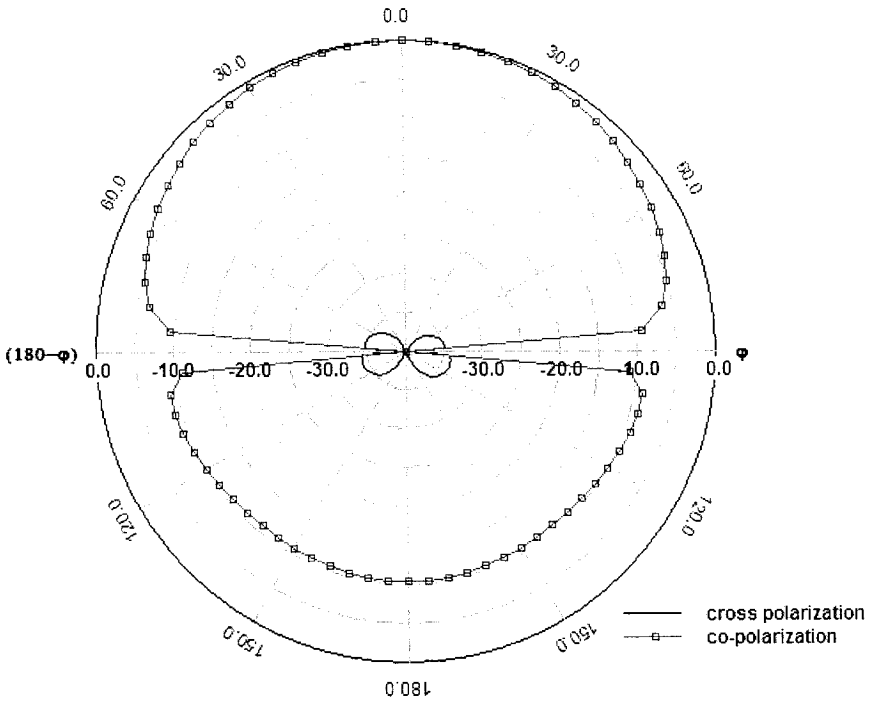

Figure 3.90 : H-Plane Radiation Patterns of Antenna with Embedded Slots at 1.76 GHz

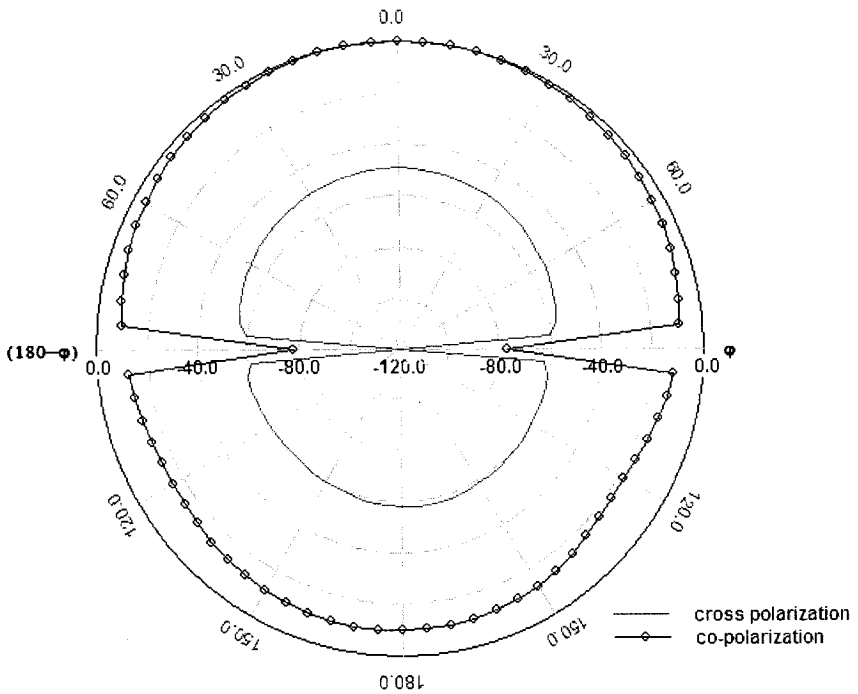

Figure 3.91 : E-Plane Radiation Patterns of Antenna with Embedded Slots at 1.76 GHz

We can tentatively summarise the performance of this particular configuration in the present sub-class of probe-fed microstrip patch antennas as follows:

- Bandwidth: limited broad bandwidth, around 5%
- Realized gain: very low, less than 0 dBi
- Antenna efficiency: very low, less than 20%
- Radiation efficiency: very low, less than 20%
- E-plane radiation pattern: stable, very low cross polarization level (cross-polarization is 50 dB less than co-polarization).
- H-plane radiation pattern: stable, very low cross polarization level (cross-polarization is 20 dB less than co-polarization).

The second antenna in this sub-class to be considered in detail is that shown in Figure 3.92, and whose modified patch geometry might be called "reactive loading" (as done by its originator [45]).

Figure 3.92 shows the geometry of a microstrip antenna with reactive loading. The antenna includes an equilateral triangular patch with a rectangular loading inserting in it. The dimensions of the antenna are based on [45], with manual optimization done using the full-wave simulator. The sideline length of the triangular is L = 50 mm. The cutting rectangular slot is 14.2 mm (length l_1) × 9.3 mm (width w_1). The rectangular loading is 6.9 mm (length l_2) × 7.3 mm (width w_2). The transmission line between the patch and the loading is 3.5 mm (length l_3) × 1 mm (width w_3). The feed point is t = 16.8 mm to the top of the triangular patch. The substrate is made of FR4 with thickness h = 1.6 mm. The ground plane is 80 mm × 80 mm. The antenna is designed to operate near 1.87 GHz.

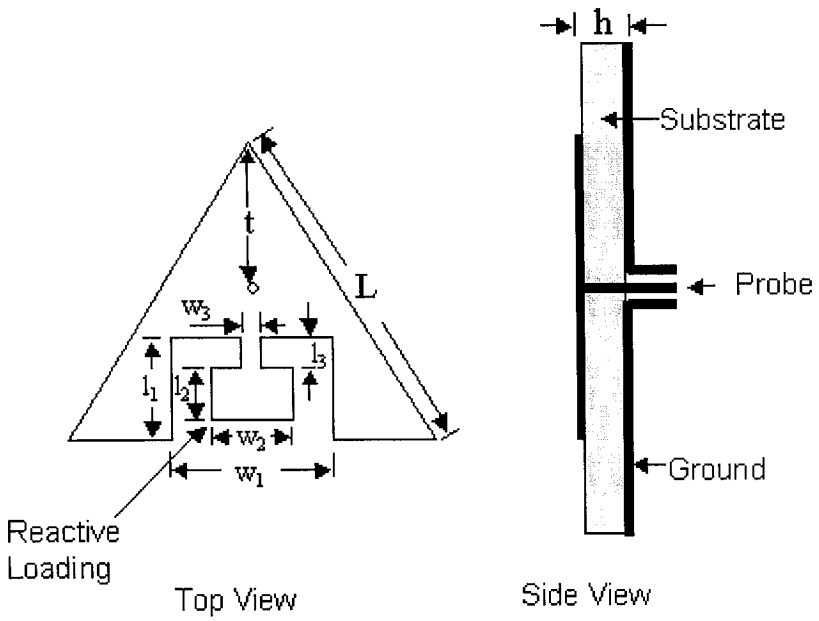

Figure 3.92 : Geometry of Antenna with Reactive Loading

We have compared return loss IE3D simulation result in Figure 3.94 to the measured result [45] in Figure 3.93. The good agreement serves to provide validation of the simulation results. The full-wave simulation results are shown in Figures 3.94 through 3.103. We observe that the return loss is less than -10 dB between 1.83 GHz and 1.91 GHz, implying an impedance bandwidth of 0.085 GHz, which is a fractional bandwidth of about 4.5% with respect to the center frequency of 1.87 GHz. As shown in Figure 3.95, the antenna realized gain varies between -8 dBi and -2 dBi over the above frequency band. Figure 3.96 reveals that the antenna efficiency is less than 20% over this same frequency range. Figure 3.97 shows that the radiation efficiency is less than 20% over the operating band. The radiation patterns at 1.83 GHz, 1.87 GHz and 1.9 GHz are shown in Figures 3.98 through 3.103. The H-plane co-polarization patterns are stable, with low cross polarization level over the operating band. The E-plane co-polarization patterns are also stable, with very low cross polarization level over the operating band.

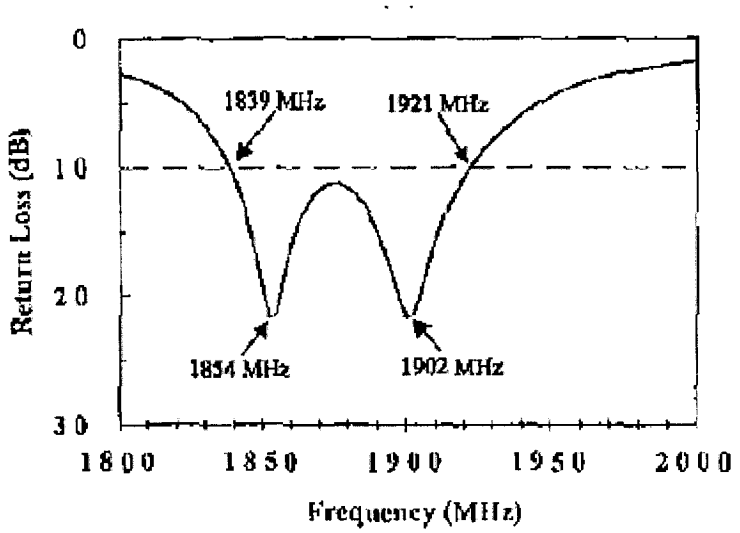

Figure 3.93 : Return Loss Measured Result of Antenna with Reactive Loading (After [45])

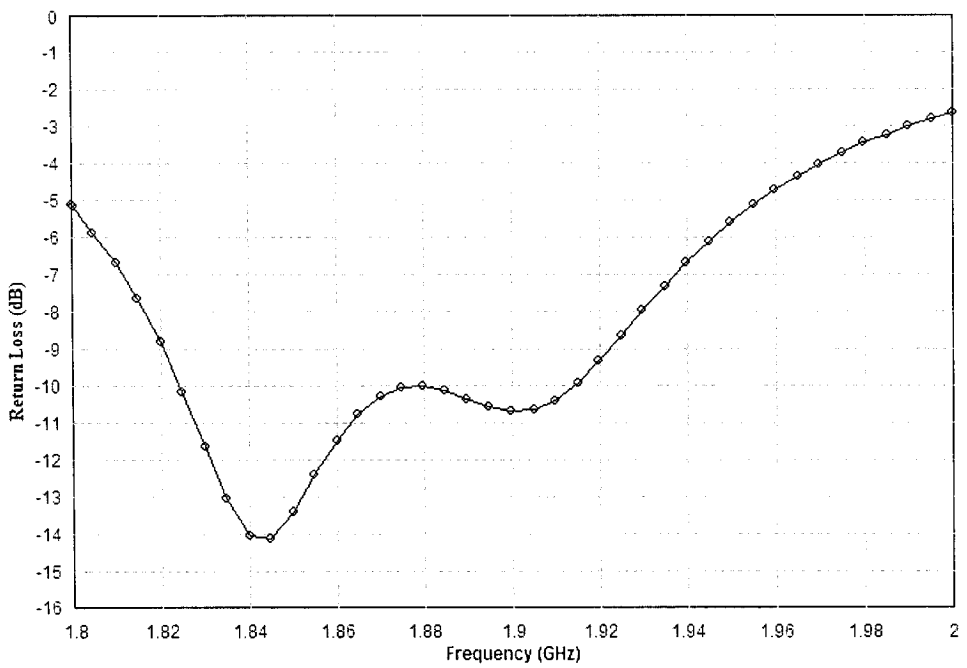

Figure 3.94 : Return Loss Simulation Result of Antenna with Reactive Loading

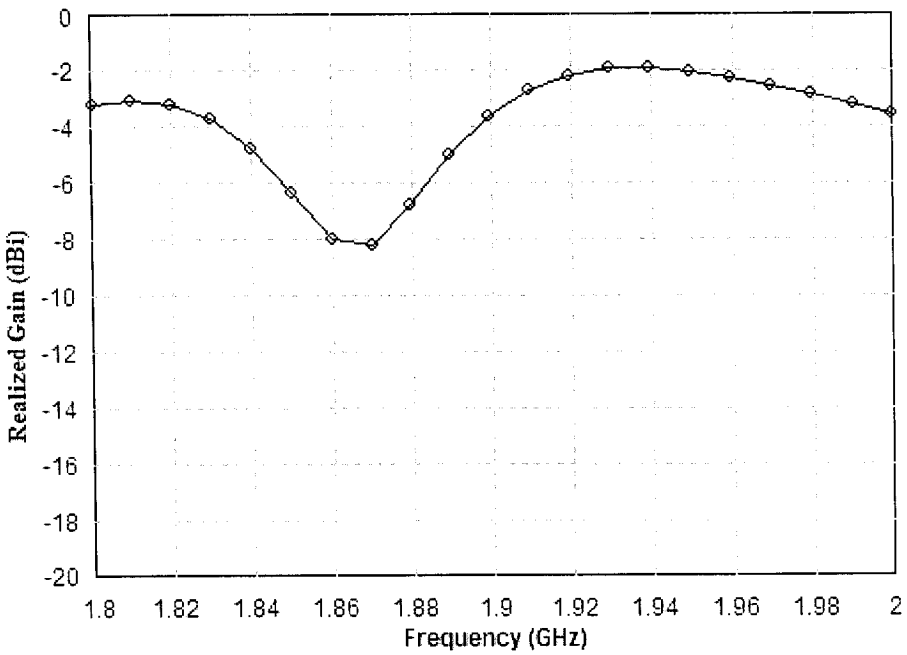

Figure 3.95 : Realized Gain of Antenna with Reactive Loading

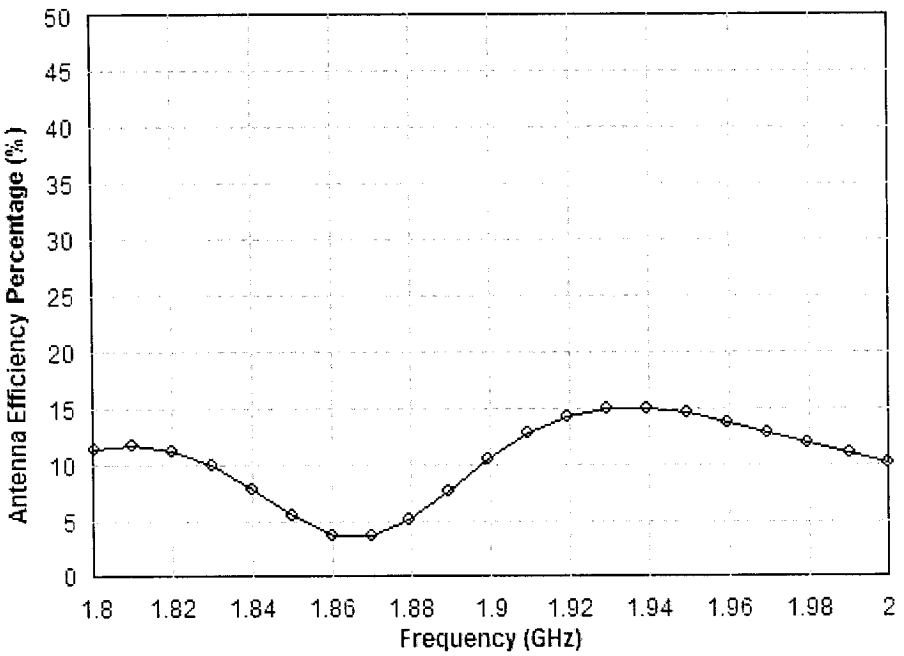

Figure 3.96 : Antenna Efficiency of Antenna with Reactive Loading

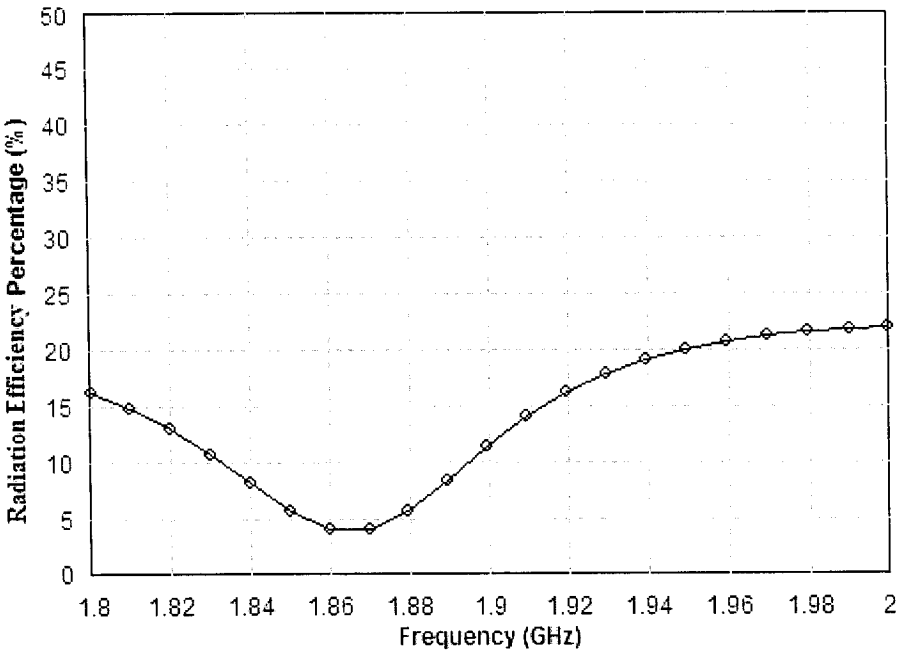

Figure 3.97 : Radiation Efficiency of Antenna with Reactive Loading

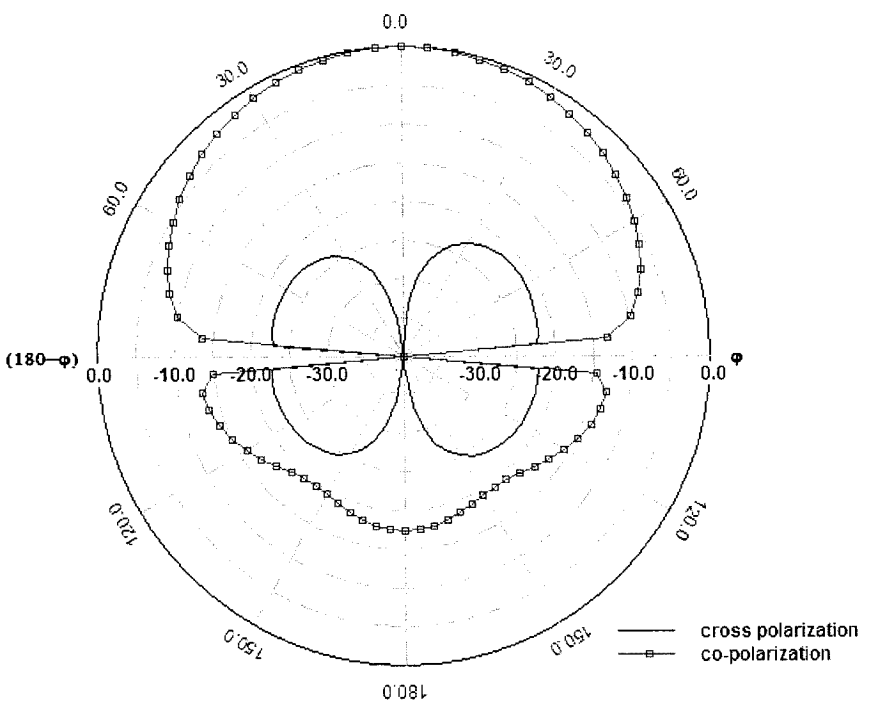

Figure 3.98 : H-Plane Radiation Patterns of Antenna with Reactive Loading at 1.83 GHz

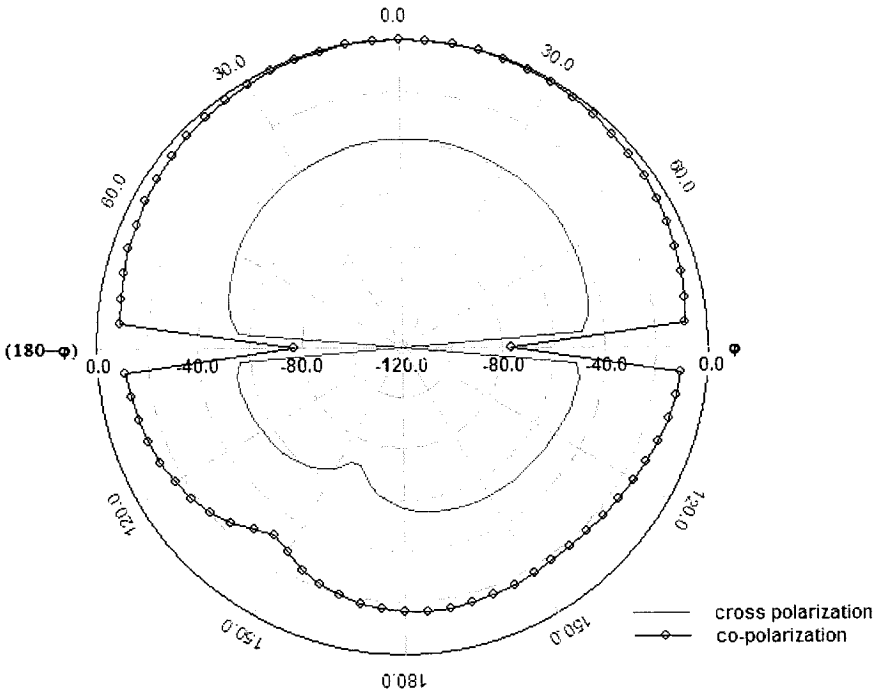

Figure 3.99 : E-Plane Radiation Patterns of Antenna with Reactive Loading at 1.83 GHz

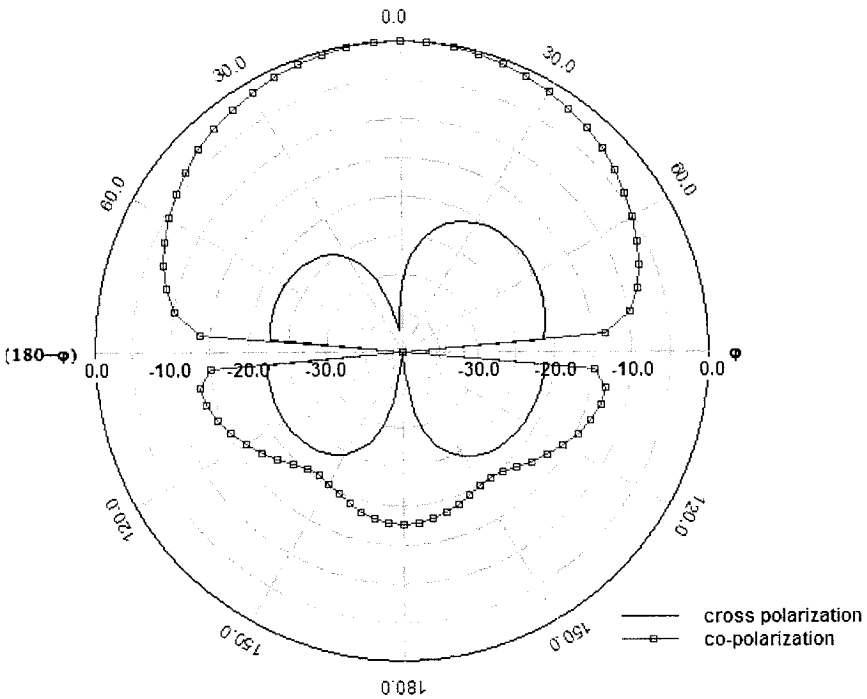

Figure 3.100 : H-Plane Radiation Patterns of Antenna with Reactive Loading at 1.87 GHz

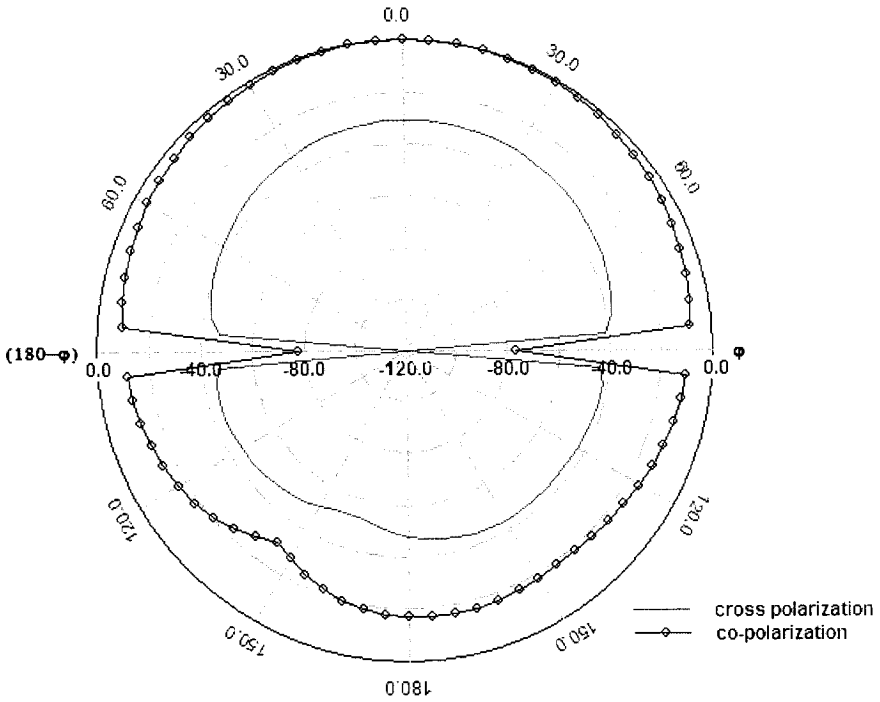

Figure 3.101 : E-Plane Radiation Patterns of Antenna with Reactive Loading at 1.87 GHz

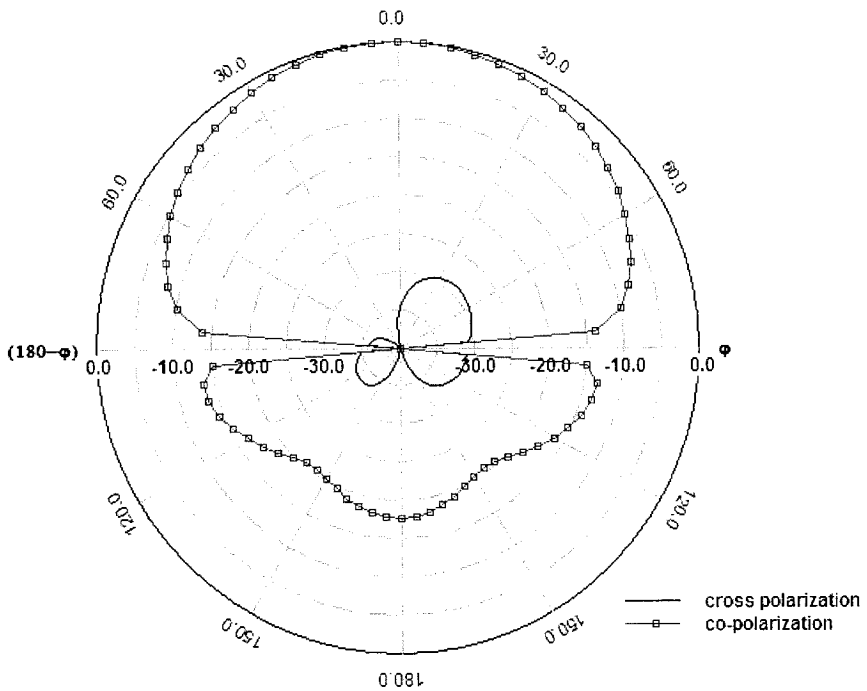

Figure 3.102 : H-Plane Radiation Patterns of Antenna with Reactive Loading at 1.90 GHz

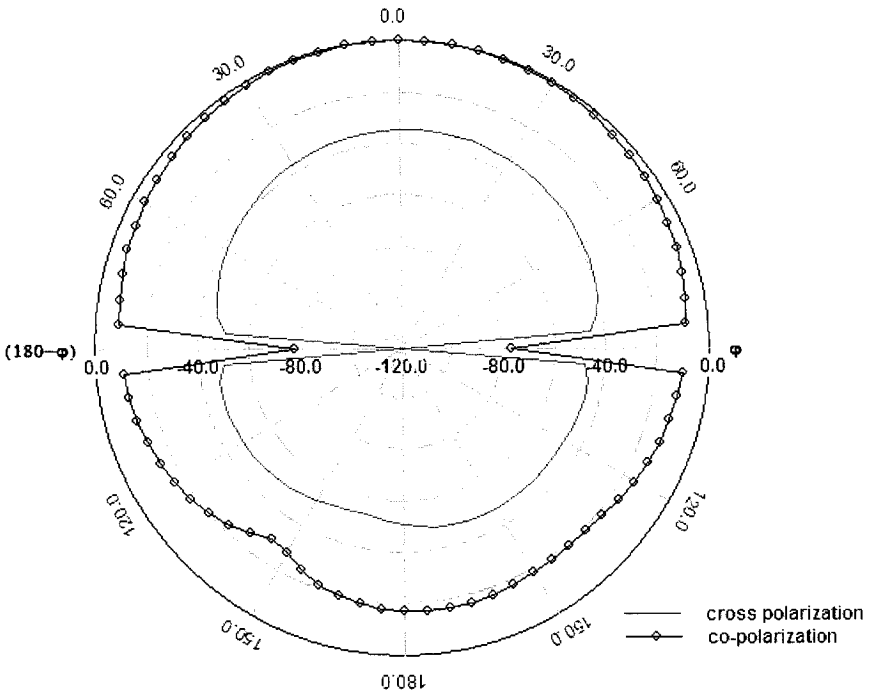

Figure 3.103 : E-Plane Radiation Patterns of Antenna with Reactive Loading at 1.90 GHz

A summary of the performance of this particular configuration in the present sub-class would read identically to that for the "embedded slot" example dealt with above. Thus that summary serves as that for the sub-class "electrically-thin high-permittivity substrate microstrip patch antenna with modified patch geometry".

We have observed that the simulation results of realized gain is relatively low for this sub-class of antennas. Unfortunately, measured results of realized gain are not given in [41] and [45].

3.5 HYBRID CONFIGURATIONS : THE USEFULNESS OF THE CHOSEN CATEGORISATION

In this section, we test the usefulness of the chosen categorization by putting quite complicated probe-fed patch antennas [47, 48, 49] into the categories we provided in Section 3.3 and 3.4. Shown in Figure 3.104 through 3.107, these antennas will be interpreted and classified in turn.

Figure 3.104 is showing that the antenna #1 has two patches in different layers and using different substrates. The new idea in this design is that: by using different substrates in different layers, the performance compensation between low-permittivity substrate antennas and high-permittivity substrate antennas becomes possible. If using low-permittivity substrate in the upper layer, this can be seen as a low-permittivity substrate antenna with modified probe, and has performances similar as Section 3.3.2. If using high-permittivity substrate in both layers, then this is a high-permittivity substrate antenna with parasitic elements, and has performances similar as Section 3.4.2. The performance results in [47] supported our classification.

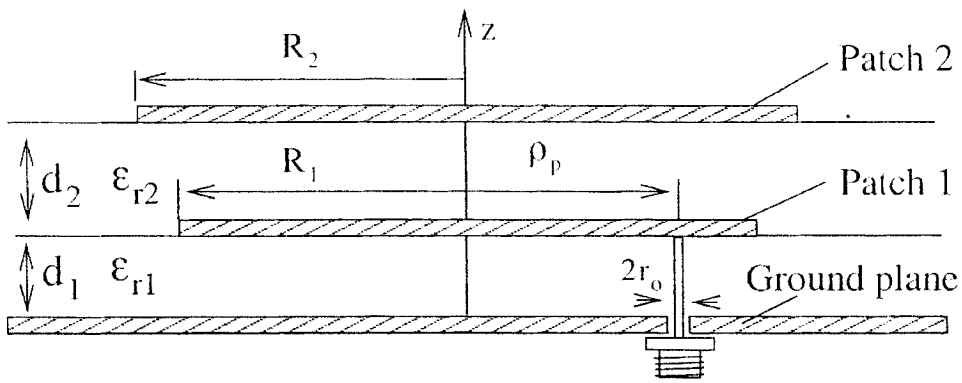

Figure 3.104 : Hybrid Microstrip Patch Antenna #1 (After [47])

The antenna #2 in Figure 3.105 is that one U-slotted patch in the lower layer and a rectangular patch in the upper layer with low-permittivity substrate in both layers. The lower patch is typical a low-permittivity substrate antenna with modified patch. The upper patch can be seen as a parasitic element. So this is a combination of antenna with modified patch and parasitic elements. We can predict that this antenna will have one more resonating frequency in the bandwidth compared to the antennas with modified patch in Section 3.3.3, so this antenna will have broader bandwidth. The performance results in [48] supported our classification.

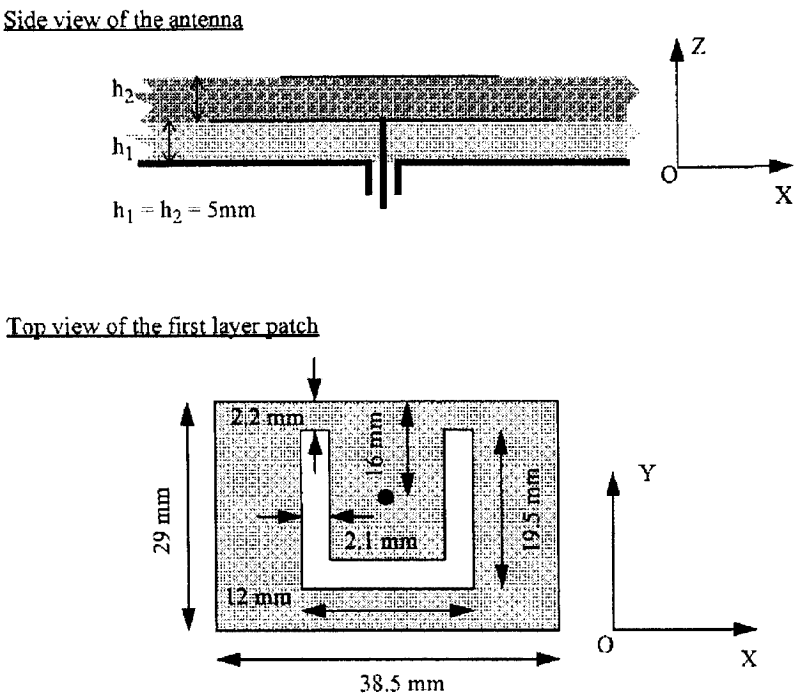

Figure 3.105 : Hybrid Microstrip Patch Antenna #2 (After [48])

The antenna #3 in Figure 3.106 is complicated because of its dual-band feature. A rectangular patch is directly fed from the probe, with another U-shaped edge-shorting patch gap-coupled to it. The substrate is low-permittivity. The ordinary rectangular patch will generate a band with less than 10% bandwidth. The U-shaped edge-shorting patch can been seen as a low-permittivity substrate antenna with shorting wall. So it will have similar performances as antennas in Section 3.3.5, such as more than 10% bandwidth. Totally, antenna #3 will generate two resonating bands, in which one is narrow and the other is broadband. The performance results in [49] supported our classification.

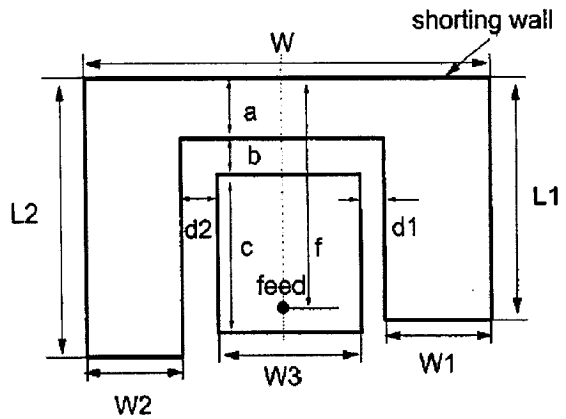

Figure 3.106 : Hybrid Microstrip Patch Antenna #3 (After [49])

The antenna #4 in Figure 3.107 is one step more complicated than the antenna #3. An E-shaped patch is directly fed from the probe, with another U-shaped edge-shorting patch gap-coupled to it. The substrate is low-permittivity. The E-shaped patch can be seen as a low-permittivity substrate antenna with modified patch as Section 3.3.3, with more than 10% bandwidth. Same as above mentioned, the U shaped edge-shorting patch

can been seen as a low-permittivity substrate antenna with shorting wall. It will have similar performances as antennas in Section 3.3.5, such as more than 10% bandwidth. Totally, antenna #4 will generate two resonating bands and both of them are broadband. The performance results in [49] supported our classification.

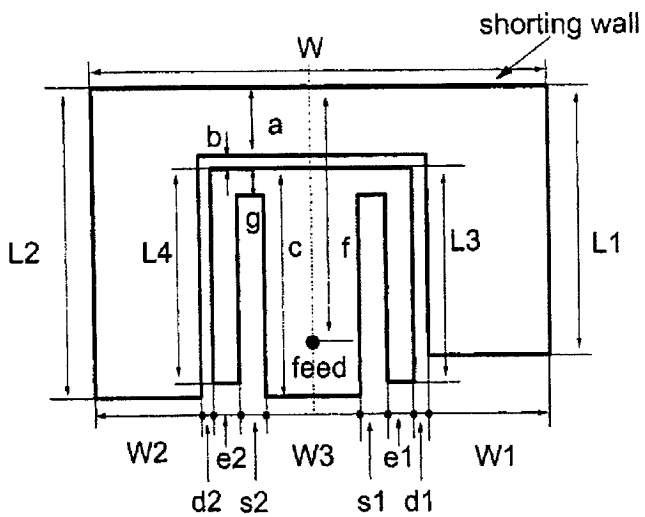

Figure 3.107 : Hybrid Microstrip Patch Antenna #4 (After [47])

In summary, some complicated hybrid microstrip patch antennas have been successfully classified into categories in Section 3.3 and 3.4. Also we can generally predict these antennas' performances. The usefulness of the chosen categorization has been proved.

3.6 CONCLUDING REMARKS

Based on an in-depth survey of the literature on bandwidth enhancement techniques for probe-fed microstrip patch antennas, this chapter has succeeded in dividing the approaches into two major classes. These are those antennas that utilize electrically-thick low-permittivity substrates, and those that use utilize electrically-thin high-permittivity substrates. These two classes have been further broken down into several sub-classes, as shown in Figure 3.3. We maintain that all probe-fed patch antennas can be either identified as belonging to one of these sub-classes or at once be seen to consist of a combination of the techniques used in two or more sub-classes. We have been able to test this hypothesis by selecting additional papers (not listed in the references) at random, and have demonstrated this using the hybrid configurations in Section 3.5. Full-wave analyses have been done of representative examples of antennas falling into each of the above-mentioned sub-classes. In each case the complete performance of the antenna has been presented: bandwidth, radiation efficiency, antenna efficiency, realized gain and radiation patterns (co- and cross-polarisation). There is a tendency, in the literature surveyed, for authors to reveal only some of the above performance indicators for a specific antenna. Information on the efficiencies is suspiciously absent! The data presented Section 3.3 and 3.4 will allow one to do a proper trade-off judgement on the best antenna for a particular application. For instance, if two given sub-classes of patch antenna provide the same acceptable bandwidth for some chosen application, how does one decide which one to use? The data presented here will allow such a decision to be made based on the performance indicators other than the bandwidth, or on the fabrication complexity (e.g.

single-layer versus double layer). It will therefore be collected and further summarised in Chapter 4.

3.7 REFERENCES FOR CHAPTER 3

[1] D.M.Pozar & D.H.Schaubert (Edits.), Microstrip Antennas : The Analysis and Design of Microstrip Antennas and Arrays (IEEE Press, 1995).

[2] Foam substrate (Rohacell HF71 and Rohacell 51 have ε_r between 1.05 and 1.07, and tan δ = 0.001 up to 40GHz. www.rohacell.com

[3] K.F.Lee & W.Chen, *Advances in Microstrip and Printed Antennas* (Wiley, 2002).

[4] K.M. Luk, C.L. Mak, Y.L. Chow, and K.F. Lee, "Broadband microstrip patch antenna", Electron. Lett., vol. 34, pp. 1442-1443, July 1998.

[5] C.L. Mak, K.F. Lee, and K.M. Luk, "Broadband patch antenna with T-shaped probe", IEE Proc. Microw. Antennas Propag., vol. 147, pp. 73–76, April 2000.

[6] Y.X.Guo, K.M.Luk & K.F.Lee, "L-probe proximity-fed annular ring microstrip antennas", IEEE Trans. Antennas Propagat., vol. 49, pp. 19 – 21, Jan. 2001.

[7] Y.X.Guo, C.L.Mak, K.M.Luk & K.F.Lee, "Analysis and design of L-probe proximity-fed patch antennas", IEEE Trans. Antennas Propagat., vol. 49, no.2, pp. 145-149, Feb. 2001.

[8] G.Mayhew-Ridgers, J.W.Odendaal & J.Joubert, "Single-layer capacitive feed for wideband probe-fed microstrip antenna elements", IEEE Trans. Antennas Propagat., vol. 51, pp. 1405-1407, June 2003.

[9] Y.X.Guo, K.M.Luk & K.F.Lee, "L-probe fed thick-substrate patch antenna mounted on a finite groundplane", IEEE Trans. Antennas Propagat., vol. 51, no.8, pp. 1955 – 1963, Aug.2003.

[10] A.A. Kishk, K.F. Lee, W.C. Mok, and K.M. Luk, "A Wide-band small size microstrip antenna proximately coupled to a hook shape probe", IEEE Trans. Antennas Propagat., vol. 52, pp. 59 – 65, Jan. 2004.

[11] T.Huynh & K.F.Lee, "Single-layer single-patch wideband microstrip antenna", Electron. Lett., vol. 31, pp. 1310-1312, Aug.1995.

[12] K.F.Lee, K.M.Luk, K.F.Tong, S.M.Shum, T.Huynh & R.Q.Lee, "Experimental and simulation studies of the coaxially fed U-slot rectangular patch antenna", IEE Proc.-Microwav. Antennas Propag., Vol.144, No.5, pp.354-358, Oct.1997.

[13] K.L. Wong and W.H. Hsu, "Broadband triangular microstrip antenna with U-shaped slot", Electron. Lett., vol. 33, pp. 2085 – 2087, Dec. 1997.

[14] Z.N.Chen & M.Y.W.Chia, "Broadband probe-fed notched plate antenna", Electron. Lett., vol. 36, pp. 599-600, March 2000.

[15] K.L. Wong and W.H. Hsu, "A broadband patch antenna with wide slits", IEEE Int. AP-S Symp. Digest, vol. 3, pp. 1414 – 1417, July 2000.

[16] Z.N.Chen & M.Y.W.Chia, "Broadband suspended plate antenna with probe-fed strip", IEE Proc.-Microwav Antennas Propag., Vol.148, No.1, pp.37-40, Feb.2001.

[17] W.H. Hsu and K.L. Wong, "Broadband probe-fed patch antenna with reduced cross-polarization radiation", IEE Conf. Antennas Propagat., vol. 2, pp. 525 – 528, April 2001.

[18] F.Yang, X.Zhang, X.Yer & Y.Rahmat-Samii, "Wide-band E-shaped patch antennas for wireless communications", IEEE Trans. Antennas Propagat., Vol.49, No.7, pp.1094-1100, July 2001.

[19] K.L. Wong and W.H. Hsu, "A broad-band rectangular patch antenna with a pair of wide slits", IEEE Trans. Antennas Propagat., Vol.49, No.9, pp.1345-1347, September 2001.

[20] W.H.Hsu & K.L.Wong, "A broad-band probe-fed patch antenna with a U-shaped groundplane for cross-polarisation reduction", IEEE Trans. Antennas Propagat., Vol.50, No.3, pp.352-355, March 2002.

[21] A.K. Shackelford, K.F. Lee, and K.M. Luk, "Design of small-size wide-bandwidth microstrip-patch antennas", IEEE Antennas Propagat. Mag., vol. 45, pp. 75 – 83, Feb. 2003.

[22] Y.Ge, K.P.Esselle & T.S.Bird, "Broadband E-shaped patch antenna for 5-6GHz wireless computer networks", IEEE Int. AP-S Symp. Digest, July 2003.

[23] Gh.Z.Rafi & L.Shafai, "Circular-arc single layer microstrip antenna for wideband applications", IEEE Int. AP-S Symp. Digest, July 2003.

[24] X.X.Zhang & F.Yang, "Study of a slit cut on a micristrip antenna and its applications", Microwave & Optical Tech. Lett., Vol.18, No.4, pp.297-300, July 1998.

[25] Z.N. Chen and M.Y.W. Chia, "Design of broadband probe-fed plate antenna with stub", IEE Proc. Microw. Antennas Propagat., vol. 148, pp. 221 – 226, Aug. 2001.

[26] R.Chair, K.F.Lee & K.M.Luk, "Bandwidth and cross-polarisation characteristics of quarter-wave shorted patch antennas", Microwave & Optical Tech. Lett., Vol.22, No.2, pp.101-103, July 1999.

[27] Y.J. Wang, C.K. Lee, and W.J. Koh, "Single-patch and single-layer square microstrip antenna with 67.5% bandwidth", IEE Proc. Microw. Antennas Propagat., vol. 148, pp. 418 – 422, Dec. 2001.

[28] W.C. Mok, R. Chair, K.M. Luk, and K.F. Lee, "Wideband quarter-wave patch antenna with shorting pin", IEE Proc. Microw. Antennas Propagat., vol. 150, pp. 56 – 60, Feb. 2003.

[29] R.Chair, W.C.Mok, K.M.Luk & K.F.Lee, "A wideband rectangular patch antenna with shorting pins", Microwave & Optical Tech. Lett., Vol.37, No.3, pp.165-167, May 2003.

[30] M.C.Huynh & W.Stutzman, "Ground plane effects on planar inverted-F antenna (PIFA) performance", IEE Proc.-Microwav Antennas Propag., Vol.150, No.4, pp.209-213, Aug.2003.

[31] P.S.Hall, C.Wood & C.Garrett, "Wide bandwidth microstrip antenna for circuit integration", Electronics Letters, Vol.15, pp.458-460, 1979.

[32] C.Wood, "Improved bandwidth of microstrip antennas using parasitic elements", IEE Proc., Pt.H, Vol.127, pp.231-234, 1980.

[33] A.Sabban, "A new broadband stacked two-layer microstrip antenna", IEEE AP-S Int. Symp. Digest, pp.63-66, 1983

[34] G. Kumar and K.C.Gupta, "Nonradiating edges and four edges gap-coupled multiple resonator broad-band microstrip antennas", IEEE Trans. Antennas Propagat., Vol. 33, No.2, pp.173-178, Feb.1985.

[35] G. Kumar and K.C.Gupta, "Directly coupled multiple resonator wide-band microstrip antennas", IEEE Trans. Antennas Propagat., Vol. 33, No.6, pp.588-593, June 1985.

[36] K.M. Luk, K.F. Tong, and T.M. Au, "Offset dual-patch microstrip antenna", Electron. Lett., vol. 29, pp. 1635 – 1636, Sept. 1993.

[37] M. Sanad, "A compact dual-broadband microstrip antenna having both stacked and planar parasitic elements", IEEE AP-S Int. Symp. Digest, Vol. 1, pp. 6 – 9, July 1996.

[38] C. K. Wu and K. L. Wong, "Broadband microstrip antenna with directly coupled and parasitic patches", Microw. Optic. Lett., vol. 22, pp. 348 – 349, Sept. 1999.

[39] Y.P.Zhang, C.W.Y.Ang, C.S.C.Lee & M.A.Do, "A stacked patch antenna of very high-permittivity material", Microwave & Optical Tech. Lett., Vol.27, No.6, pp.395-396, Dec.2000.

[40] G. Kumar and K.P. Ray, "Stacked gap-coupled multi-resonator rectangular microstrip antennas", IEEE AP-S Int. Symp. Digest, Vol. 3, pp. 514 – 517, July 2001.

[41] J. Y. Sze & K.L.Wong, "Designs of broadband microstrip antennas with embedded slots", IEEE Antennas Propagat. Soc. Int. Symp., vol. 2, pp. 936 – 939, July 1999.

[42] J. W. Wu and J. H. Lu, "Slotted circular microstrip antenna for bandwidth enhancement", IEEE Antennas Propagat. Soc. Int. Symp., vol. 2, pp. 272 - 275, June 2003.

[43] T. W. Chiou and K. L. Wong, "Designs of compact microstrip antennas with a slotted ground plane", IEEE Antennas Propagat. Soc. Int. Symp., vol. 2, pp. 732 – 735, July 2001.

[44] K. L. Wong and J. Y. Jan, "Broadband circular microstrip antenna with embedded reactive loading", Electron. Lett., vol. 34, pp. 1804 – 1805, Sept. 1998.

[45] K. L. Wong, J. S. Kuo, S. T. Fang, and T. W. Chiou, "Broadband microstrip antennas with integrated reactive loading", 1999 Asia Pacific Microw. Conf., vol. 2, pp. 352 – 354, Nov. Dec.

[46] J. Y. Jan and K. L. Wong, "Broadband circular microstrip antennas with embedded reactive loading in the patch and the ground plane", IEEE Antennas Propagat. Soc. Int. Symp., vol. 3 , pp. 56, June 2002.

[47] A.Mitchell, M.Lech, D.M.Kokotoff & R.B.Waterhouse, "Search for high-performance probe-fed stacked patches using optimization", IEEE Trans. Antennas Propagat., vol. 51, no.2, pp.249-255, Feb.2003.

[48] M.Clenet, C.B.Ravipati & L.Shafai, "Bandwidth enhancement of U-slot microstrip antenna using a rectangular stacked patch", Microwave & Optical Tech. Lett., Vol.21, No.6, pp.393-395, Dec.2000.

[49] Y.X.Guo, K.M.Luk, K.F.Lee & R.Chair, "A quarter-wave U-shaped patch antenna with two unequal arms for wideband and dual-frequency operation", IEEE Trans. Antennas Propagat., vol. 50, no.8, pp. 1082-1087, Aug.2002.

CHAPTER 4

PERFOMANCE TRADE-OFF SUMMARY & NEW MICROSTRIP PATCH ANTENNA STRUCTURE

4.1 GOALS

In Section 4.2 we will collect and summarised in tabular form the performance findings of Chapter 3. We will in Section 4.3 demonstrate how the increased understanding afforded by the classification of the broadbanding techniques, that formed the subject of Chapter 3, can be used to devise further improvements. In the process we will demonstrate the performance of novel antenna that has not previously been described in the literature. Section 4.4 concludes the chapter.

4.2 PERFORMANCE TRADE-OFF SUMMARY OF PROBE-FED MICROSTRIP PATCH ANTENNA BROADBANDING TECHNIQUES

As shown in the Table 4.1, broadband microstrip antennas with electrically thick low permittivity substrate usually use thick air/foam substrate. The antennas performances include: very broad bandwidth (20% or broader, some of them can easily have 40% bandwidth); high realized gain (8~10 dBi without shorting); high antenna efficiency and radiation efficiency (> 80% dBi without shorting); and poor H-plane polarization purity (10 dB or less difference between co-polarization and cross-polarization).

On the other hand, broadband microstrip antennas with electrically thin high permittivity substrate usually use thin FR4 substrate, which is commonly used material in

print circuit board. The antennas performances include: 10% or less bandwidth; low realized gain (3 dBi or less), very low antenna efficiency and radiation efficiency (<20%); and good polarization purity in both H-plane and E-plane.

Table 4.1 : Comparison of Techniques for Microstrip Antennas with Electrically Thick Low Permittivity Substrate and Techniques for Microstrip Antennas with Electrically Thin High Permittivity Substrate

Items for Comparison		***Techniques for microstrip antennas with electrically thick low permittivity substrate***	***Techniques for microstrip antennas with electrically thin high permittivity substrate***
Physical Character	Thickness	Thick (about 0.1 λ)	Thin (about 0.01 λ)
	Substrate Permittivity	Air/Foam	FR4
Broadband Principle		Reactance compensation	Multiple resonating elements
Antenna Performance	Bandwidth	> 20%	Around 10% or less
	Realized Gain	Around 9 dBi (without shorting) Around 3 dBi (with shorting)	< 3 dBi
	Antenna Efficiency	> 80% (without shorting) > 50% (with shorting)	< 30%
	Radiation Efficiency	> 80% (without shorting) > 60% (with shorting)	< 30%
	Radiation Patterns	Good polarization purity in E-plane; Poor polarization purity in H-plane	Good polarization purity in both E-plane and H-plane

In a word, broadband microstrip antennas with electrically thick low permittivity substrate have broader bandwidth, higher realized gain, higher antenna efficiency and radiation efficiency, but worse H-plane polarization purity than the ones with electrically thin high permittivity substrate.

Table 4.2 gives the features of broadband techniques for microstrip antennas with electrically thick low permittivity substrate. Among them, antenna with modified feed technique can achieve the broadest bandwidth (> 40%), high realized gain, high antenna efficiency and radiation efficiency, the second worst polarization purity in H-plane; Antenna with modified patch technique and antenna with stub technique both have broad bandwidth (20%) highest realized gain, high antenna efficiency and radiation efficiency, and the best polarization purity in H-plane; Antenna with shorting walls and pins technique can achieve broad bandwidth (20%), moderate realized gain, moderate antenna efficiency and radiation efficiency, and the worst polarization purity in H-plane. We also notice that antenna with modified feed technique usually need more complicate feeding structure, and antenna with shorting walls and pins technique can largely reduce antenna size.

Table 4.2 : Comparison of Broadband Techniques for Microstrip Patch Antennas With Electrically Thick Low Permittivity Substrate

Antenna Performances	***Antenna with modified feed***	***Antenna with modified patch***	***Antenna with stub***	***Antenna with shorting walls and pins***
Bandwidth	> 35%	Around 20%	Around 20%	Around 20%
Realized Gain	Around 8 dBi	Around 9 dBi	Around 9 dBi	Around 3.5 dBi
Antenna Efficiency	> 80%	> 90%	> 80%	> 50%
Radiation Efficiency	> 90%	> 90%	> 90%	> 60%
Radiation Patterns	Very high cross-pol in H-plane, -5 dB to co-pol	High cross-pol in H-plane, -10 dB to co-pol	High cross-pol in H-plane, -10 dB to co-polar	Very high cross-pol in H-plane, may higher than co-pol; max co-pol excursive from center in E-plane

As shown in Table 4.3, antenna with parasitic elements technique can achieve broader bandwidth (10%), higher realized gain, higher antenna efficiency and radiation efficiency, good polarization purity; antenna with modified patch technique can achieve limited broad bandwidth (5%), low realized gain, low antenna efficiency and radiation efficiency, and good polarization purity.

Table 4.3 : Comparison of Broadband Techniques for Microstrip Patch Antennas with Electrically Thin High Permittivity Substrate

Antenna Performances	*Antenna with parasitic elements*	*Antenna with modified patch*
Bandwidth	Around 10%	Around 5%
Realized Gain	Flat, around 2 dBi	Not flat, < 0 dBi
Antenna Efficiency	< 30%	< 30%
Radiatin Efficiency	< 30%	< 30%
Radiation Patterns	Good polarization purity, max co-polarization may offset from center	Good polarization purity

4.3 A NEW PROBE-FED MICROSTRIP PATCH ANTENNA USING TWO FORMS OF MODIFIED PROBE GEOMETRY : EMBEDDED SLOTS AND REACTIVE LOADING

4.3.1 Antennas with Embedded Slots and Reactive Loading Geometries

Two forms of modified patch geometry were discussed in Section 3.4.3 for electrically-thin high-permittivity substrate antennas, namely embedded slots and reactive loading. The patch antenna overall performance using these techniques was found to be very similar, with a fractional bandwidth of 5%. Both of these approaches to modifying

the patch geometry utilize closely-spaced multiple resonances to enhance the antenna bandwidth. Based on the understanding afforded by the classifications in Chapter 3, in order to further improve the antenna bandwidth, we combined both the embedded slot and reactive loading approaches to patch geometry modification, as shown in Figure 4.1. This constitutes a new probe-fed patch geometry that has not been previously proposed by other authors. We will demonstrate through full-wave simulation that this increases the antenna bandwidth from 4.6% to 9.1%.

The dimensions of the patch and the pair of toothbrush-shape slots are based on [41] and the Figure 3.80 from Section 3.4.3. The dimensions of toothbrush-shape slots are the same as [41]: The patch is 37.3 mm (length L) × 24.87 mm (width W). The slots consist of a pair of bent slots with 15° bent angle and a pair of three protruding slots, which are 2 mm spacing to the next one and different widths as 9 mm (w_1), 8.5mm (w_2) and 8 mm (w_3). A reactive loading is added in the middle. The cutting rectangular slot is 22.65 mm (length l_4) × 2 mm (width w_4). The rectangular reactive loading is 22.5 mm (length l_5) × 1.2 mm (width w_5). The feed point is g = 11.15 mm from lower edge of the patch. The substrate is made of FR4 with thickness h = 2.6 mm. The ground plane is 60 mm × 60 mm.The antenna is designed to operate near 1.75 GHz.

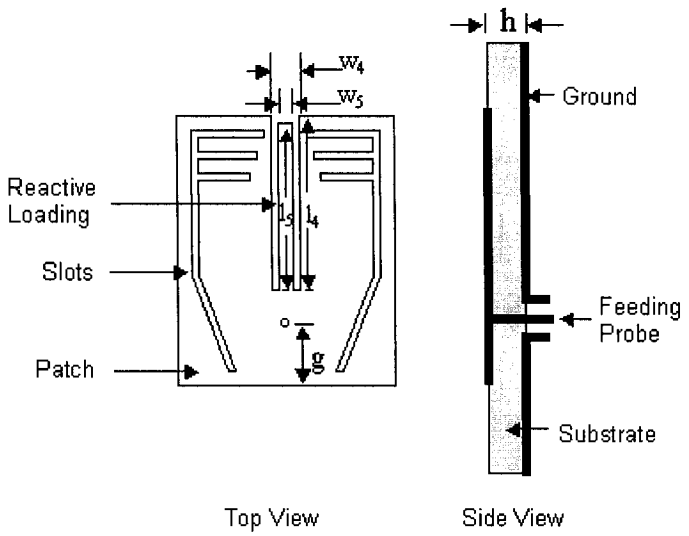

Figure 4.1 : Geometry of Antenna with Two Forms of Patch Geometry Modification Combined

The full-wave simulation results are shown in Figures 4.2 through 4.11. We observe that the return loss is less than -10 dB between 1.68 GHz and 1.84 GHz, implying an impedance bandwidth of 0.16 GHz, which is a fractional bandwidth of about 9.1% with respect to the center frequency of 1.75 GHz. As shown in Figure 4.3, the antenna realized gain varies between -9 dBi and 0 dBi over the above frequency band. Figure 4.4 reveals that the antenna efficiency is less than 25% over this same frequency range. Figure 4.5 shows that the radiation efficiency is less than 30% over the operating band. The radiation patterns at 1.69 GHz, 1.75 GHz and 1.84 GHz are shown in Figures 4.6 through 4.11. The H-plane and E-plane co-polarization patterns are stable, with low cross polarization level over the operating band.

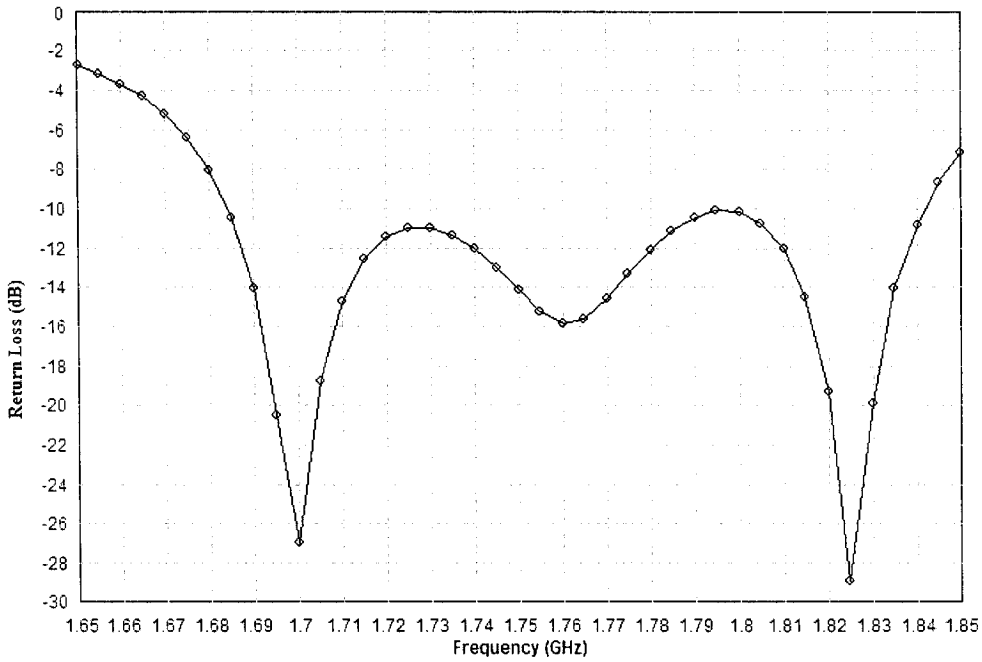

Figure 4.2 : Return Loss of Antenna with Embedded Slots and Reactive Loading

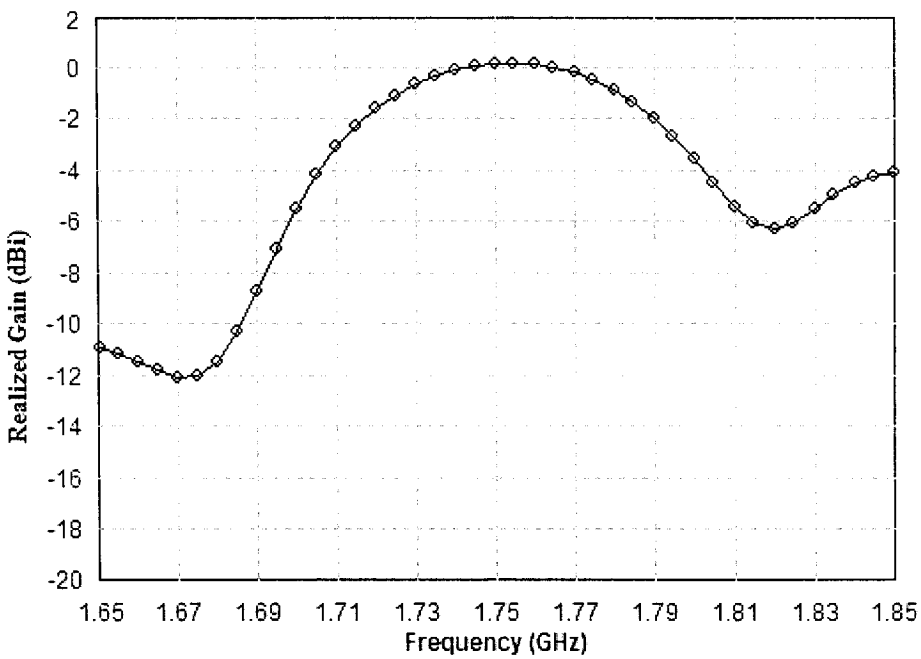

Figure 4.3 : Realized Gain of Antenna with Embedded Slots and Reactive Loading

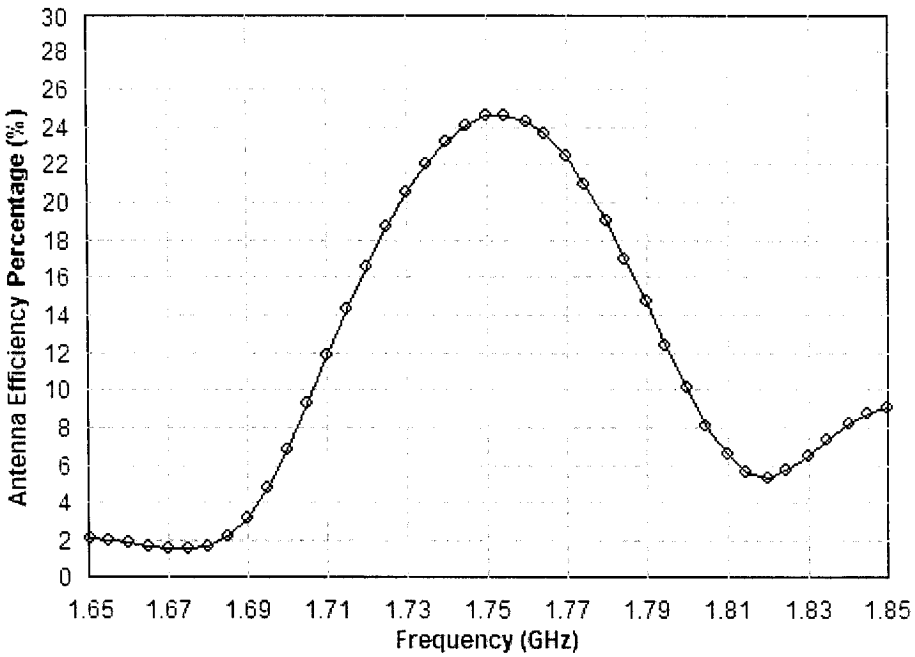

Figure 4.4 : Antenna Efficiency of Antenna with Embedded Slots and Reactive Loading

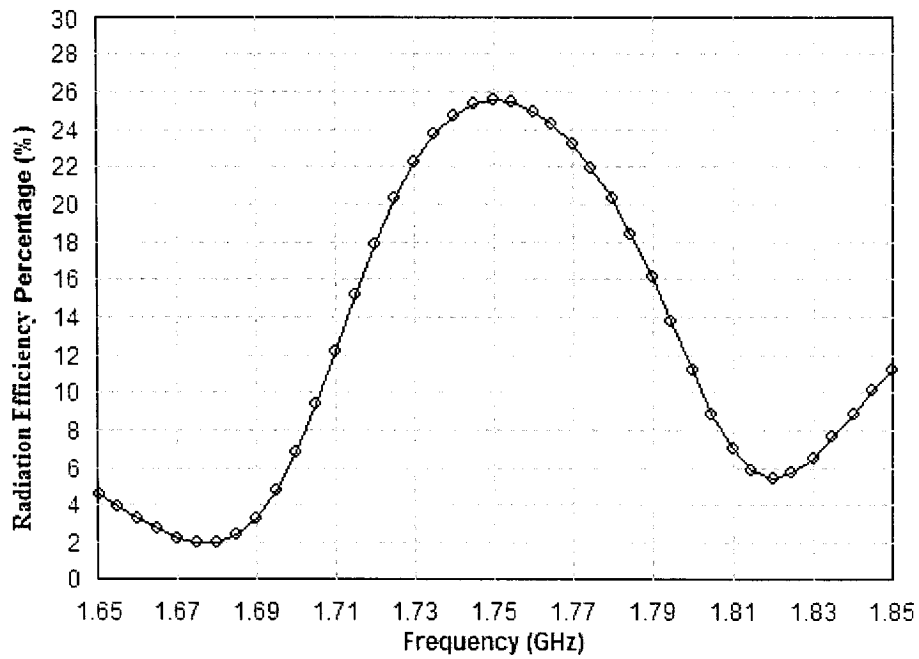

Figure 4.5 : Radiation Efficiency of Antenna with Embedded Slots and Reactive Loading

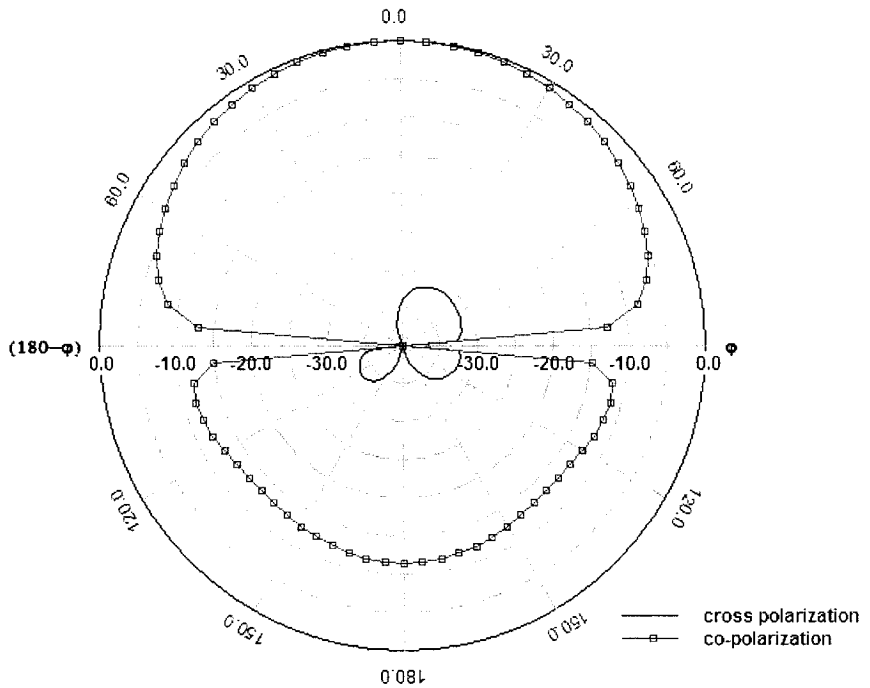

Figure 4.6 : H-Plane Radiation Patterns of Antenna with Embedded Slots and Reactive Loading at 1.69 GHz

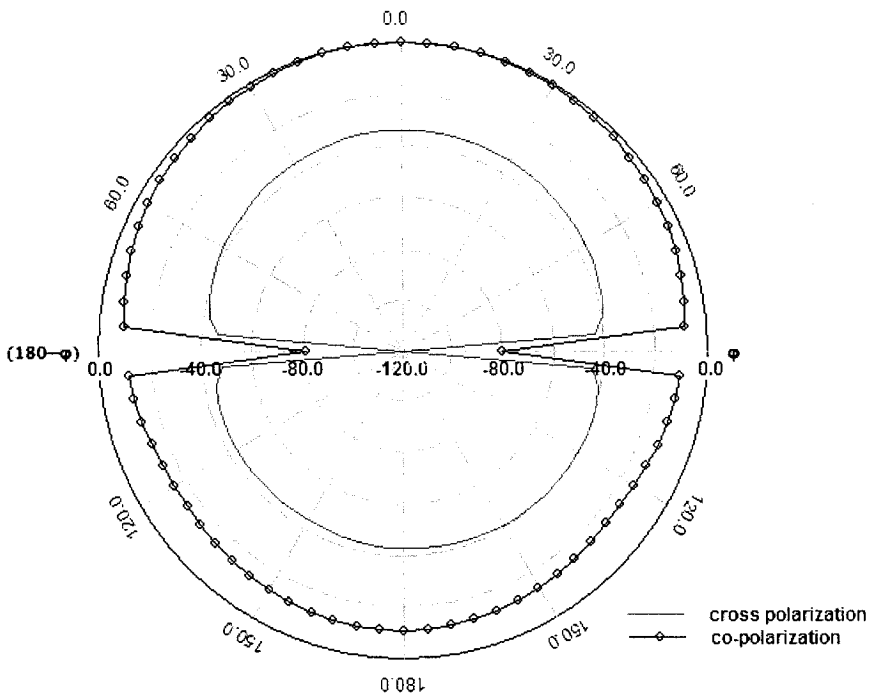

Figure 4.7 : E-Plane Radiation Patterns of Antenna with Embedded Slots and Reactive Loading at 1.69 GHz

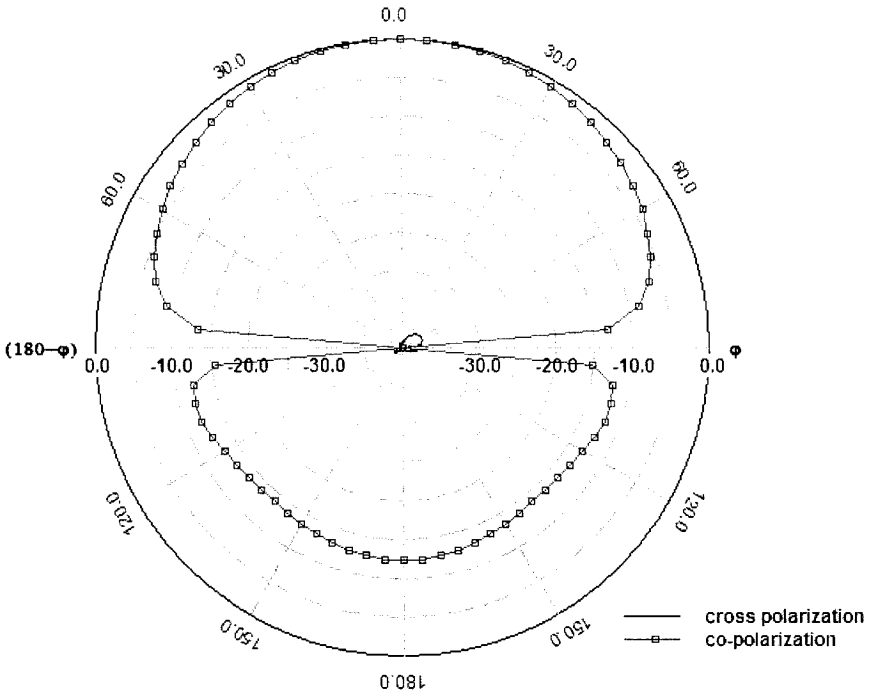

Figure 4.8 : H-Plane Radiation Patterns of Antenna with Embedded Slots and Reactive Loading at 1.75 GHz

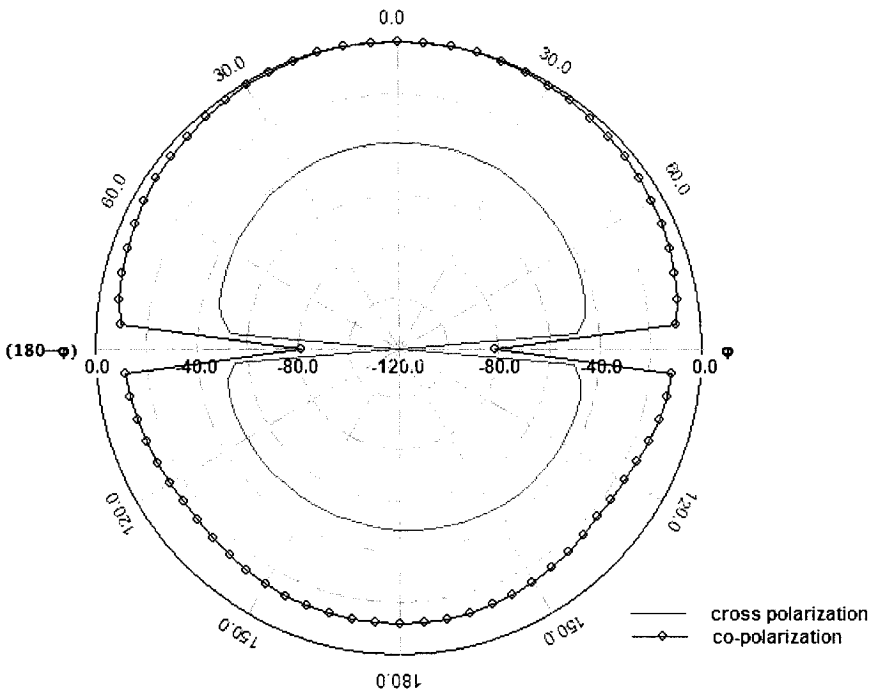

Figure 4.9 : E-Plane Radiation Patterns of Antenna with Embedded Slots and Reactive Loading at 1.75 GHz

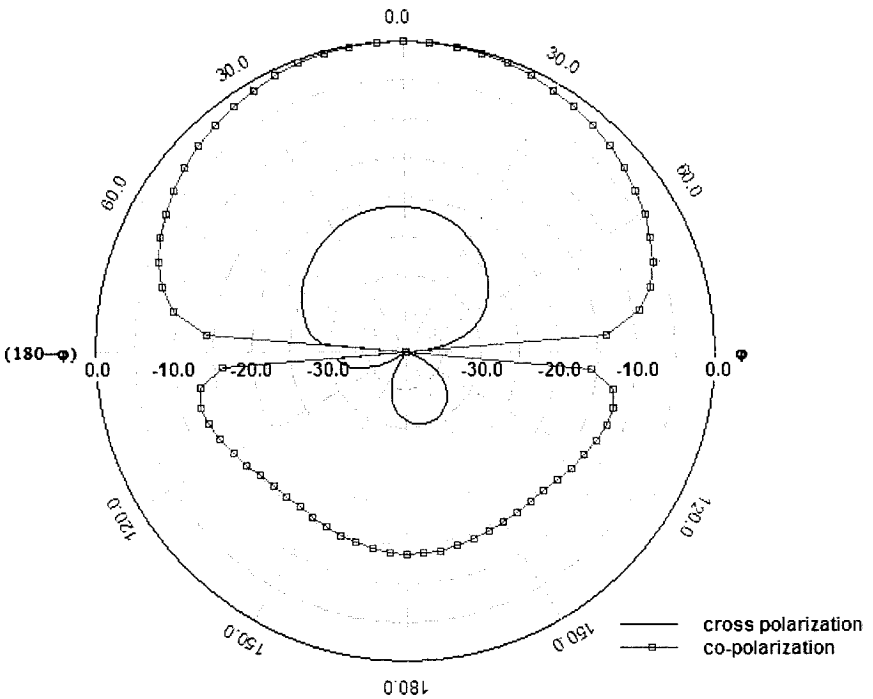

Figure 4.10 : H-Plane Radiation Patterns of Antenna with Embedded Slots and Reactive Loading at 1.84 GHz

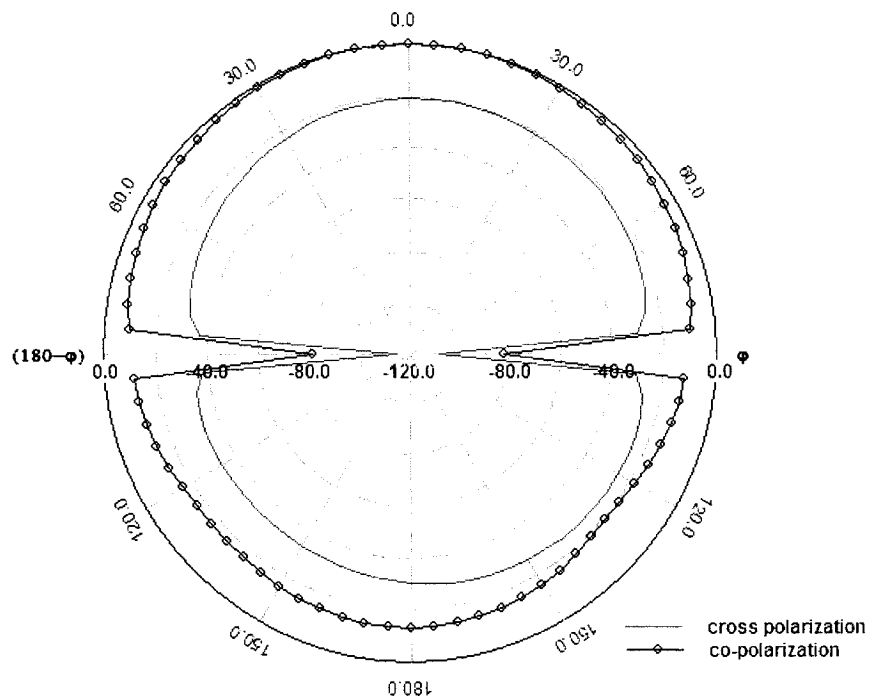

Figure 4.11 : E-Plane Radiation Patterns of Antenna with Embedded Slots and Reactive Loading at 1.84 GHz

In summary, compared to the antenna with modified patch in Section 3.4.3, since more resonating frequencies are introduced, this novel probe-fed microstrip patch antenna has almost doubled bandwidth, similar realized gain, higher antenna efficiency and radiation efficiency, similar good polarization purity. Its overall performance is as follows:

- Bandwidth: broad bandwidth, around 10%
- Realized gain: very low, less than 0 dBi
- Antenna efficiency: very low, less than 25%
- Radiation efficiency: very low, less than 30%
- E-plane radiation pattern: stable, low cross polarization level (cross-polarization is 20 dB less than co-polarization).
- H-plane radiation pattern: stable, low cross polarization level (cross-polarization is 20 dB less than co-polarization).

4.3.2 Investigations of the Effect of Reactive Loading Geometries

In order to investigate the reactive loading dimensions effect on the antenna return loss performance, in this section, we compared return loss results with different cutting length l_4, cutting width w_4, reactive loading length l_5, reactive loading width w_5, feeding point g and substrate thickness h.

Figure 4.12 shows antenna return loss results with cutting length l_4 = 22.15 cm, 22.65 cm and 23.15 cm. As cutting length l_4 increasing, the antenna bandwidth slightly shifts to higher frequency, meanwhile the return loss peak value between two lower resonant frequency dips decreases with the return loss peak value between two high resonant frequency dips increasing at the same time. Cutting length l_4 = 22.15 cm is the optimal value, which keeps both return loss peak values lower than –10 dB.

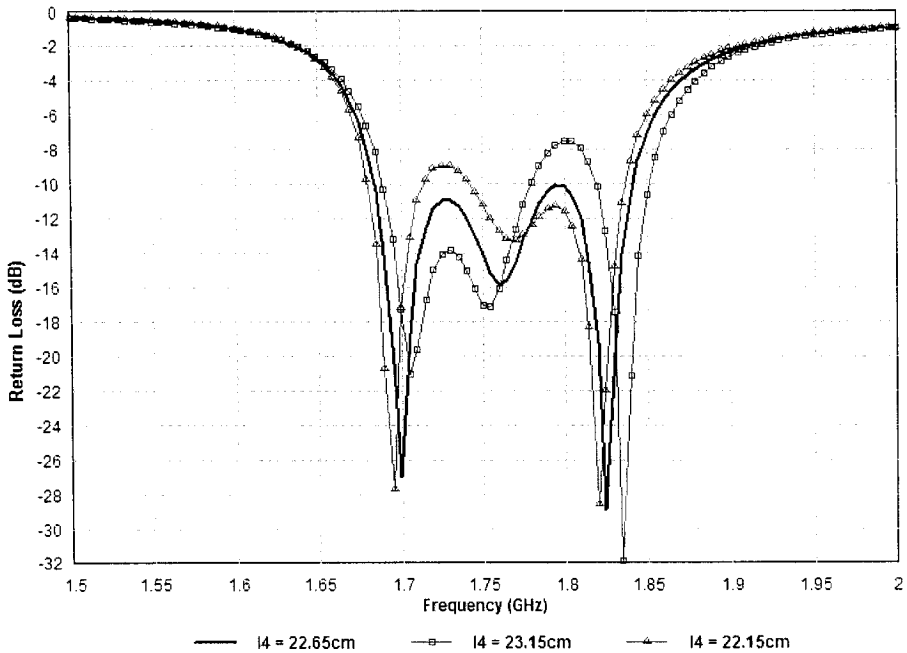

Figure 4.12 : Return Loss with Different Cutting Length l_4

Figure 4.13 compares antenna return loss results with cutting width w_4 = 1.8 cm, 2cm and 2.2 cm. As cutting width w_4 increasing, the return loss span between the lowest resonant frequency and highest frequency becomes broader, but the return loss peak value between two high resonant frequency dips increases. Cutting width w_4 = 2 cm is the optimal value, which keeps the antenna bandwidth as broad as possible with the return loss peak value between two high resonant frequency dips lower than –10 dB.

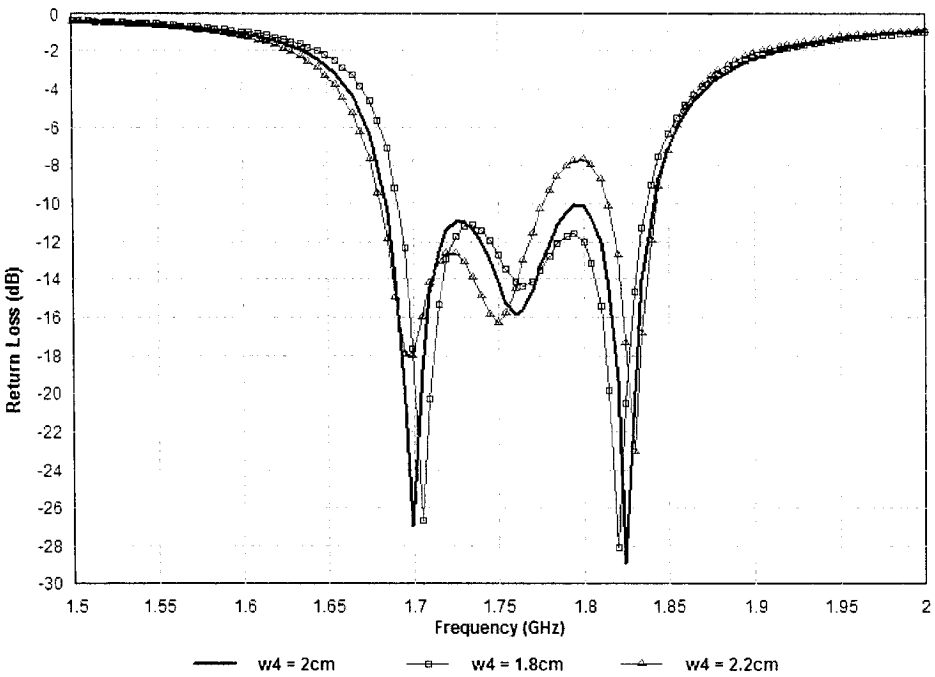

Figure 4.13 : Return Loss with Different Cutting Width w_4

Figure 4.14 shows antenna return loss results with reactive loading length l_5 = 22 cm, 22.5 cm and 23 cm. Reactive loading length controls the position of the reactive loading resonant frequency, which in this case is the highest resonant frequency of the antenna, with also slight effect on the position of the lowest resonant frequency. As reactive loading length l_5 decreases, the reactive loading resonant frequency moves toward a higher frequency. Reactive loading length l_5 = 22.5 cm is the optimal value, which keeps the antenna bandwidth as broad as possible with the return loss peak value between two high resonant frequency dips lower than –10 dB.

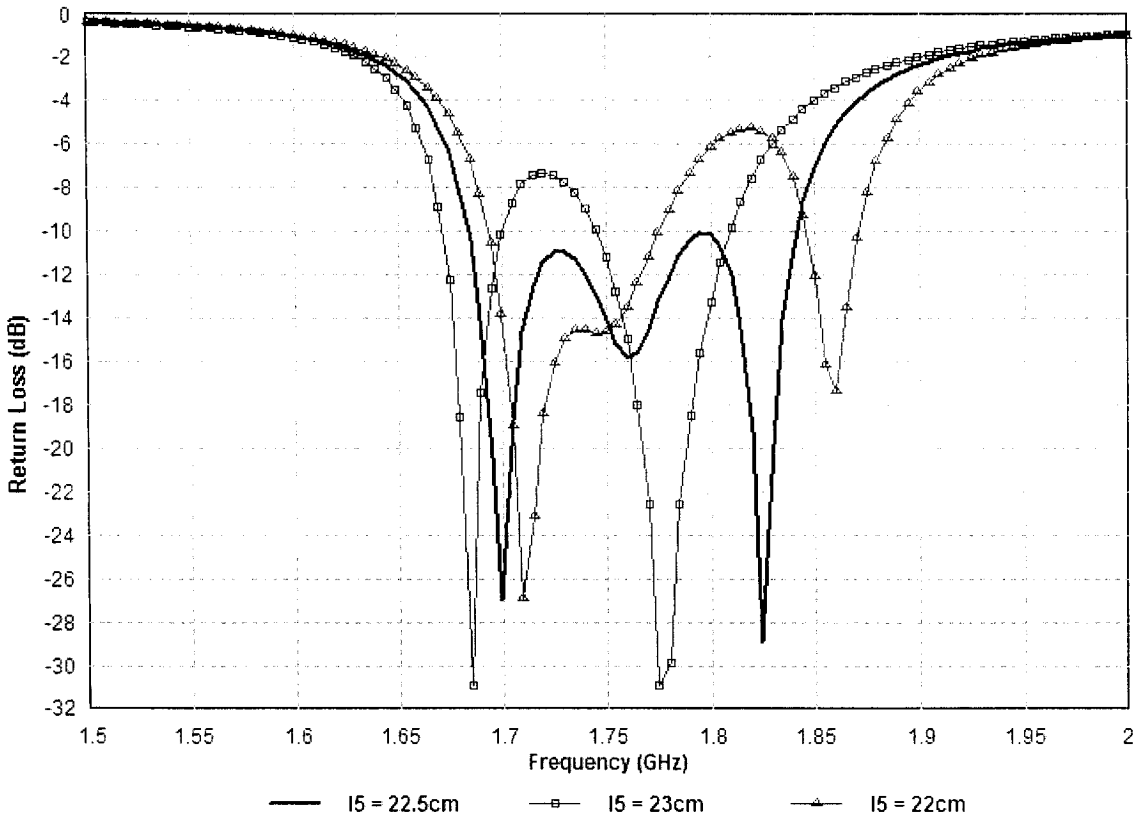

Figure 4.14 : Return Loss with Different Reactive Loading Length l_5

Antenna return loss results with reactive loading width w_5 = 1 cm, 1.2 cm and 1.4 cm are shown in Figure 4.15. Reactive loading width has only a slight effect on return loss peak values between resonant frequencies. Reactive loading width w_5 = 1.2 cm is the optimal value, which keeps the return loss peak value between two high resonant frequency dips lower than –10 dB.

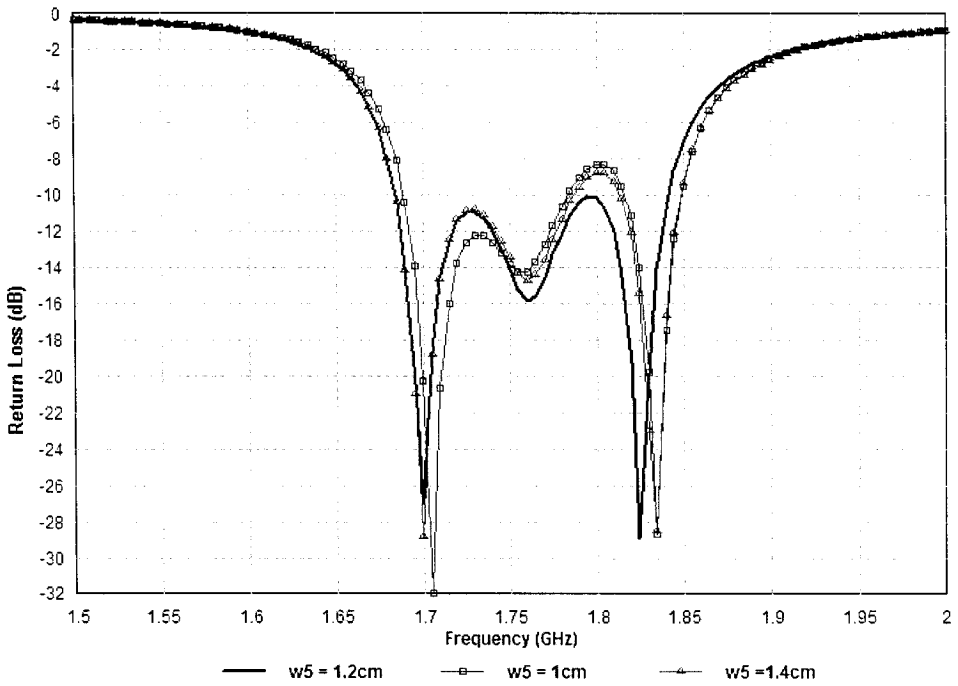

Figure 4.15 : Return Loss with Different Reactive Loading Width w_5

Figure 4.16 shows antenna return loss results with feed point g = 10.65 cm, 11.15 cm and 11.65 cm from patch lower edge. As we've discussed in Section 2.4.2, the feed point location has a great effect on the antenna input impedance. In this case, the main effects of feed point location are the return loss peak value between two high resonant frequencies and the position of the highest resonant frequency. The feed point location g = 11.15 cm from the patch lower edge is the optimal value, which keeps the return loss peak value between two high resonant frequency dips lower than –10 dB.

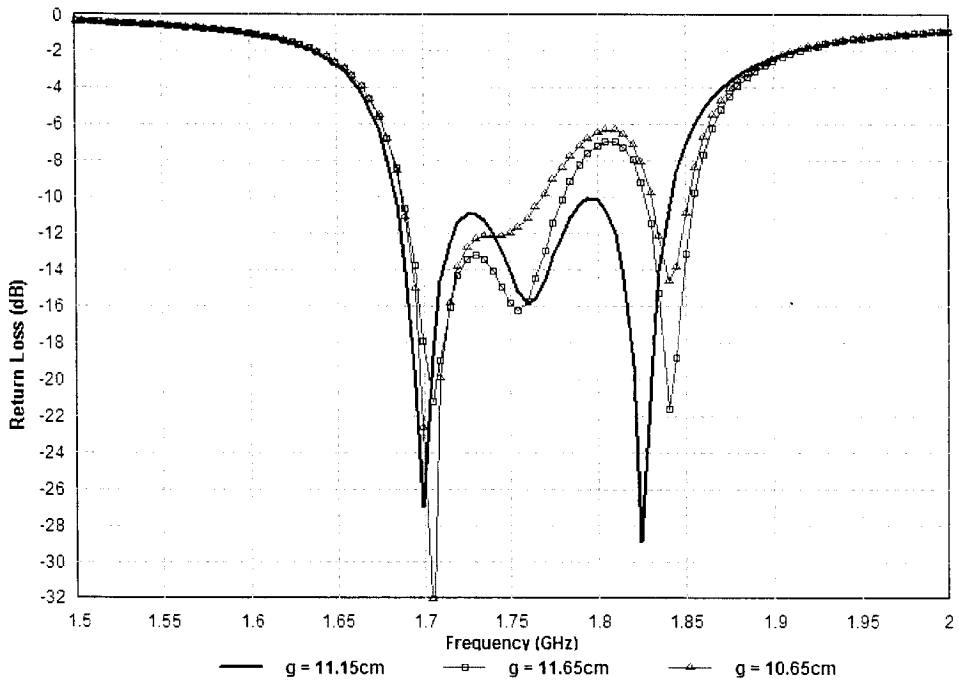

Figure 4.16 : Return Loss with Different Feed Point g

Antenna return loss results with substrate thickness h = 2.4 cm, 2.6 cm and 2.8 cm are shown in Figure 4.17. As substrate thickness h increases, the return loss span between the lowest resonant frequency and highest frequency becomes narrower, and the return loss two peak values between resonant frequency dips decrease. Substrate thickness h = 2.6 cm is the optimal value, which keeps the antenna bandwidth as broad as possible with the return loss peak values between resonant frequency dips lower than –10 dB.

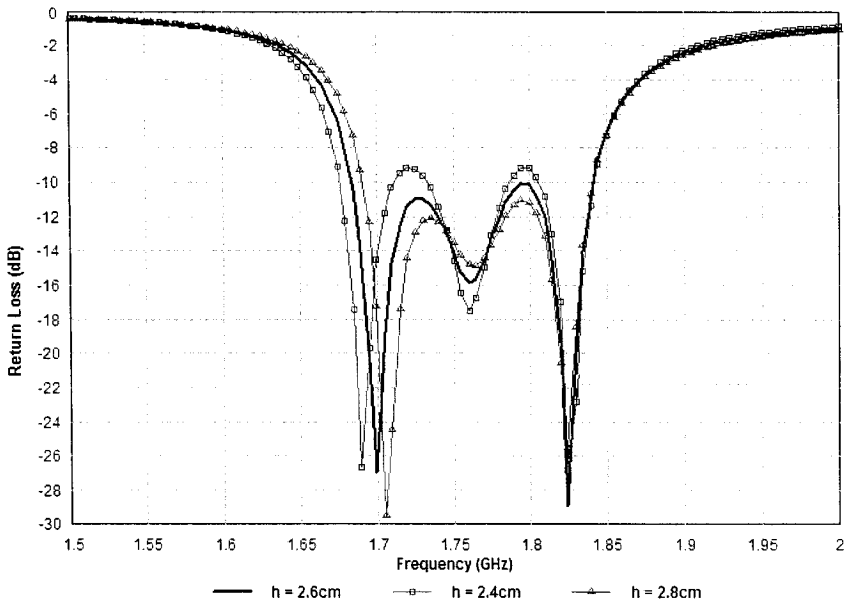

Figure 4.17 : Return Loss with Different Substrate Thickness h

4.4 CONCLUDING REMARKS

The large amount of data presented in Chapter 3 has been succinctly collected and summarised in tabular form in this chapter to allow a designer to do a proper trade-off selection on the best broadband probe-fed microstrip patch antenna for a particular application. We have also demonstrated how the increased understanding afforded by the classification of the broadbanding techniques, which allows one to put the contributions from virtually all papers on the subject into context, can be used to devise further improvements.

4.5 REERENCES FOR CHAPTER 4

[1] J. Y. Sze, "Designs of broadband microstrip antennas with embedded slots", IEEE Antennas Propagat. Soc. Int. Symp., vol. 2, pp. 936 – 939, July 1999.

[2] K. L. Wong, J. S. Kuo, S. T. Fang, and T. W. Chiou, "Broadband microstrip antennas with integrated reactive loading", 1999 Asia Pacific Microw. Conf., vol. 2, pp. 352 – 354, Nov. Dec.

CHAPTER 5

GENERAL CONCLUSIONS

5.1 THESIS CONTRIBUTIONS

The contributions of this thesis are as follows:

- We have been able to usefully reduce the plethora of geometries used for broadbanding probe-fed microstrip patch antennas, that have been described in numerous publications, into several categories. This classification provides a way of thinking about and evaluating future broadbanding methods that may be proposed by others. It also serves to relate existing methods of doing so, and makes objective decision-making on the matter possible. The topic need no longer consist of a disparate list of apparently unrelated techniques.

- By applying the identical full-wave electromagnetic analysis method to selected cases from each of the bandwidth enhancement categories we have provided what can be called the first "unprejudiced" comparison of their performance. This complete performance data (both good and bad aspects) has been summarised in tabular form, and will allow a designer to do a proper trade-off selection for the most suitable broadband probe-fed microstrip patch antenna for a particular application.

- In the process of demonstrating how the increased understanding afforded by the classification of the broadbanding techniques can be used to devise further improvements, we have devised a novel antenna (with double the bandwidth performance of other examples in its class) that has not previously been described in the literature.

5.2 SUGGESTIONS FOR FUTURE WORK

An examination of the overall performance review in Section 4.2 reveals that the many bandwidth enhancement techniques for probe-fed microstrip patch antennas still have some performance parameters which could be improved. Further researches on the topic could attempt the development of the following:

- Techniques to improve the polarization purity of broadband microstrip patch antennas on electrically-thick low-permittivity substrates.
- Techniques to further improve bandwidth for broadband microstrip patch antennas with electrically-thin high-permittivity substrates (such as FR4) above 10 %.
- Techniques to improve the realized gain for broadband microstrip patch antennas with electrically-thin high-permittivity substrates (such as FR4).

Since each technique introduced in Chapter 3 has certain advantages with respect to some performance parameter, the above could be attempted by considering combinations of the different categories. The fact that this *modus operandi* might lead to success is supported by the example discussed in Section 4.4, where the bandwidth was almost doubled.

APPENDIX I

FULL-WAVE ANALYSIS CODE *IE3D*

A. INTRODUCTION

In order to get optimized dimension values and more accurate performance results, full-wave electromagnetic simulation software is needed. IE3D software is used in this thesis. (Other software, such as Ensemble and HFSS, can also be used.) The IE3D is a full-wave, method of moment (MOM) simulator solving the current distribution on 3D and multi-layered structures of general shape. It has many good features, including the ability to model different true 3D metallic structures in multiple dielectric layers in different boundary conditions, high efficiency and accuracy, the ability to model structures with finite ground planes and differential feed structures, electromagnetic optimization and so on.

B. USE OF THE CODE IE3D

The IE3D package consists of the four major application programs:

MGRID :	Layout editor for the construction of geometry.
MODUA :	Schematic editor for parameter display and nodal circuit simulation.
CURVIEW :	Post-processor for display and animation of current distribution and field distribution.
PATTERNVIEW:	Post-processor for radiation patterns.

Return loss, realized gain, antenna efficiency, radiation efficiency and radiation patterns, as defined in Section 2.5, can all be generated by these IE3D programs. More detailed information on IE3D can be found in [1]

C. EXPLANATION OF SHARP DIPS IN IE3D RADIATION PATTERN RESULTS

In Chapter 3, sharp dips close to the groundplane have been found in radiation patterns computed using IE3D. It is obvious that these sharp dips will not occur in practice. Discussions with the IE3D code developers at Zeland Softwares Inc. confirmed our suspicion that this is a code issue. We have used a finite size groundplane in all the examples discussed. Yet the code forces one to use an infinitely large substrate. Fortunately, the problem arises only at angles 0° and 180°. The rest of the pattern is smoothly varying.

D. REFERENCES FOR APPENDIX I

[1] Zeland Software Inc., "IE3D User's Manual", http://www.zeland.com.